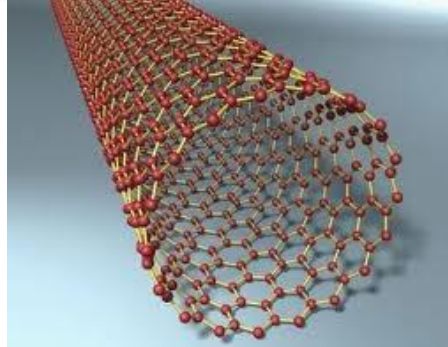




Aalto University



Studies on CVD growth and oxidation of SWCNTs

Prof. Dr. Esko I. Kauppinen

NanoMaterials Group

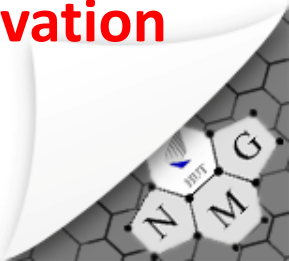
Department of Applied Physics, Aalto University School of Science

esko.kauppinen@aalto.fi

Global Center of Excellence for Mechanical Systems Innovation

Tokyo University, Tokyo, Japan

September 20, 2012



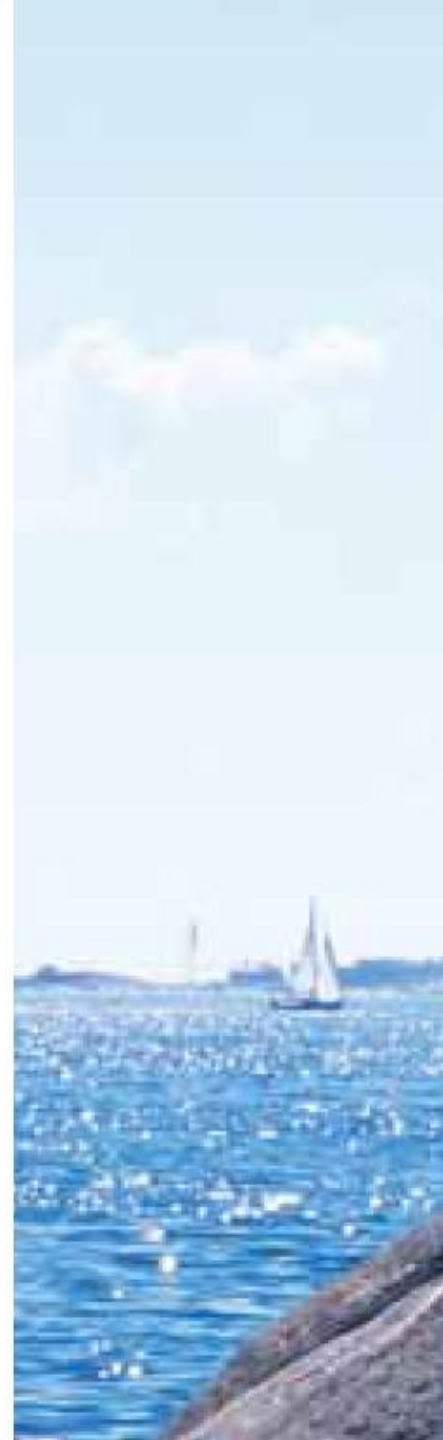
NT13

**Fourteenth International
Conference on the
*Science and Applications
of Nanotubes***

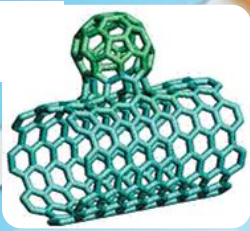
24-28 June 2013

Dipoli Congress Center, Espoo, Finland

www.nt13.org



Finland is Centrally Located



NOKIA

Bangkok	9 h 45 min
Beijing	7 h 40 min
Berlin	1 h 55 min
Brussels	2 h 40 min
Chicago	9 h 35 min
Copenhagen	1 h 40 min
Frankfurt	2 h 40 min
Hong Kong	9 h 50 min
London	3 h 10 min
Moscow	1 h 45 min
Delhi	6 h 45 min
New York	8 h 40 min
Osaka	9 h 35 min
Paris	3 h 05 min
Seoul	8 h 45 min
Shanghai	8 h 55 min
Singapore	11 h 30 min
St Petersburg	1 h
Stockholm	55 min
Tokyo	9 h 40 min
Toronto	8 h 50 min



About Finland

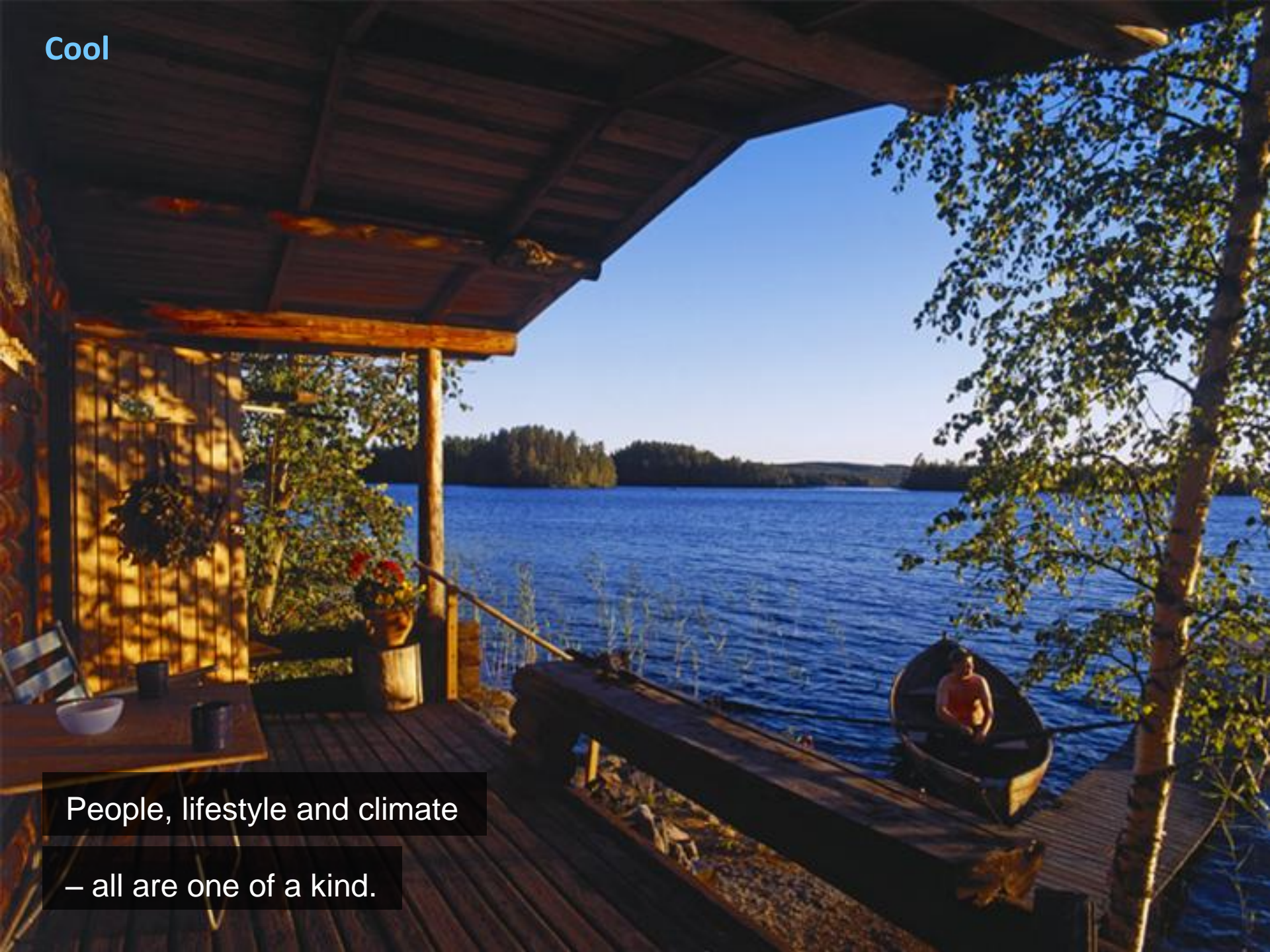
- 5.4 million people
- World's top 3 in:
 - Innovation (Harvard Business Review ranking 2009)
 - Highest Availability of Scientists and Engineers
 - World's best IPR protection
- Capital city Helsinki
- Espoo city in metropolitan area
- Home of **Otaniemi**, Northern Europe's biggest hitech hub, home of Angry Birds, Venture Garage, Nokia etc
- Birthplace of Linux, MySQL



Cool

People, lifestyle and climate

– all are one of a kind.



Midsummer midnight in Helsinki



Finland is full of interesting contrasts, such as the four seasons, the midnight sun and the period of darkness, urban and rural, East and West - you name it.

Contrasts

A small country holds a quite big amount of variety.

- In Finland all the four seasons have their own personality in different parts of the country, especially in Lapland where summer lasts less than 2,5 months.

- The maximum and the minimum temperatures at January vary between -3°C and -30°C .

- There is also a time in winter when the sun won't raise at all for weeks.

On the contrary the sun won't go down for 73 days in the summer.

- The average temperature in sauna is $+70-100^{\circ}\text{C}$. That is about $+70-100^{\circ}\text{C}$ warmer than the water where Finns like to swim in winter.



Venue – Dipoli

Located on the Aalto campus area

Affordable yet modern and comfortable

10 min bus ride to Helsinki center



NT 13 Organizers

Conference chairs

Prof. Esko I. Kauppinen (chair)

Prof. Risto Nieminen (co-chair)

Prof. Pertti Hakonen (co-chair)

Co-organizer

Prof. David Tomanek

National committee

Albert G. Nasibulin (Aalto, chair), Hua Jiang (Aalto), Markus Ahlskog (U. Jyväskylä), Arkady Krasheninnikov (U. Helsinki), Harri Lipsanen (Aalto), Kai Nordlund (U. Helsinki), Yutaka Ohno (Aalto & Nagoya U. Japan), Mika Pettersson (U. Jyväskylä), Yuri Svirko (U. Eastern Finland)

Local organizing committee

Toma Susi (chair), Marita Halme, Alexander Savin, Antti-Pekka Eskelinen

Supported by NT Steering Committee and International Advisory Board

Satellite Meetings

June 29-30, 2012

In Tallin, Estonia (80 km from Helsinki)

- Metrology, biomedical
- Modeling
- Graphene
- Thin films
- Composites

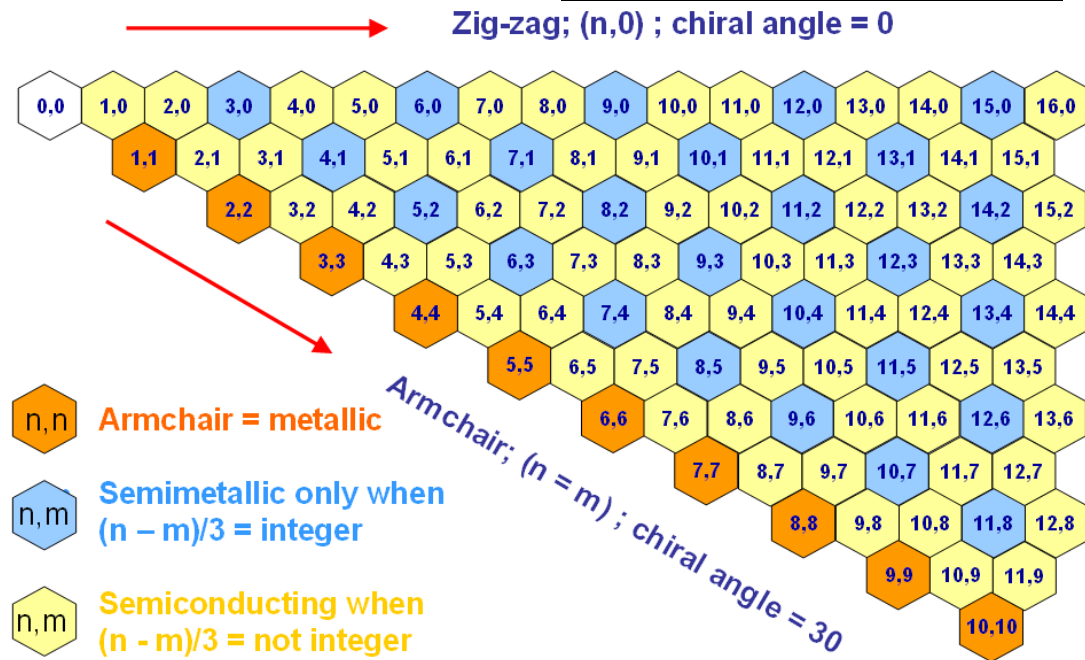
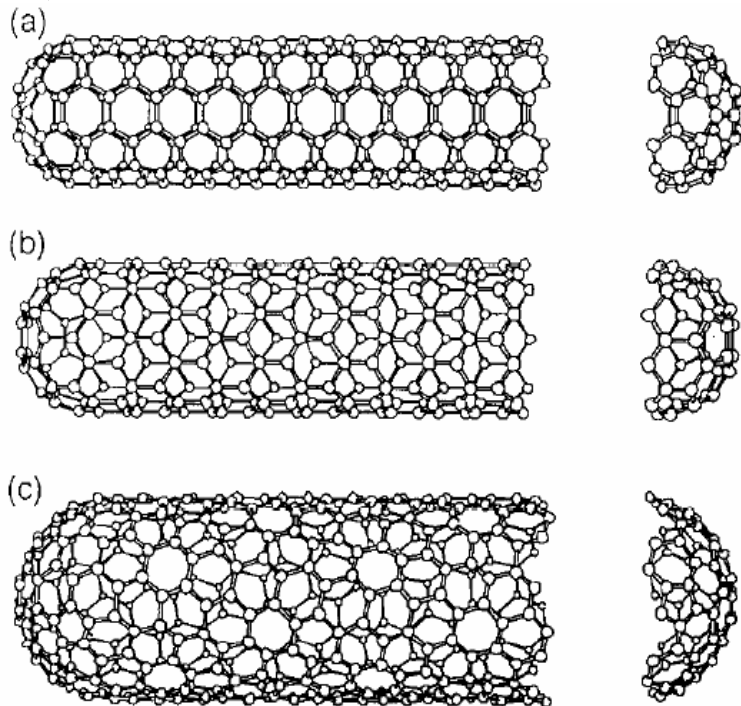
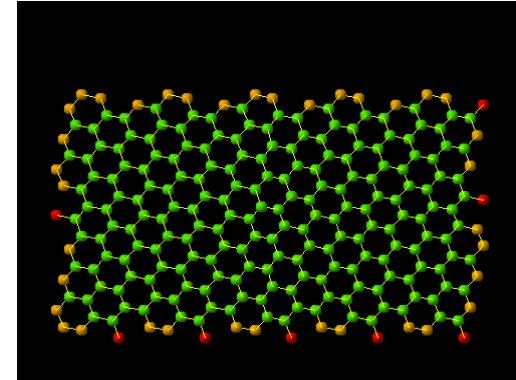
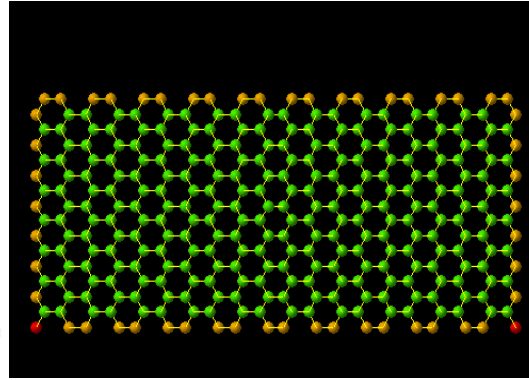
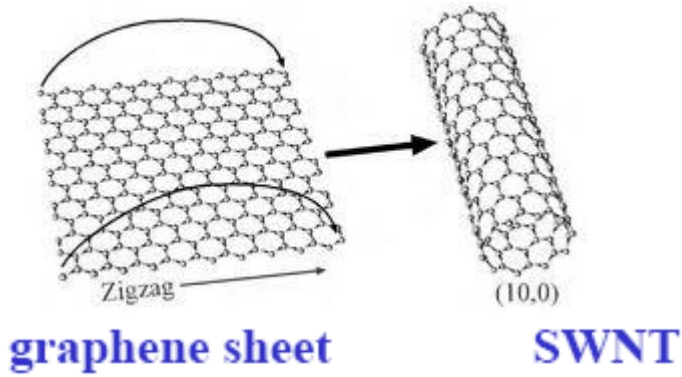


Content

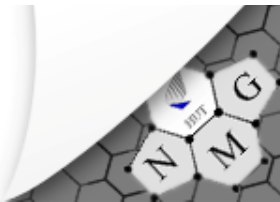
- Status of Aalto Direct Dry Printing (DPP) method for TCE and TFT-FET manufacturing – brief summary
- What do we know about SWCNT (n,m) distributions ?
- Experiments on SWCNT oxidation vs. (n,m)
- Fundamental studies towards monochiral SWCNTs - in-situ Cs-TEM (ETEM) studies on growth mechanisms from CO
- Future steps



Carbon Nanotube



Rolling in different directions makes different kinds of tubes



Nokia Flexible phone with CNTs ?

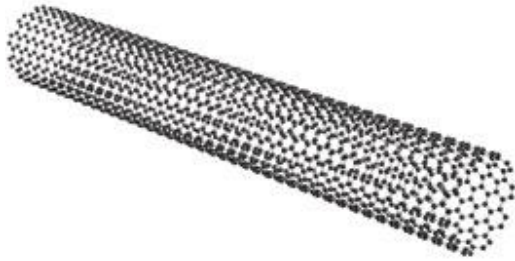


Samsung Flexible phone with Graphene ?

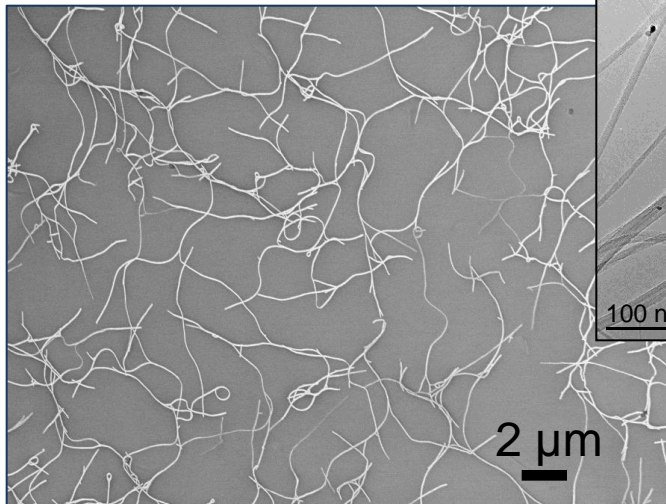
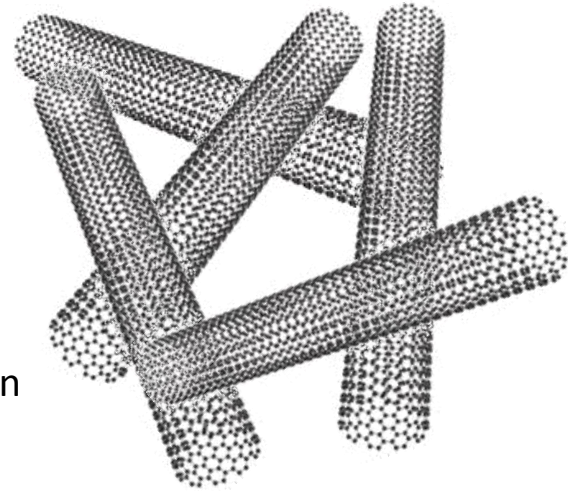


Single Walled Carbon Nanotube Thin Film Material

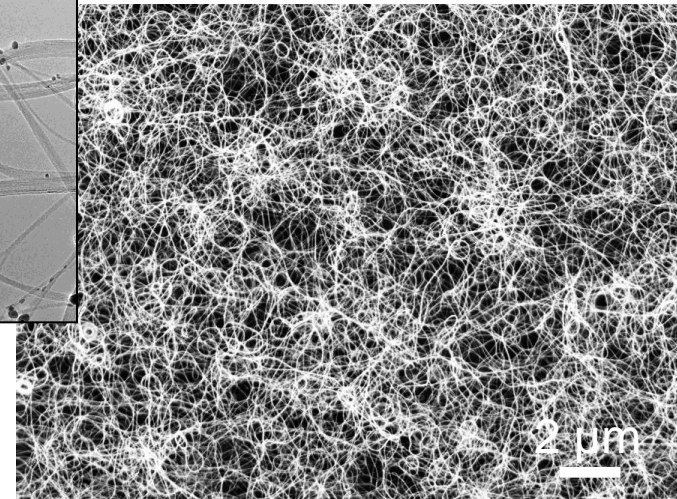
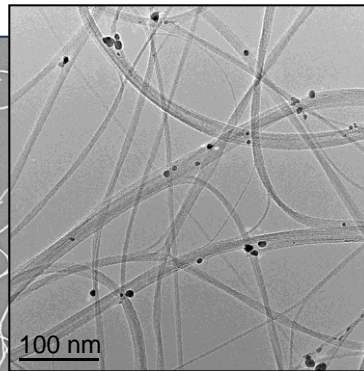
Carbon Nanotube



- Highly conductive
- Flexible, tough
- Transparent
- Simple and fast formation
(depend on method)



Carbon Nanotube Network –
semiconductor



Carbon Nanotube Film -metallic

Aalto University Novel dry, direct CNT film deposition method: DPP – Direct Dry Printing

Synthesis

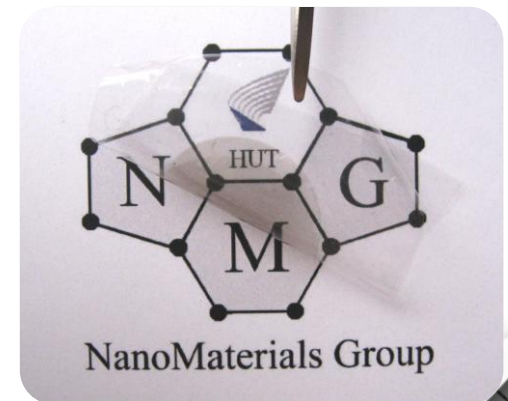
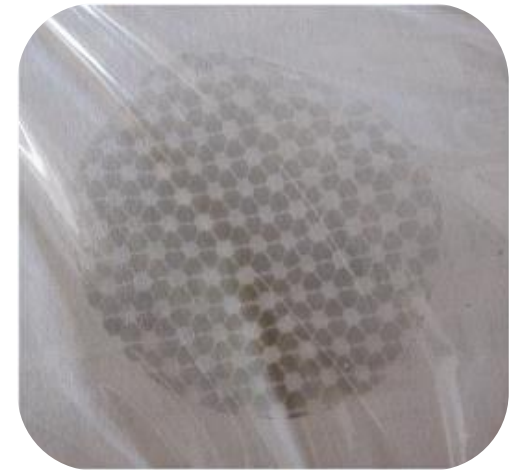
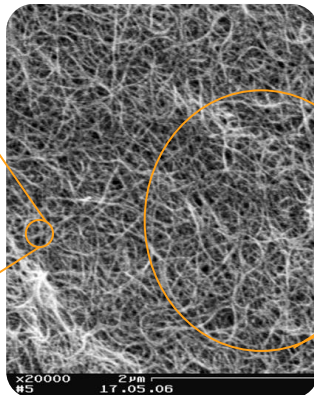
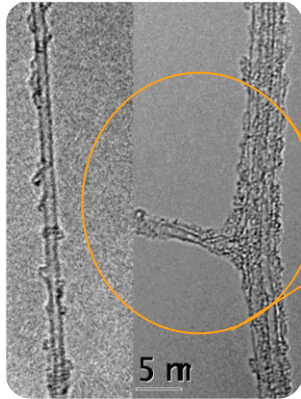
Deposition

Thin Films

SWCNTs in the reactor gas

Control of SWCNT properties

Patterned/non-patterned



NanoMaterials Group

Bundling $\propto N_{CNT}^2 \propto N_{Cat}^2$

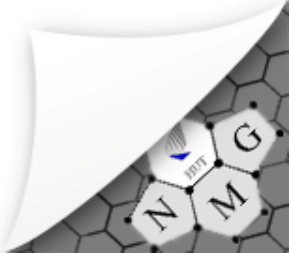
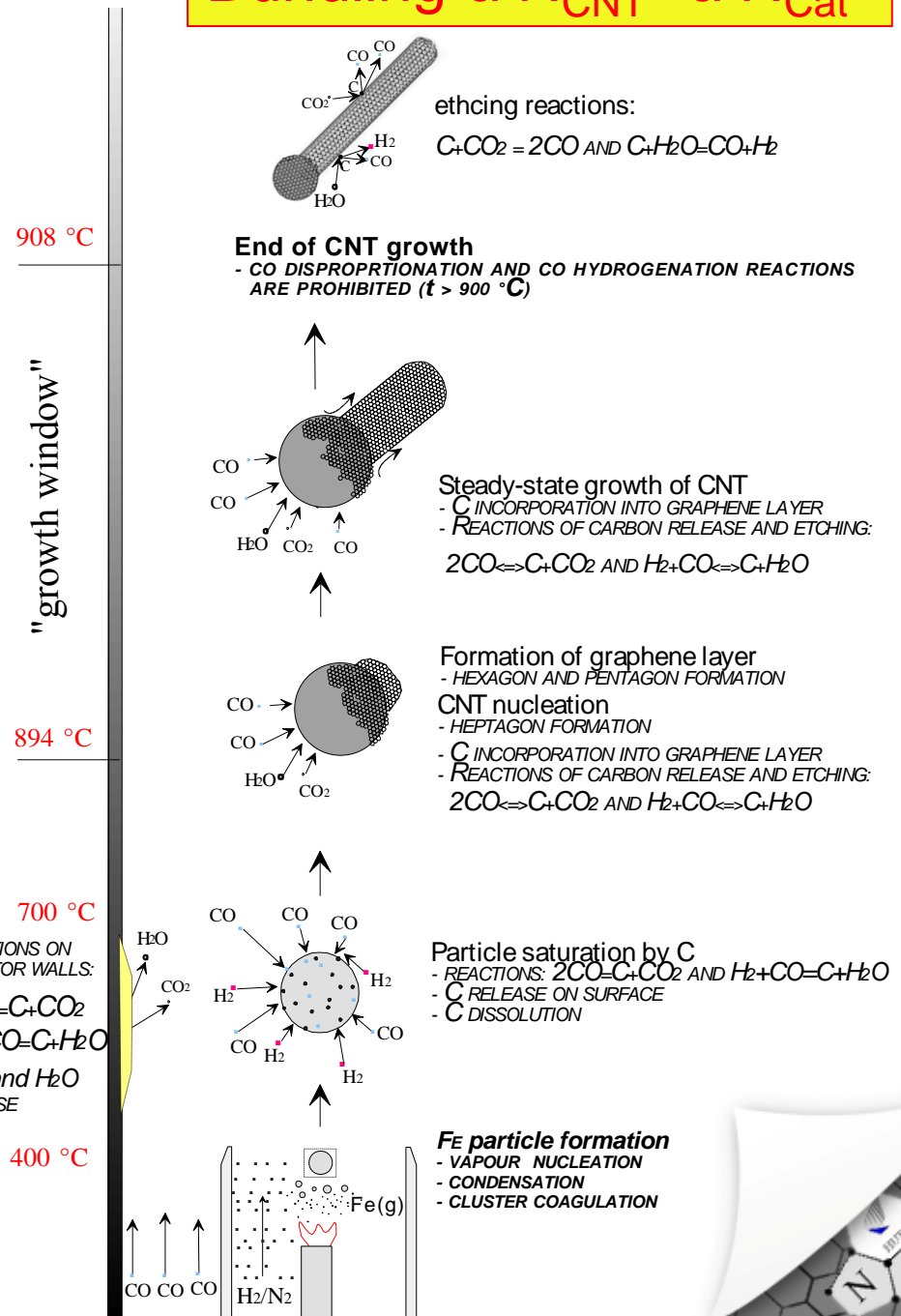
Schematics of SWCNT formation mechanism during FC-CVD CO using Fe clusters

Nasibulin, Queipo, Shandakov, Brown, Jiang, Pikhitsa, Tolochko, Kauppinen, *J. Nanosci. Nanotech.* 6

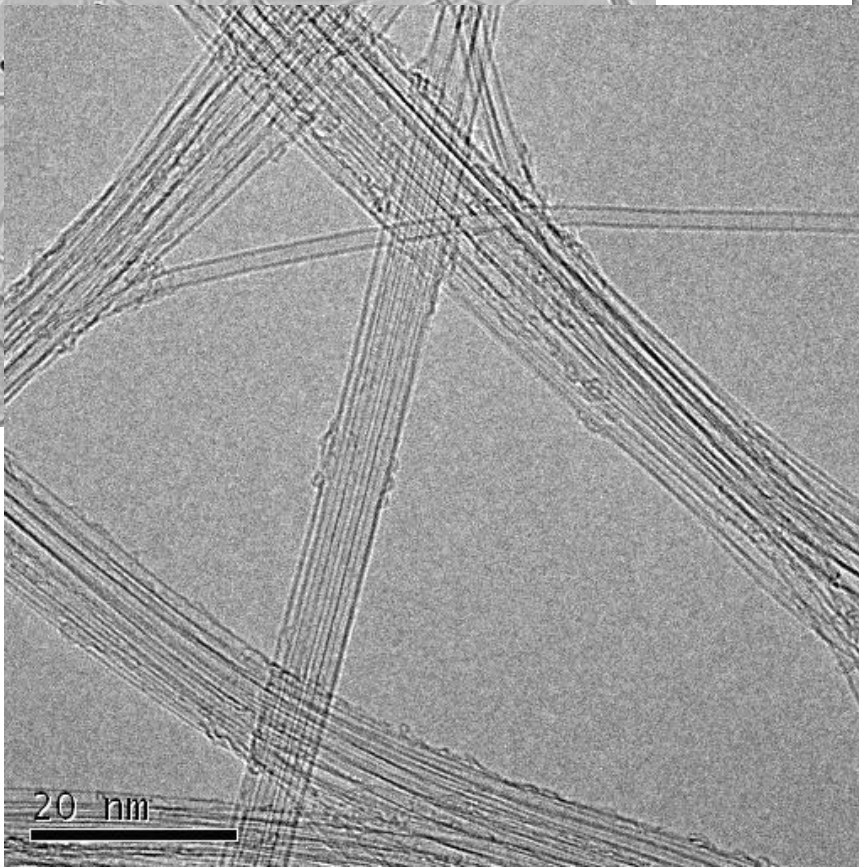
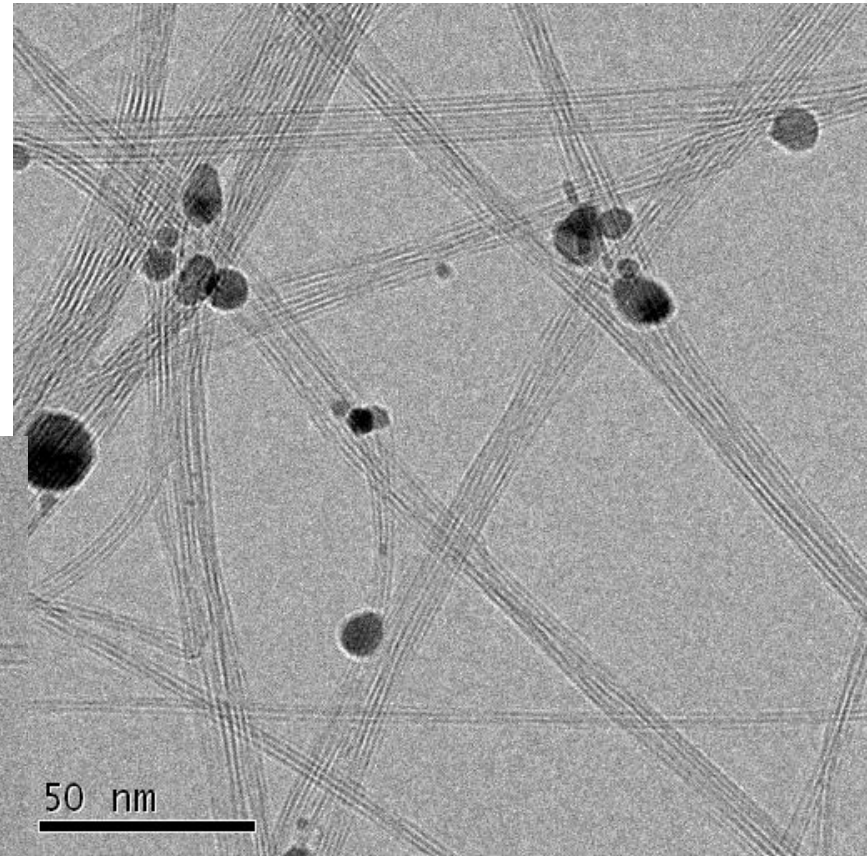
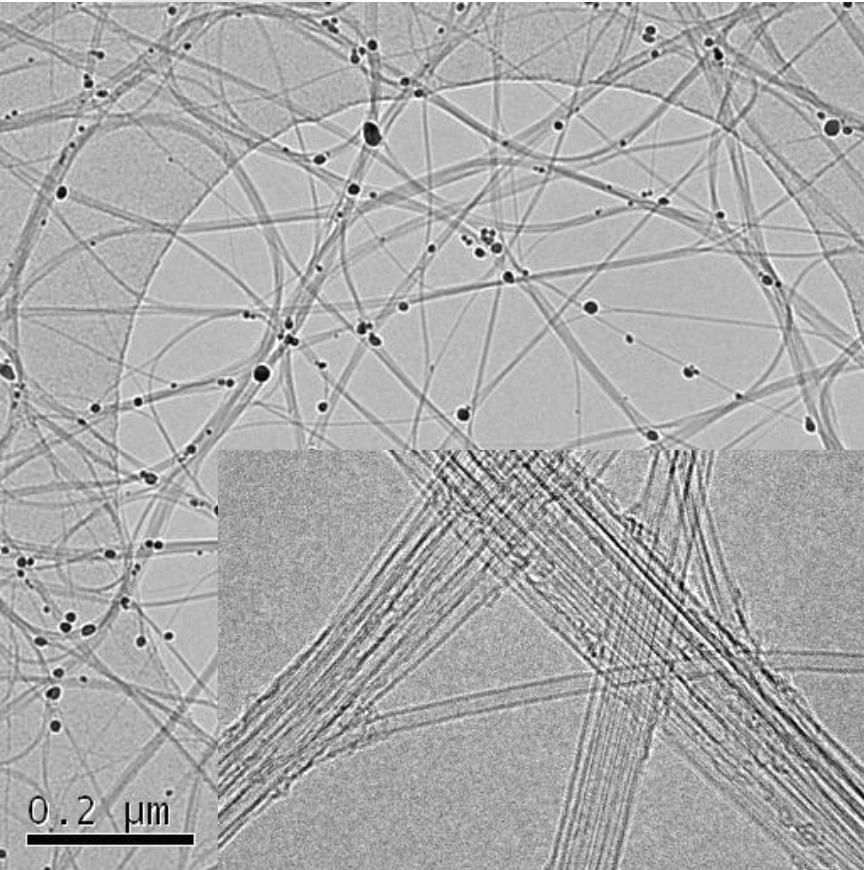
1233.

Control :

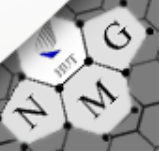
- Diameter and length via temperature and oxidant (e.g. CO₂, NH₃, H₂O) concentration
- Bundling via catalyst concentration



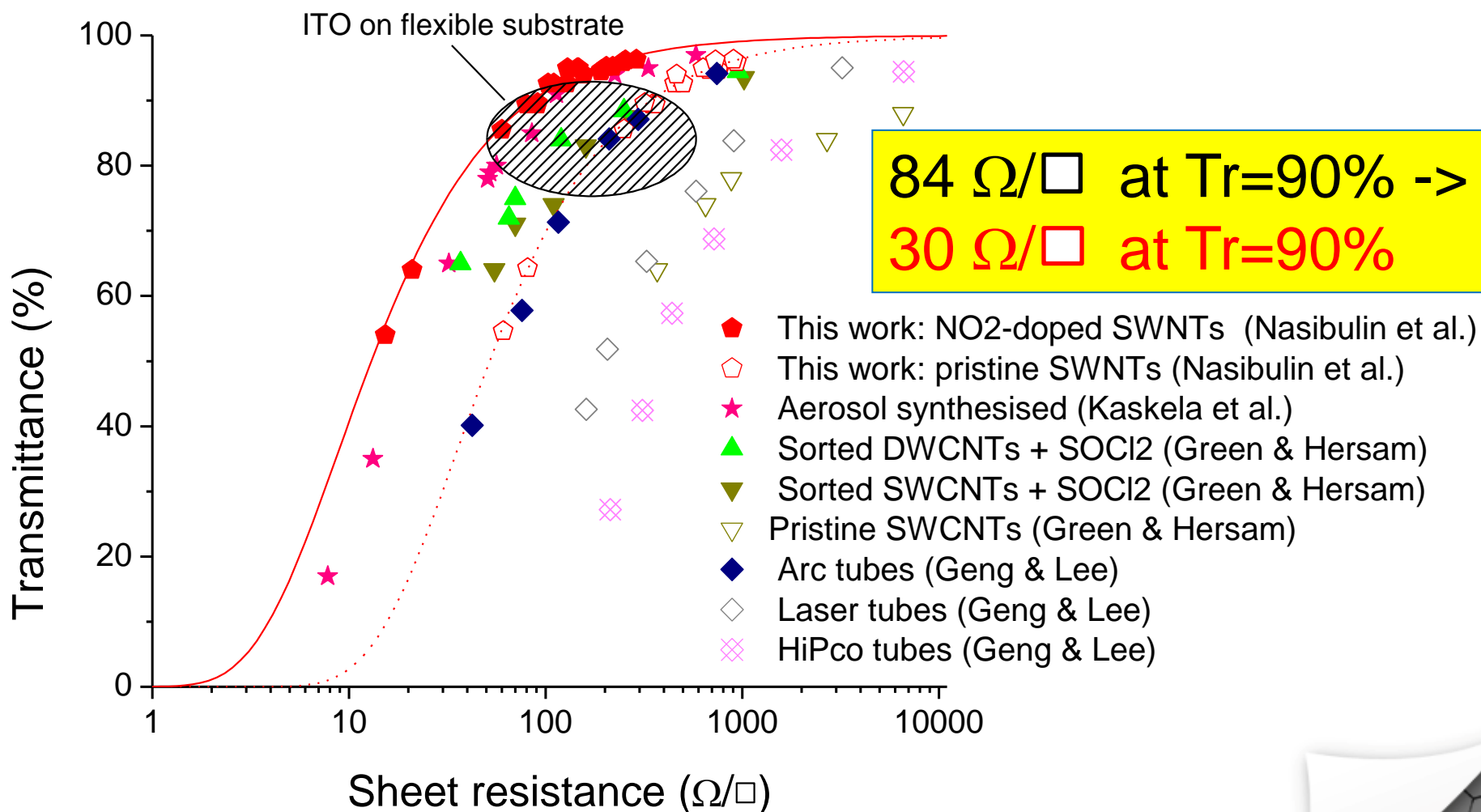
TEM of large reactor SWCNTs – 10 μm long bundles



Collaboration with
Prof. Florian Banhart
Strasbourg Univ.
France



Record performance level of SWCNT-based transparent electrodes (1.7 nm tubes)

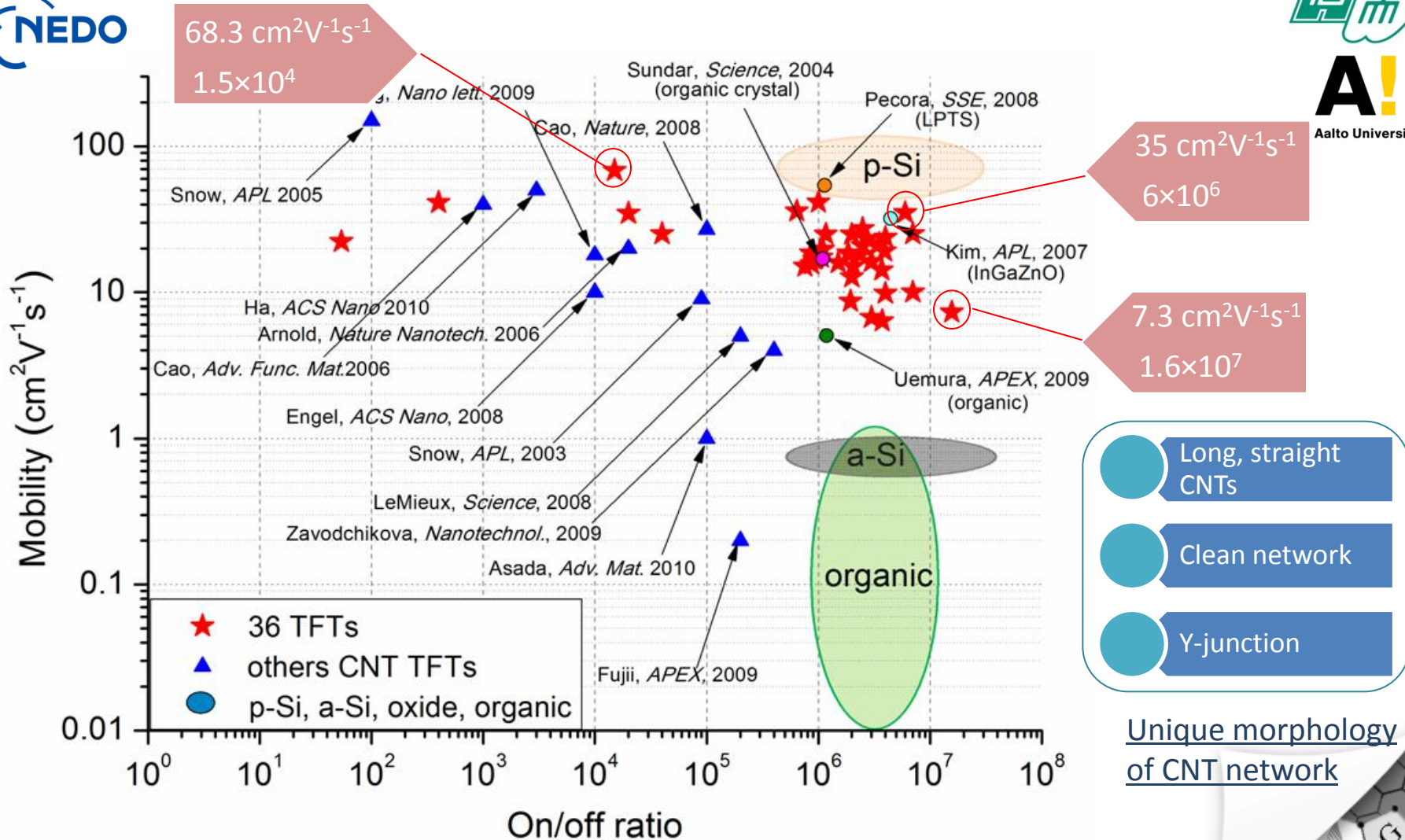


Nasibulin, Kaskela, Mustonen, Anisimov, Kauppinen, *et al.* (2011)
ACS Nano, 5(4), p.3214

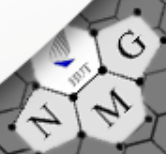


World's highest performance carbon nanotube TFTs

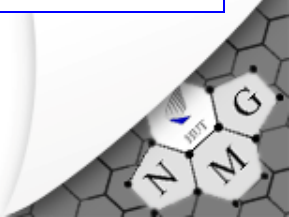
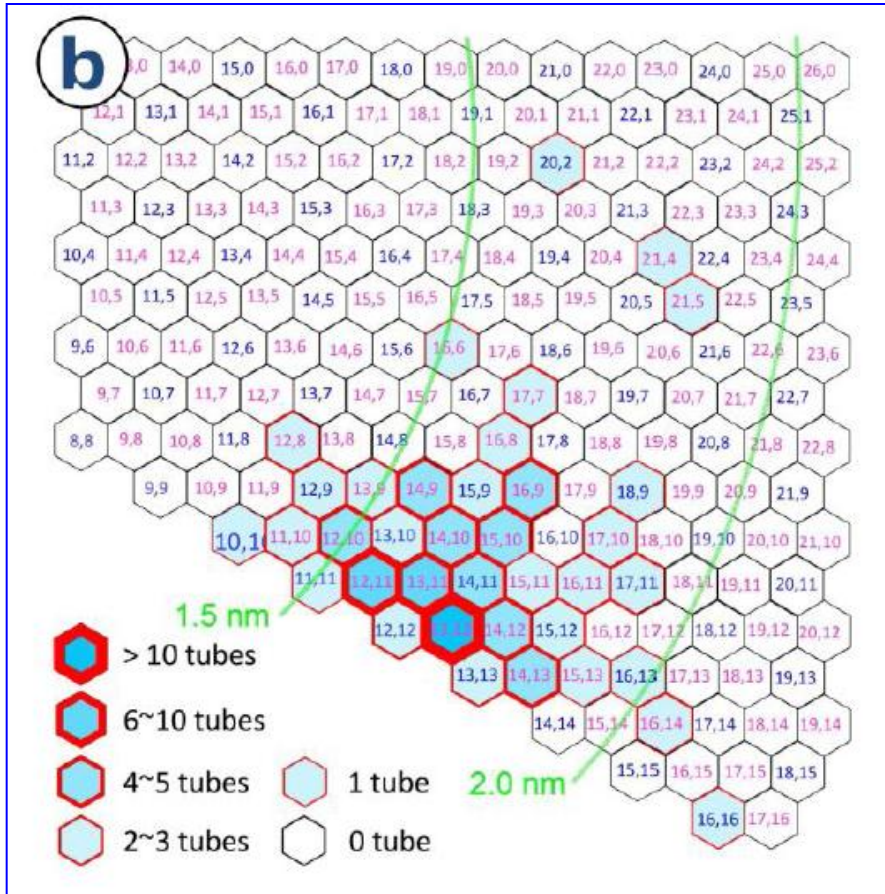
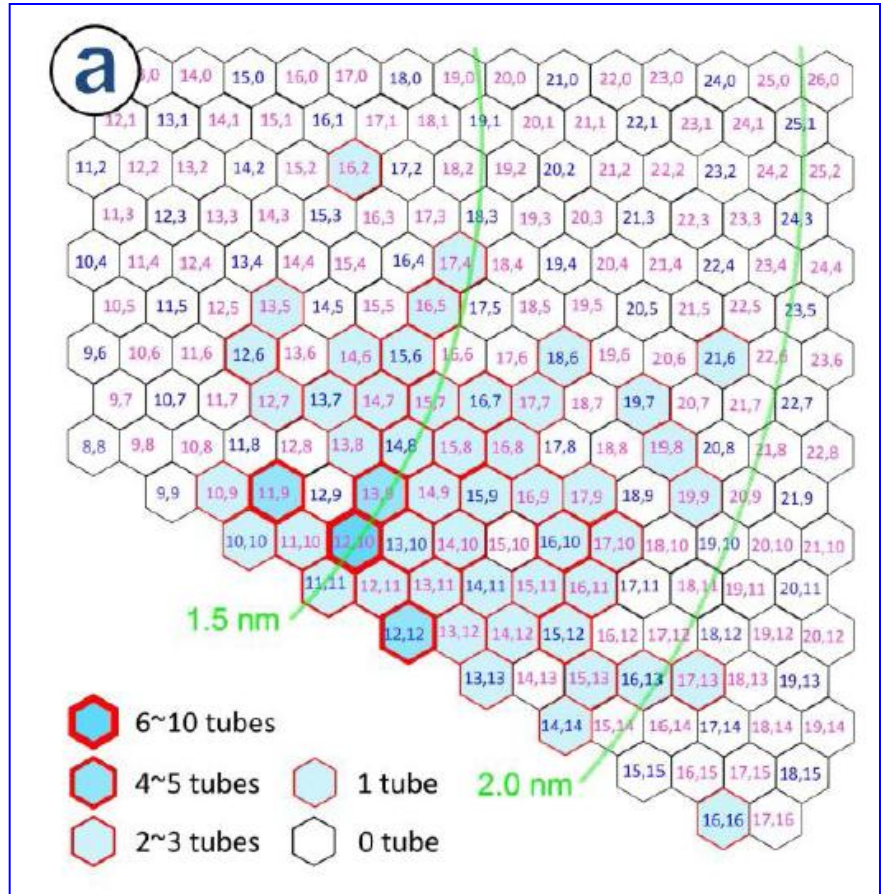
- High mobility and high on/off achieved concurrently -



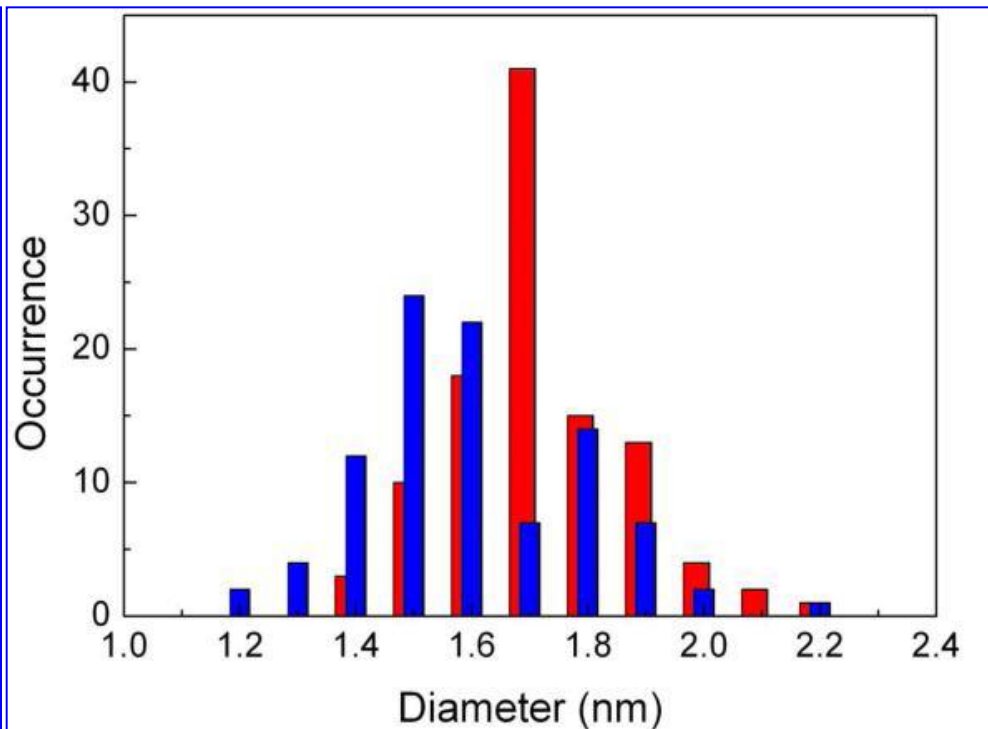
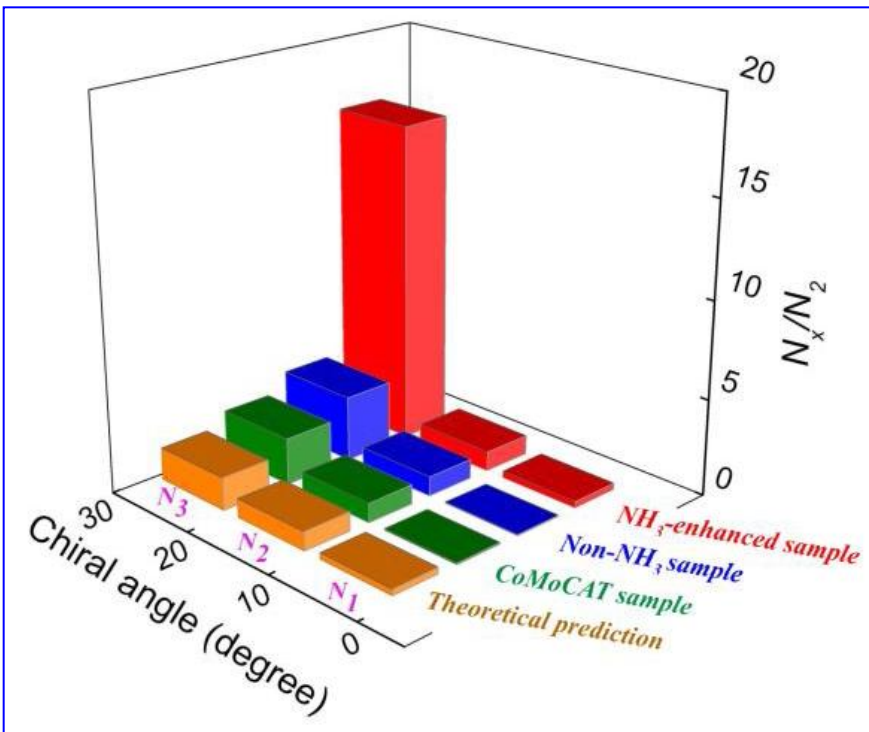
Sun, Timmermans, Tian, Nasibulin, Kauppinen, Kishimoto, Mizutani and Ohno, *Nature Nanotechnology* (2011) **6**, 156–161.



Chirality i.e. (n,m) maps for samples produced with (a) 0 ppm NH₃, and (b) 500 ppm NH₃ as determined with electron diffraction of individual SWCNTs – *large chiral angle due to enhanced etching of low chiral angle tubes*



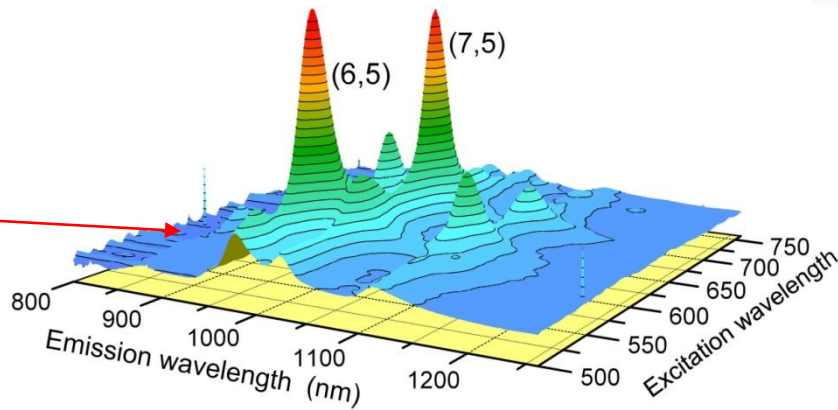
Chiral angle maps for samples and diameter distributions produced with 0 ppm NH₃ (blue) and 500 ppm NH₃ (red).



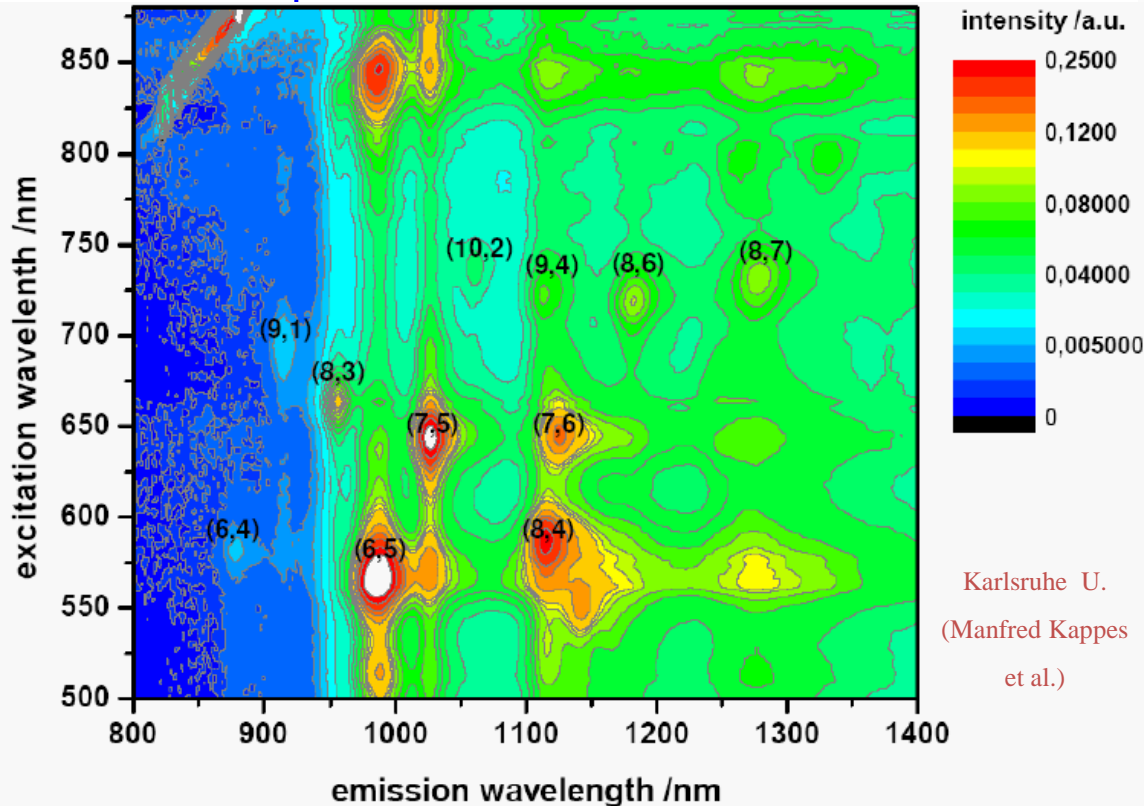
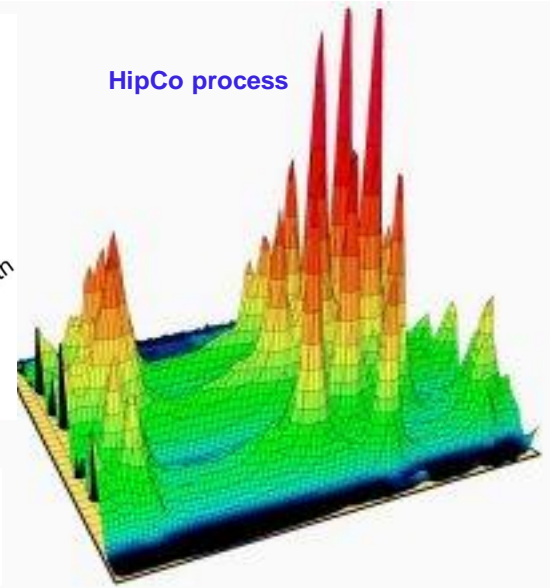
SWCNTs with NH₃ show the world narrowest chiral angle distribution



CoMoCat



HipCo process

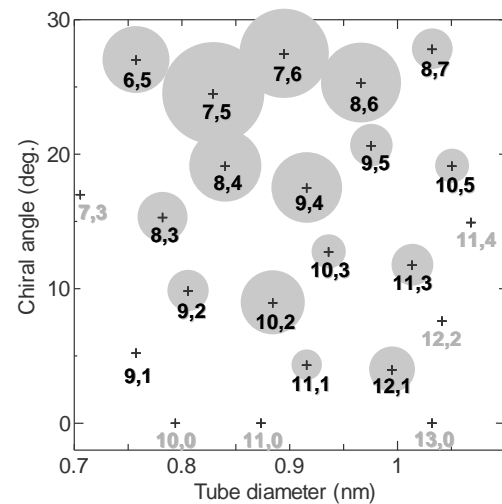
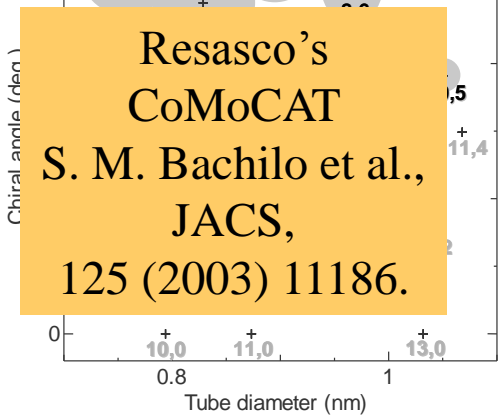
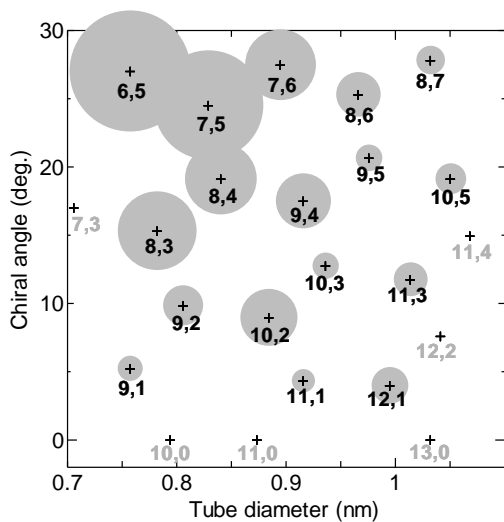
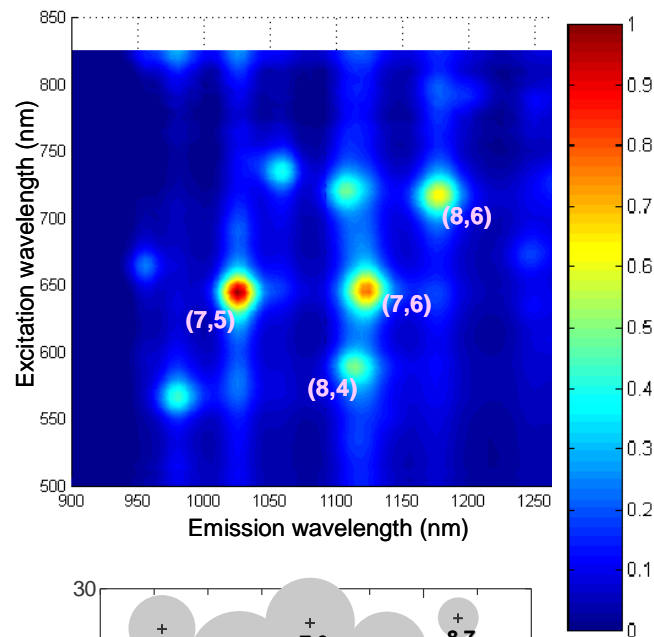
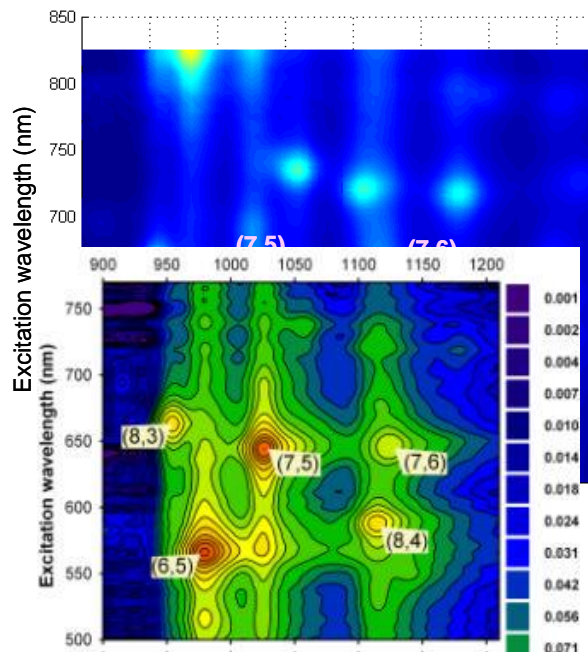
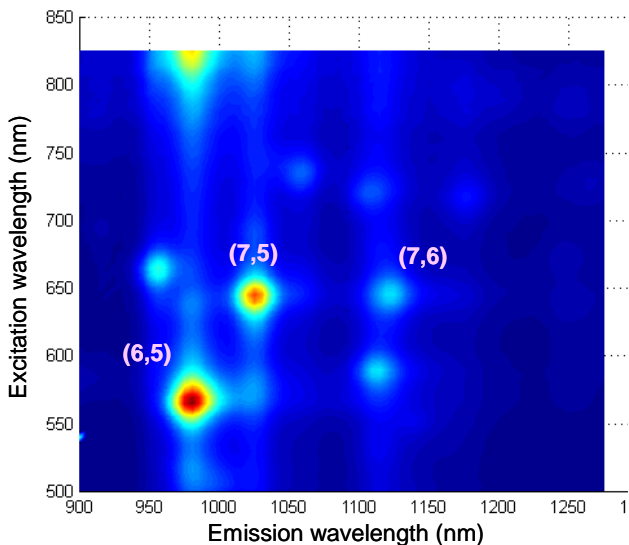


Comparison of (n,m)
Distribution of
CoMoCAT Vs. HIPCO PL
- Photo-luminescence
**SEMICONDUCTING
TYBES ONLY**

Courtesy –Prof. D. Resasco

ACCVD Chirality – PL -Semiconducting

Carbon source : Ethanol, CVD time : 10min
S. Maruyama et al.

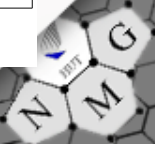


Resasco's
CoMoCAT
S. M. Bachilo et al.,
JACS,
125 (2003) 11186.

650°C

750°C

850°C



Carbon nanotubes are grown by chemical vapor deposition (CVD) on highly doped Si substrates with a 200 nm oxide layer. Different CVD growth conditions were used, as described in Refs. [42–44]. A grid structure is prepared on top of the nanotubes by electron beam lithography, thermal evaporation of 3nm Cr and 110nm Au, and a lift-off process. The sample is cleaved so that the structure is on the cleaved edge of the substrate (Fig. 1a). There are two possible etching processes to obtain the free-standing structure (Fig. 1b)

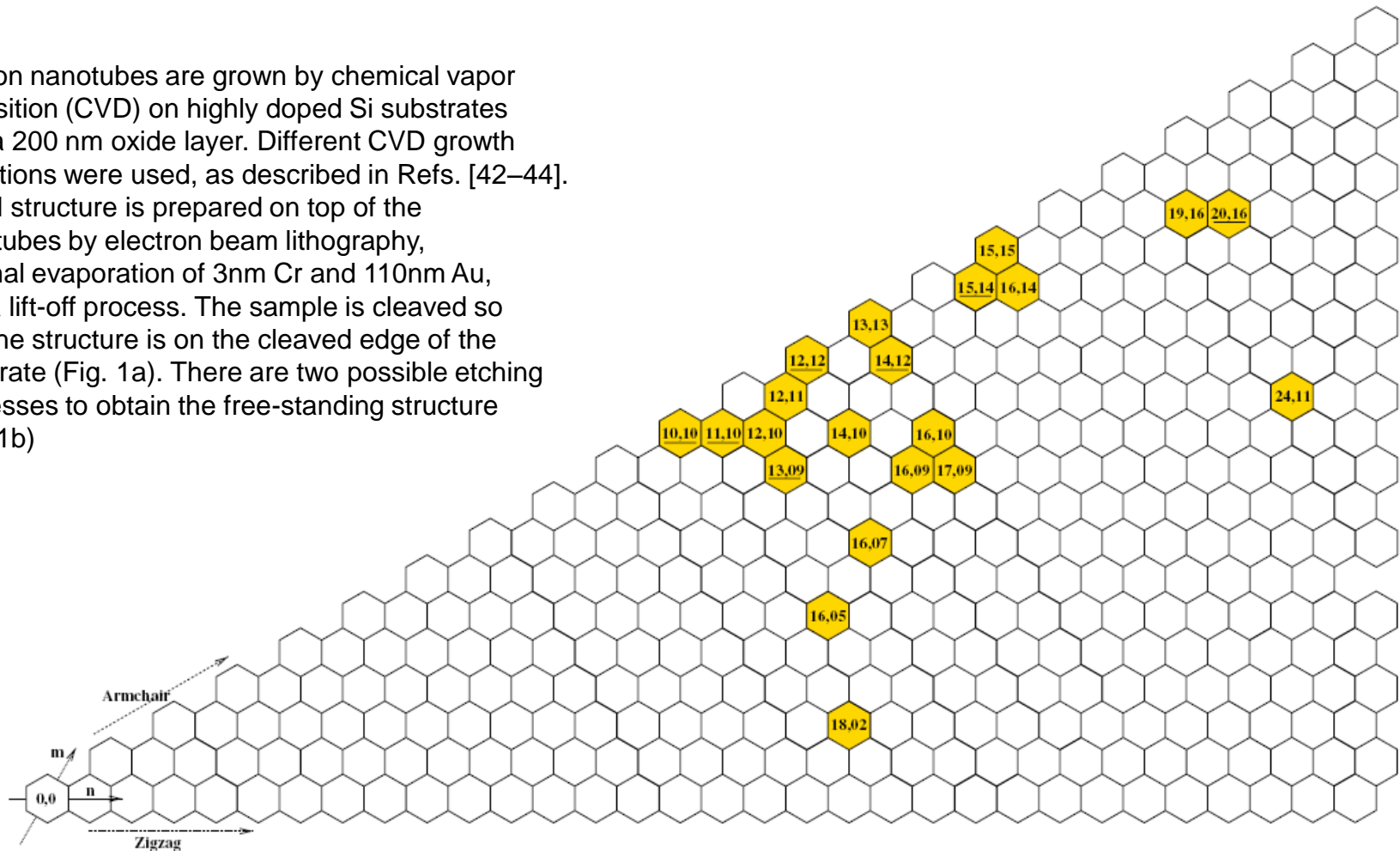
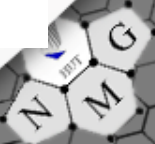
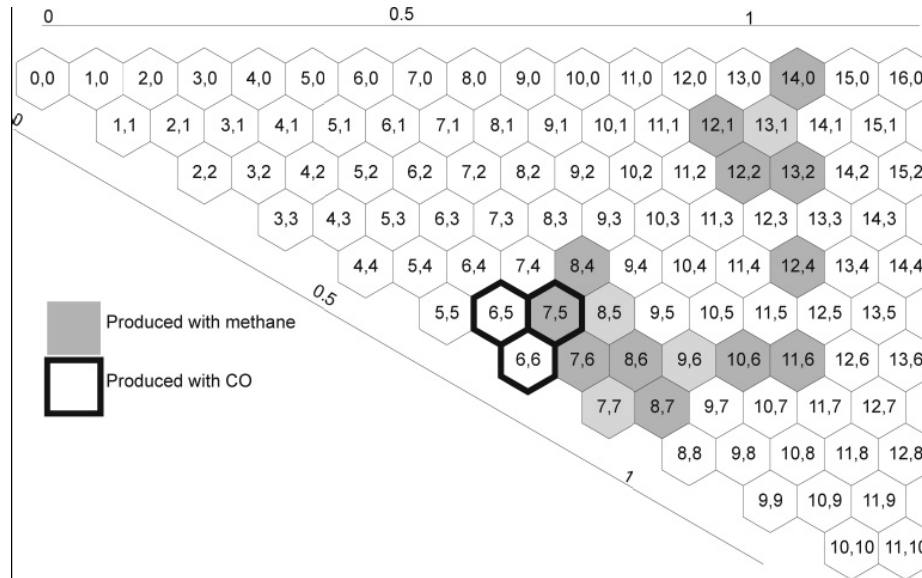


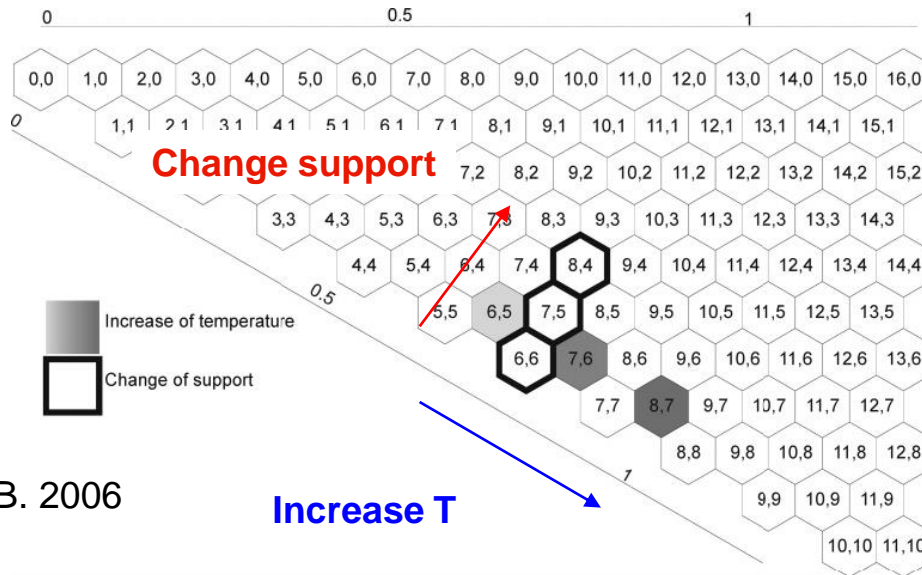
Fig. 9. Nanotube indices of 28 tubes grown in the same CVD process. The underlined indices were encountered twice. The rolling angle is not randomly distributed, but is close to the armchair direction (30°) in the majority of the nanotubes in this material.



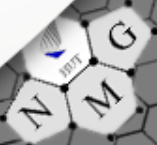
COMoCA: (n,m) map, effect of gas feed at 800 °C on the produced SWNT.



(n,m) map, effect of temperature and support morphology on the produced SWNT

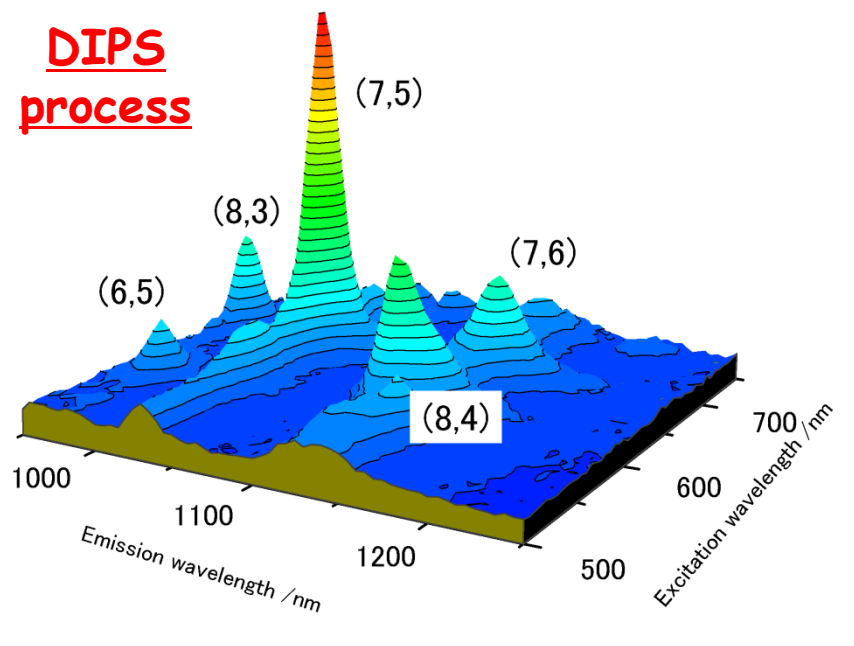


Lolli et al., Phys. Chem. B. 2006



Comparison of DIPS (FC-CVD) and CoMoCat (supported CVD) PL - Semiconducting fraction

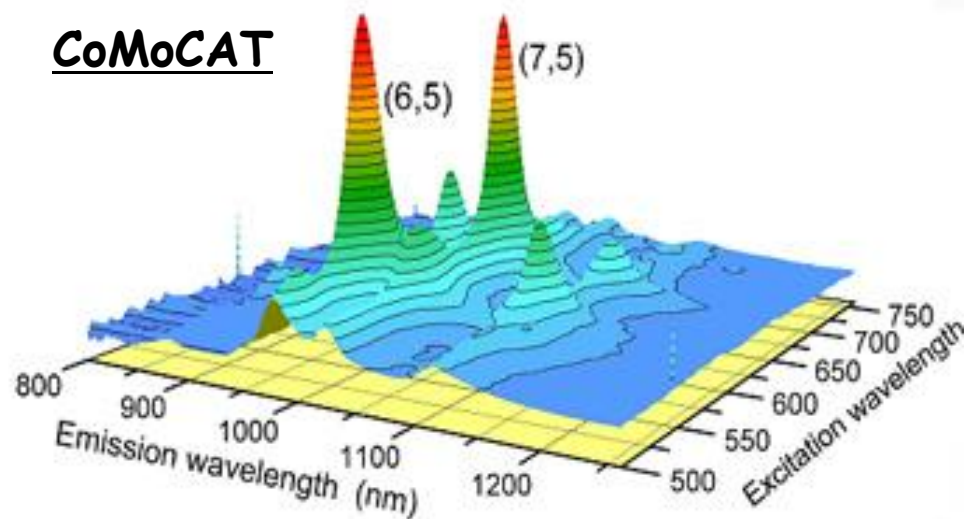
DIPS
process



**DIPS – bimetallic (Fe-Mo)
catalyst**

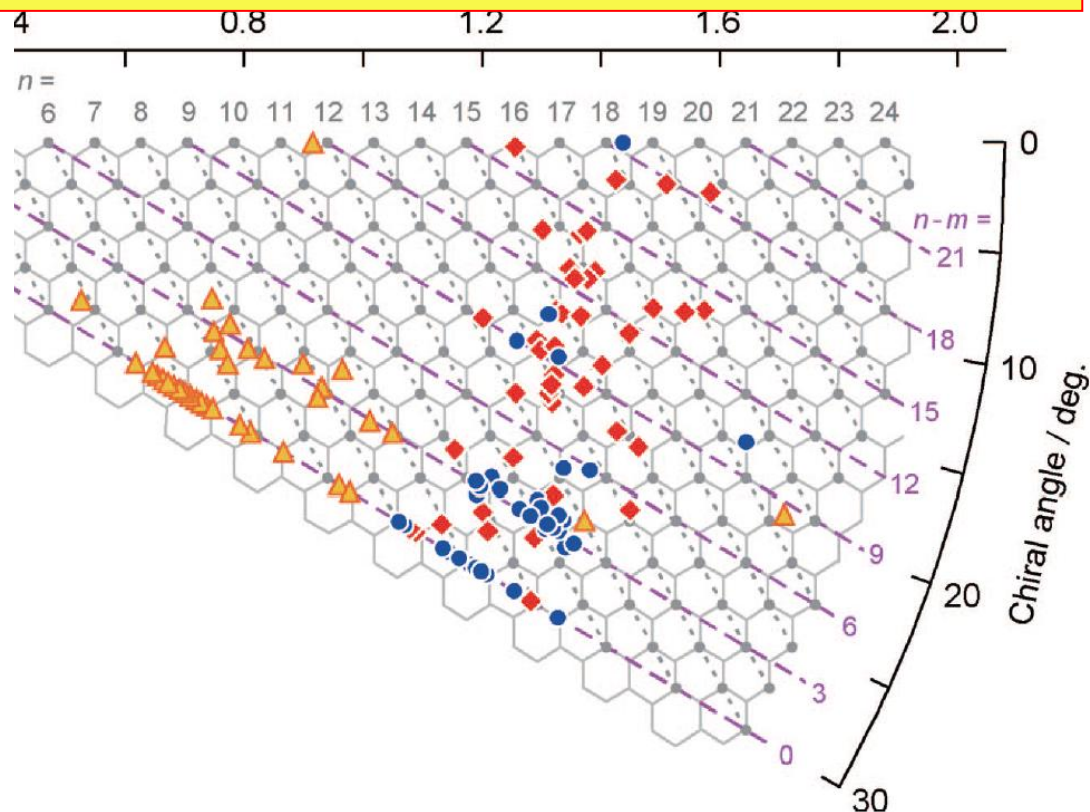
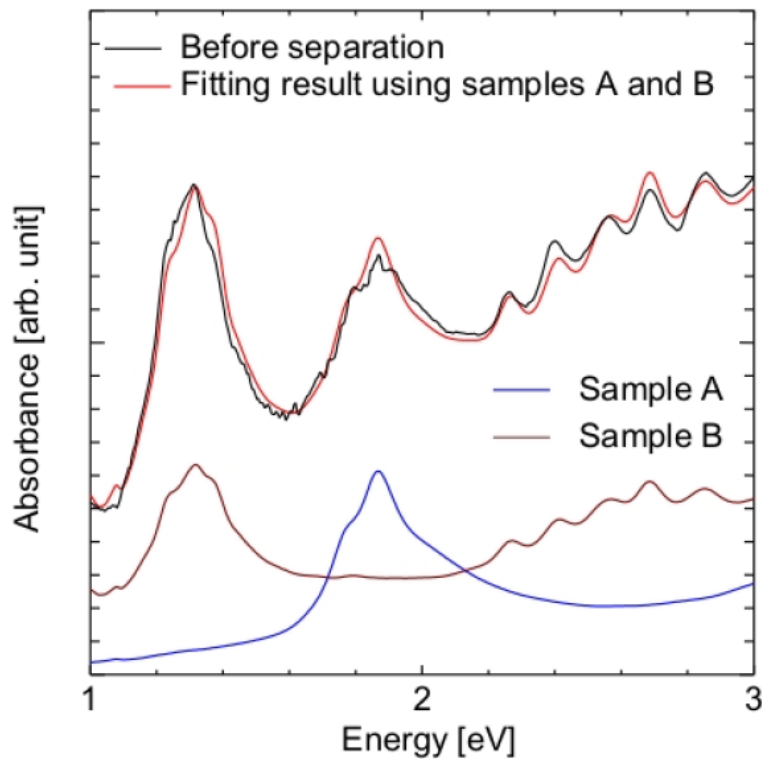
T. Saito, S. Iijima et al.

CoMoCAT



Spectrofluorimetric analysis (courtesy Prof. Weisman) of SWeNT™ (Left) and HiPCO™ (Right) samples. The comparison reflects the much narrower distribution of diameter and chirality

Comparison study of Optical Absorption (OA) to TEM/ED – chirality separated samples - *Optical absorption gives narrower chiral distribution*



Samples based on OA

A (blue circles) – metallic LV tubes

B (red diamonds) – semicond. LV tubes

C (yellow triangles) – metallic CoMoCAT tubes

Yuta Sato, Kazuhiro Yanagi, Yasumitsu Miyata,
Kazu Suenaga, Hiromichi Kataura and Sumio Iijima (2008)
NanoLetters 8, 3151-3154.

Table 1. Summary of TEM Observation for Separated SWNT Samples

sample	number of observed SWNTs			average d (nm)	average α (deg)
	total	metallic	semiconducting		
A	45 (41) ^a	36	5	1.42	25.3
B	44 (42) ^a	11	31	1.40	15.6
C	41 (38) ^a	28	10	0.87	26.3

^a Number of SWNTs whose chiral indices (n, m) were uniquely determined.

CoMoCat – comparison of TEM/ED and Resonance Raman

JORIO *et al.* Resonance Raman
 PHYSICAL REVIEW B 72, 075207 (2005)

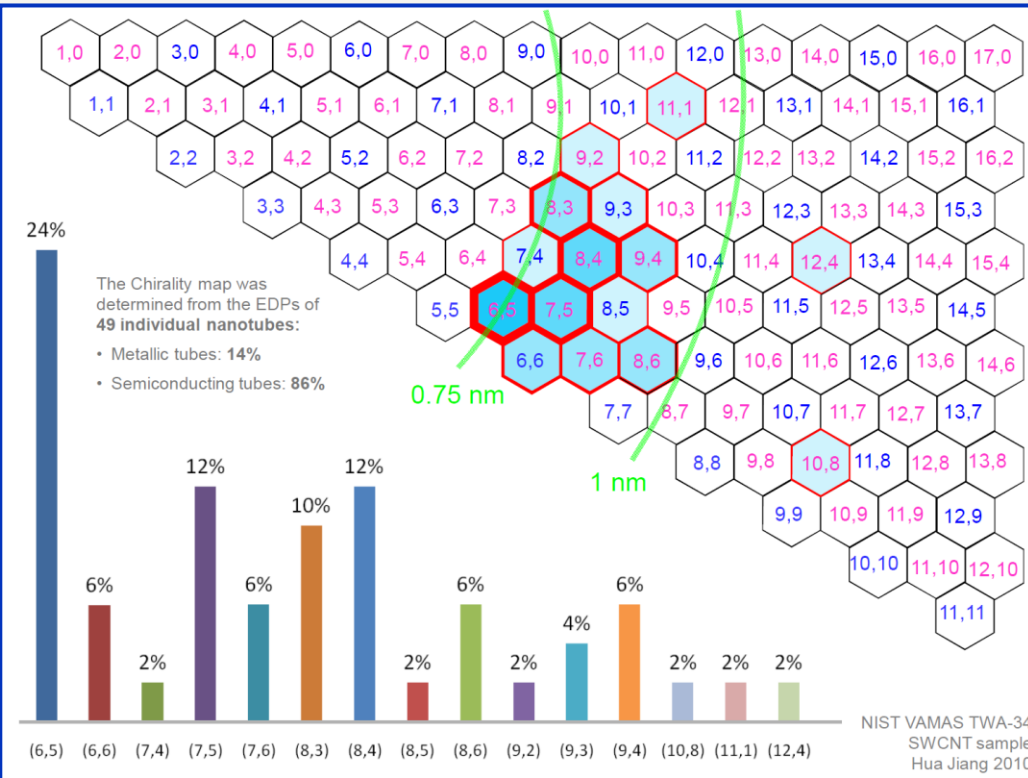


TABLE I. The (n,m) , $2n+m$ family number, diameter $d_t = 0.142\sqrt{n^2+m^2+nm}\sqrt{3}/\pi$ (nm), chiral angle θ (deg), E_{ii} (eV) (Ref. 7), ω_{RBM} (cm^{-1}), measured RBM intensity $I_{\text{RBM}}^{\text{EXP}}$ (normalized), calculated intensity $I_{\text{RBM}}^{\text{CALC}}$ (arb. unit) (Ref. 16, 17), and population $P = I_{\text{RBM}}^{\text{EXP}}/I_{\text{RBM}}^{\text{CALC}}$ (normalized), for semiconducting and metallic Co-MoCAT SWNTs in solution. The results are obtained by fitting all the spectra with a sum of Lorentzians. The $I_{\text{RBM}}^{\text{EXP}}$ and P values are normalized to give 100 to the largest values.

(n,m)	$2n+m$	d_t	θ	E_{22}^S	ω_{RBM}	$I_{\text{RBM}}^{\text{EXP}}$	$I_{\text{RBM}}^{\text{CALC}}$	P
(6,4)	16	0.68	23.4	2.11	337	21.9	0.94	7.9
(6,5)	17	0.75	27.0	2.18	309	42.5	0.14	100.0
(7,5)	19	0.82	24.5	1.92	284	85.7	0.57	51.2
(7,6)	20	0.88	27.5	1.92	266	7.0	0.08	28.9
(8,3)	19	0.77	15.3	1.86	299	100.0	1.32	25.7
(9,2)	20	0.79	9.8	2.24	291	4.3	0.34	4.2
(10,3)	23	0.92	12.7	1.95	254	6.0	0.22	9.4
(11,1)	23	0.90	4.3	2.03	259	6.3	0.50	4.3

(n,m)	$2n+m$	d_t	θ	E_{11}^M	ω_{RBM}	$I_{\text{RBM}}^{\text{EXP}}$	$I_{\text{RBM}}^{\text{CALC}}$	P
(6,6)	18	0.81	30.0	2.69	288	5.65	2.83	0.7
(7,4)	18	0.75	21.1	2.61	308	31.75	1.93	5.6
(7,7)	21	0.95	30.0	2.43	250	4.32	1.74	0.8
(8,2)	18	0.72	10.9	2.43	318	10.86	2.99	1.2
(8,5)	21	0.89	22.4	2.43	265	9.68	1.24	2.6
(9,3)	21	0.85	13.9	2.35	274	12.98	2.19	2.0
(9,6)	24	1.02	23.4	2.24	233	1.14	0.84	0.5
(9,9)	27	1.22	30.0	2.03	198	0.41	0.77	0.2
(10,1)	21	0.82	4.7	2.27	280	21.62	2.76	2.6
(10,4)	24	0.98	16.1	2.22	242	2.79	1.54	0.6
(10,7)	27	1.19	24.2	2.07	204	0.41	0.60	0.2
(11,2)	24	0.95	8.2	2.19	245	8.54	2.13	1.4
(11,5)	27	1.11	17.8	2.06	215	0.57	1.10	0.2
(12,0)	24	0.94	0	2.16	247	3.43	2.36	0.5
(12,3)	27	1.08	10.9	2.04	220	0.92	1.62	0.2
(13,1)	27	1.06	3.7	2.02	224	1.08	1.93	0.2
(14,2)	30	1.18	6.6	1.92	202	3.43	1.54	0.8

TEM/ED: Jiang et al. unpublished

CoMoCat – comparison of TEM/ED and PL

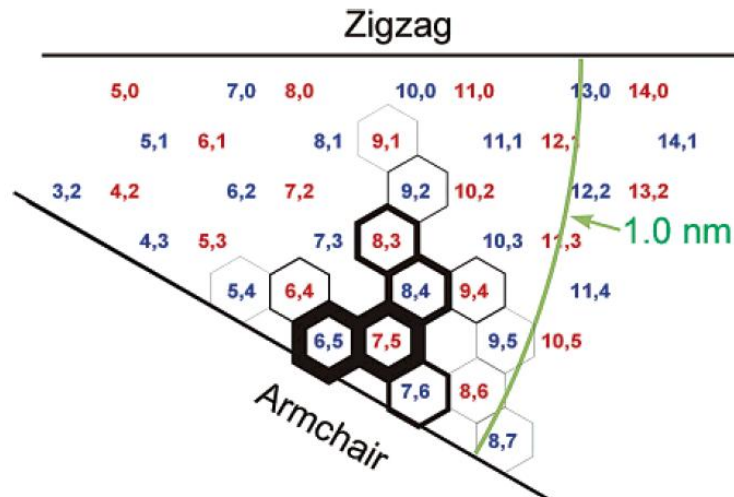
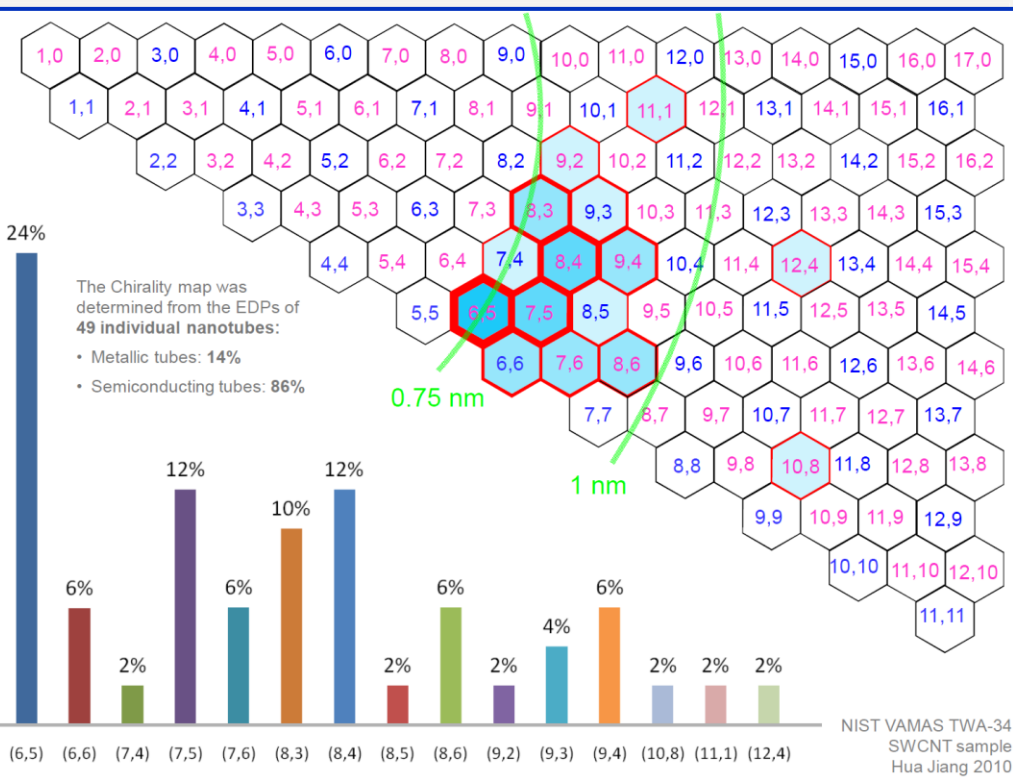
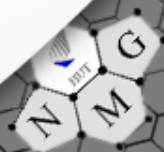


Table 1. (n,m)-Resolved Spectral Intensities from SWNT Samples

n,m	diameter (nm)	chiral angle (deg)	fractional intensity (%), CoMoCAT	fractional intensity (%), HiPco
5,4	0.620	26.3	0.3	0.0
6,4	0.692	23.4	2.8	0.3
9,1	0.757	5.2	0.8	0.2
6,5	0.757	27.0	28	3.7
8,3	0.782	15.3	11	2.9
9,2	0.806	9.8	1.7	0.4
7,5	0.829	24.5	28	4.9
8,4	0.840	19.1	14	4.2
10,2	0.884	9.0	0.0	4.5
7,6	0.895	27.5	8.5	7.1
9,4	0.916	17.5	2.3	7.6
10,3	0.936	12.7	0.0	4.3
8,6	0.966	25.3	0.8	8.3
9,5	0.976	20.6	0.3	5.7
9,5	0.976	20.6	0.0	5.7
12,1	0.995	4.0	0.0	3.8
11,3	1.014	11.7	0.0	4.6
8,7	1.032	27.8	0.3	5.6
10,5	1.050	19.1	0.0	4.6

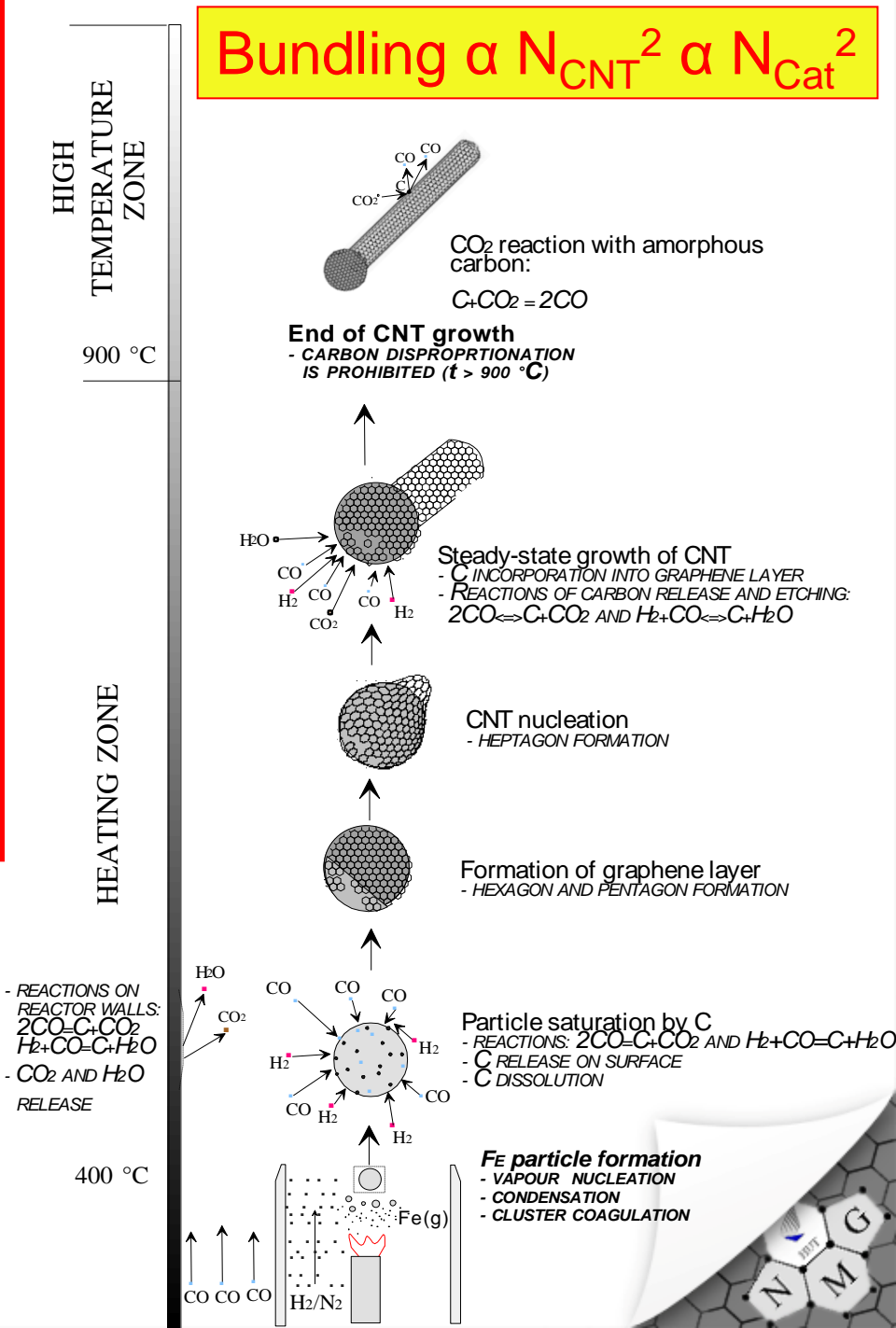
TEM/ED: Jiang et al. unpublished

Sergei M. Bachilo, Leandro Balzano, Jose E. Herrera, Francisco Pompeo, Daniel E. Resasco and R. Bruce Weisman
J. AM. CHEM. SOC. 2003, 125, 11186-11187.

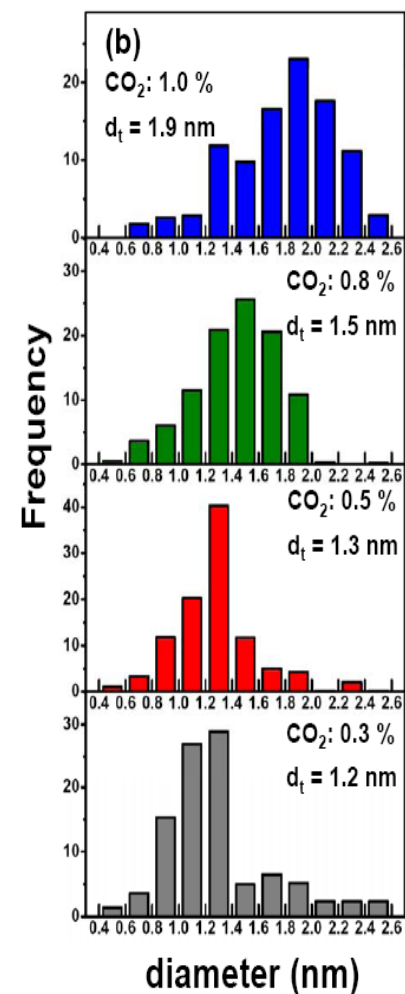
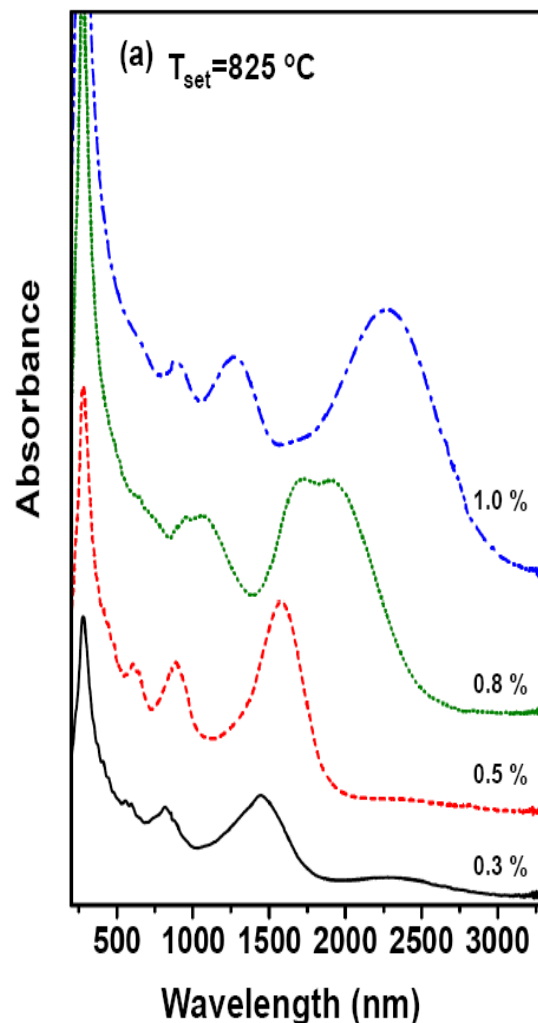
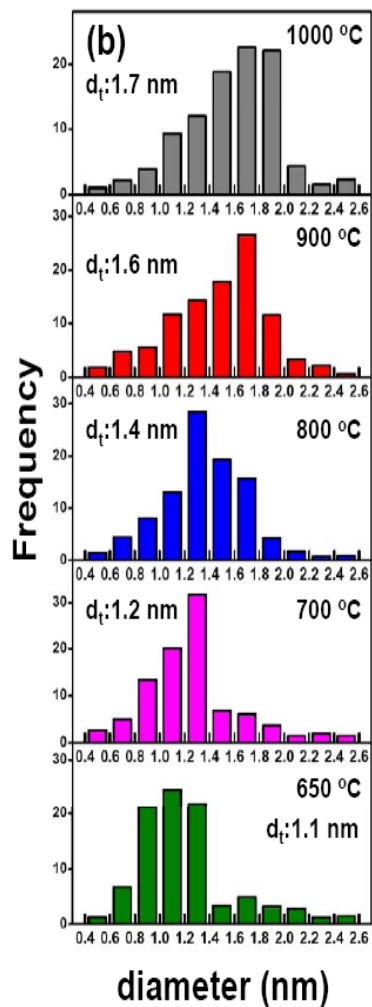
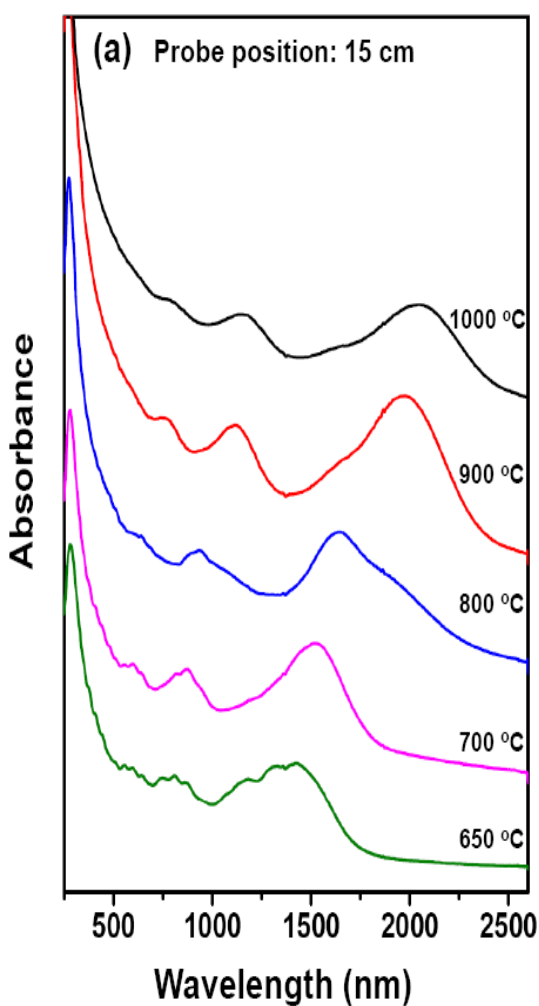


Schematic presentation of mechanism of CNT formation – the role of oxidation

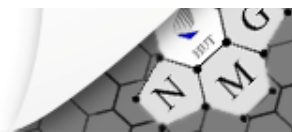
A. G. Nasibulin, D. P. Brown, P. Queipo, D. Gonzalez, H. Jiang, E. I. Kauppinen (2005) An essential role of CO_2 and H_2O during single-walled CNT synthesis from carbon monoxide. *Chemical Physics Letters* **417**, 179-184



Optical absorption derived SWCNT diameter distributions vs. wall temperature with probe at 15 cm and vs. CO₂ concentration with probe at 6.5 cm



Ying et al. (2011) Carbon





Chirality-dependent reactivity of individual single-walled carbon nanotubes (submitted)

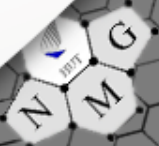
Bilu Liu^{1,2}, Hua Jiang¹, Arkady V. Krasheninnikov^{1,3},
Albert G. Nasibulin¹, Wencai Ren², Chang Liu²,
Esko I. Kauppinen^{1*}, Hui-Ming Cheng^{2*}

1. Department of Physics, Aalto University, Finland
2. Institute of Metal Research, Chinese Academy of Sciences, China
3. Department of Physics, University of Helsinki, Finland



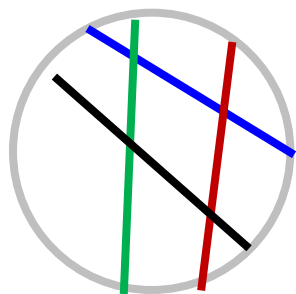
Background & Motivations

- It has been shown that a suitable chemical process is good for chirality selectivity or separation. But Why and How?
- To investigate this issue, many early efforts have been made based on optical analysis of CNT bundles or CNTs with support.
- In this study, we present our study of the chirality-dependent intrinsic chemical reactivity of free-standing individual SWCNTs by means of electron diffraction in electron microscope.

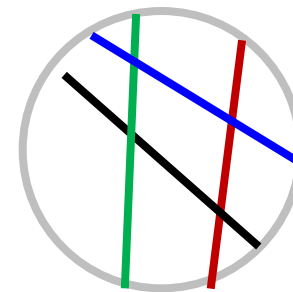


Experimental setup

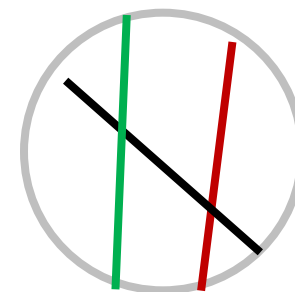
CNTs on
a TEM grid



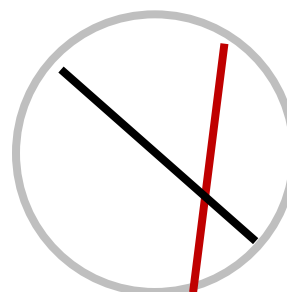
400°C
in air, 30min



450°C
in air



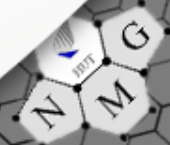
490°C
in air, 30 min



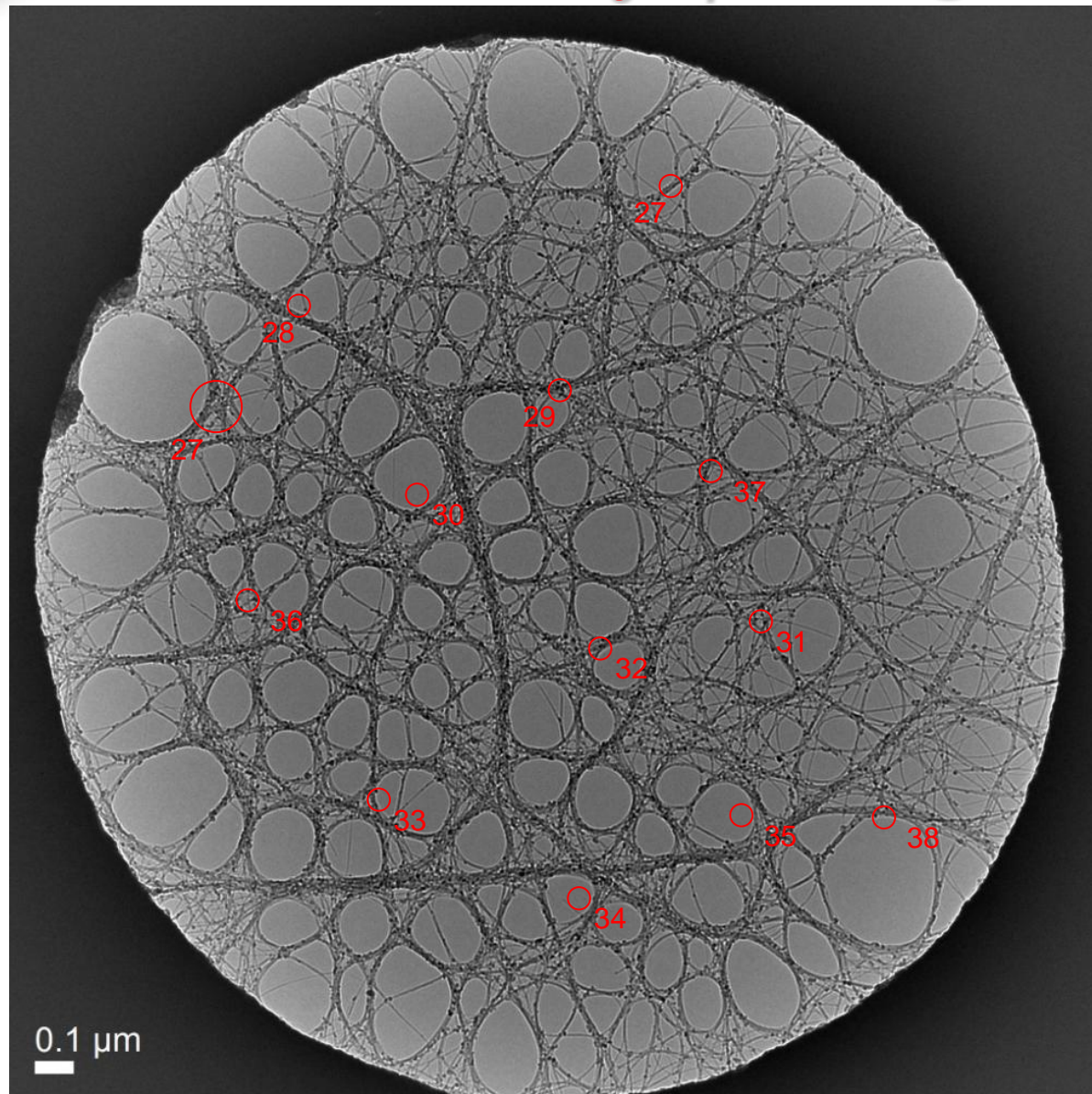
- HRTEM
- Election diffraction



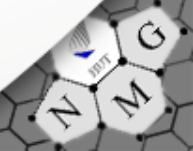
chirality-dependent reactivity



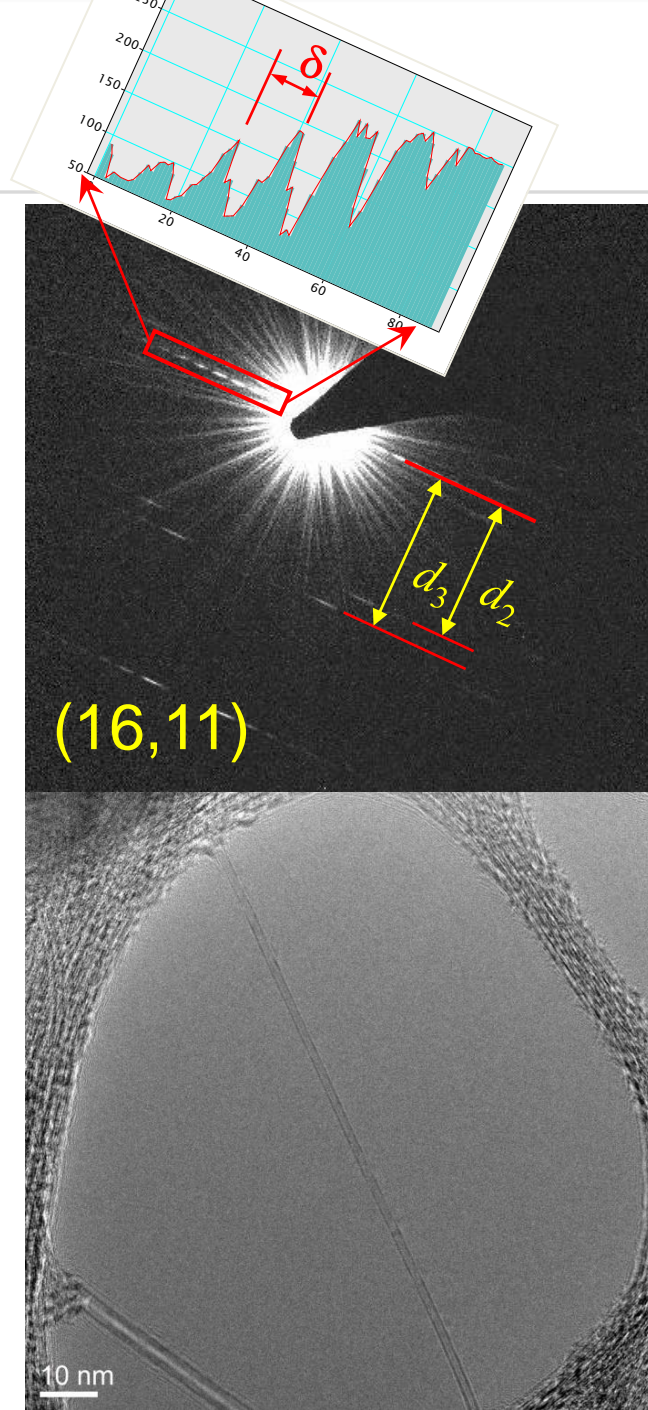
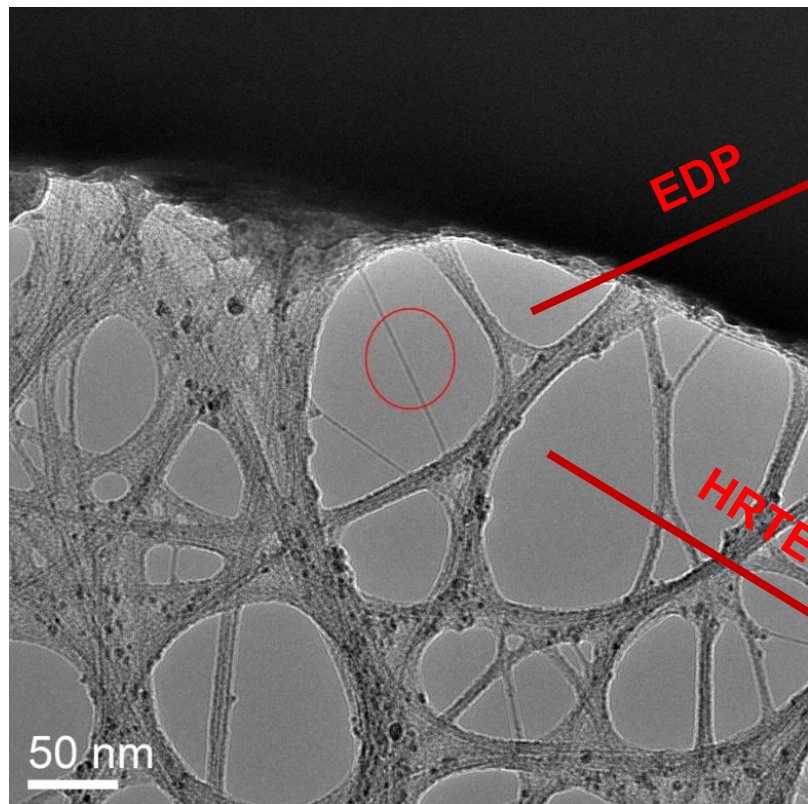
SWCNTs on a Si_3N_4 TEM grid



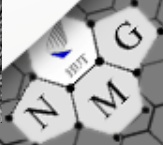
We are interested in individual tubes that can hardly be seen here!
They are usually **straight, clean, defect-free** and **well separated**.



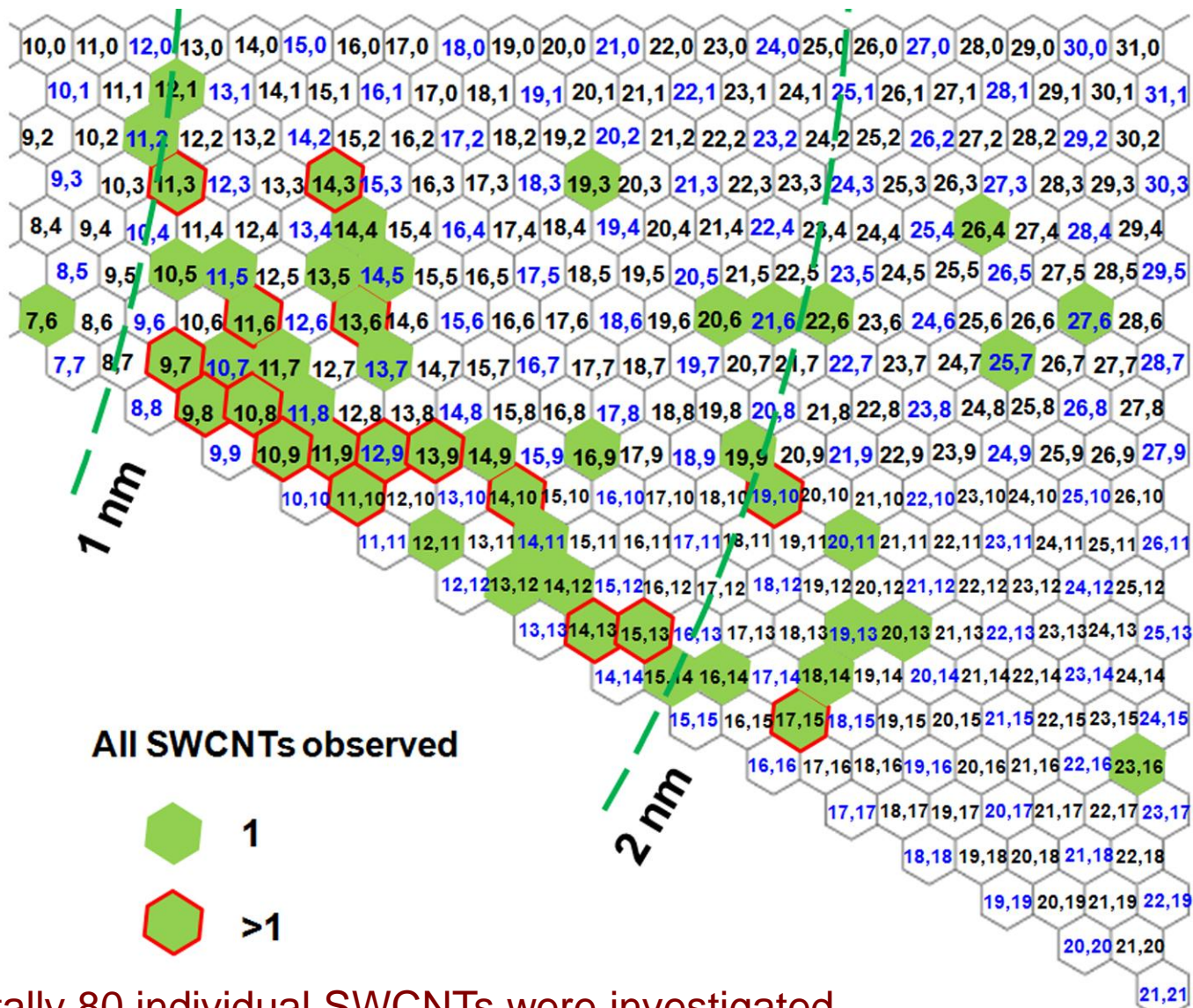
TEM characterization



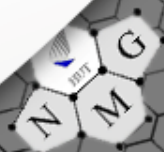
H Jiang et al, CARBON 45 (2007), 662



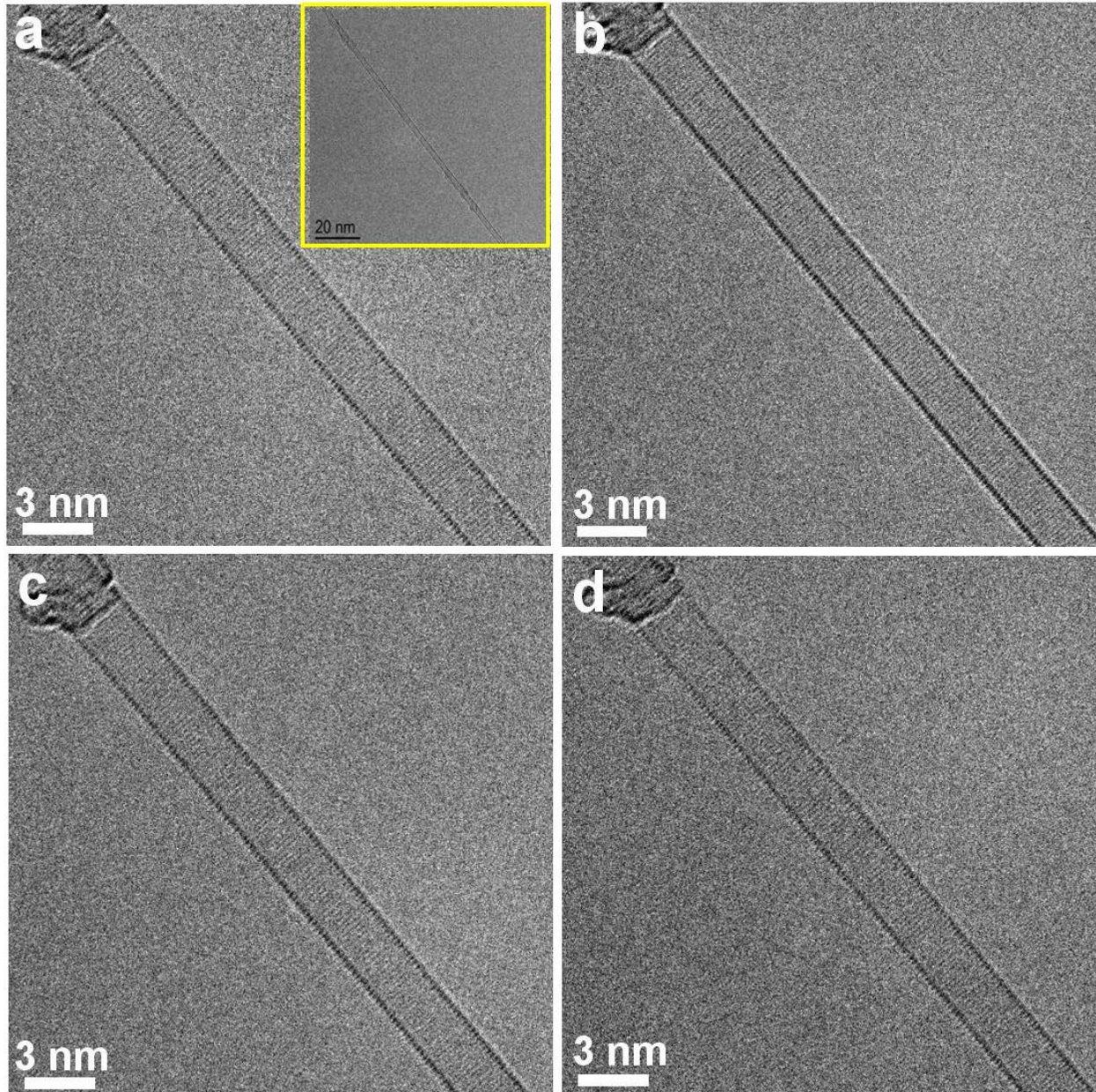
A chirality map of all SWCNTs under investigation



Totally 80 individual SWCNTs were investigated.



No defect is generated in CNTs by e-beam at 80 kV



e-beam irradiation time:

(a) 387s

(b) 526s

(c) 730s

(d) 960s

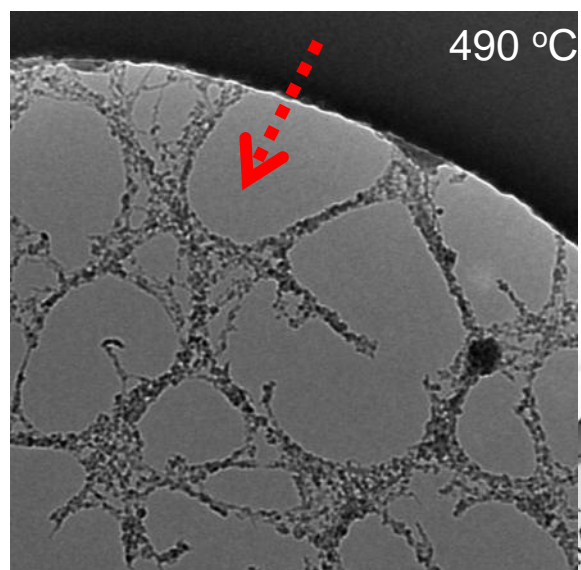
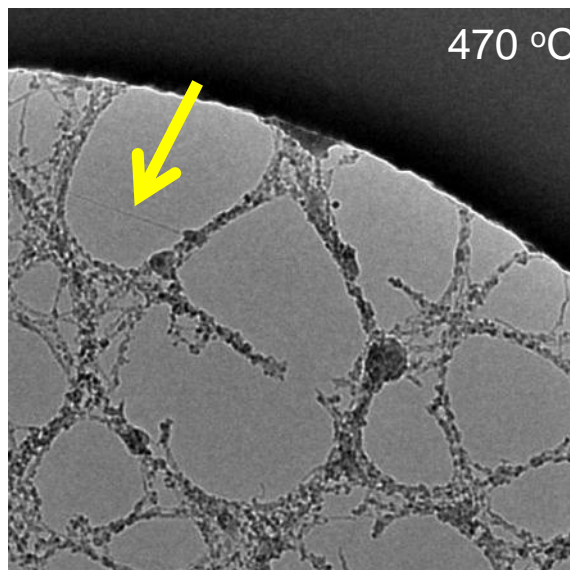
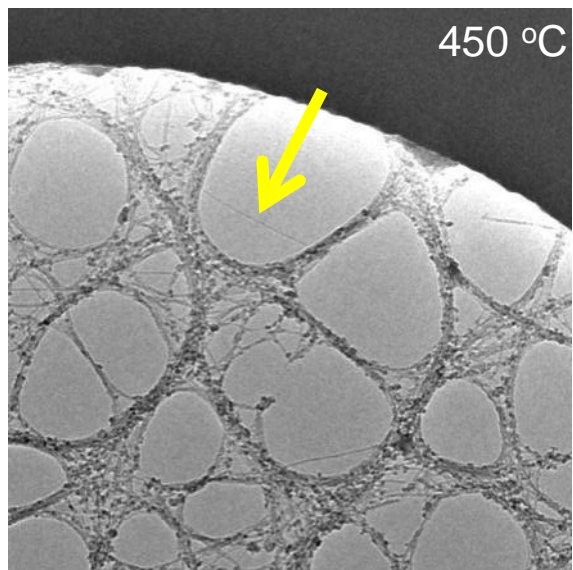
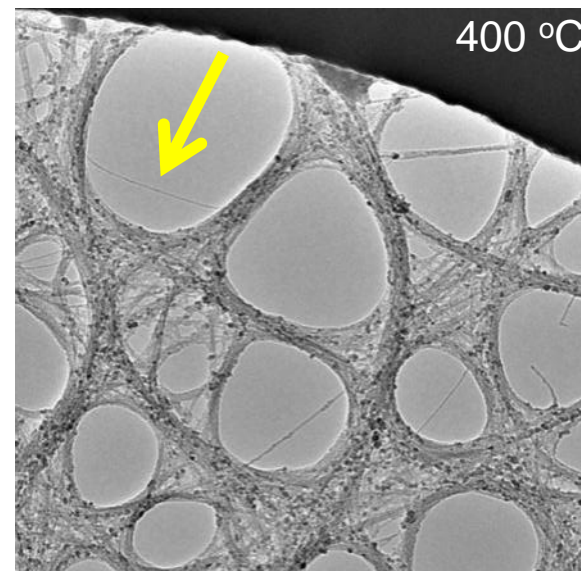
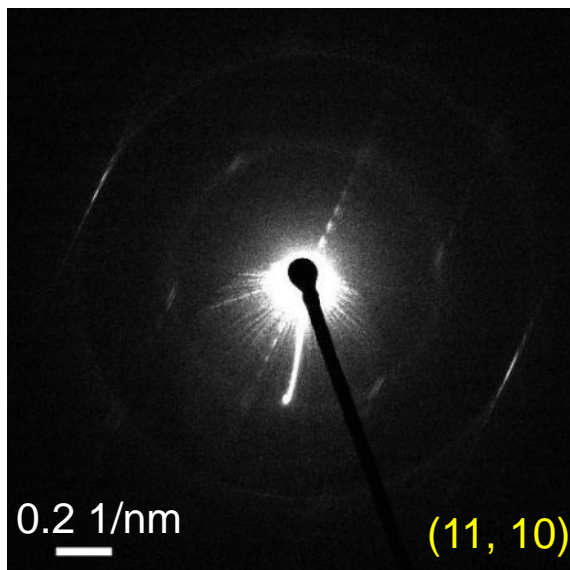
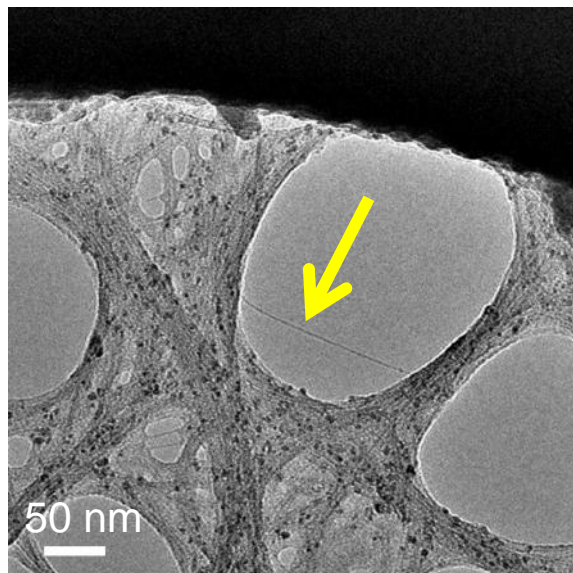
The typical exposure time for taking an electron diffraction pattern is 5s - 10s

So, CNTs are safe under electron beam irradiation!



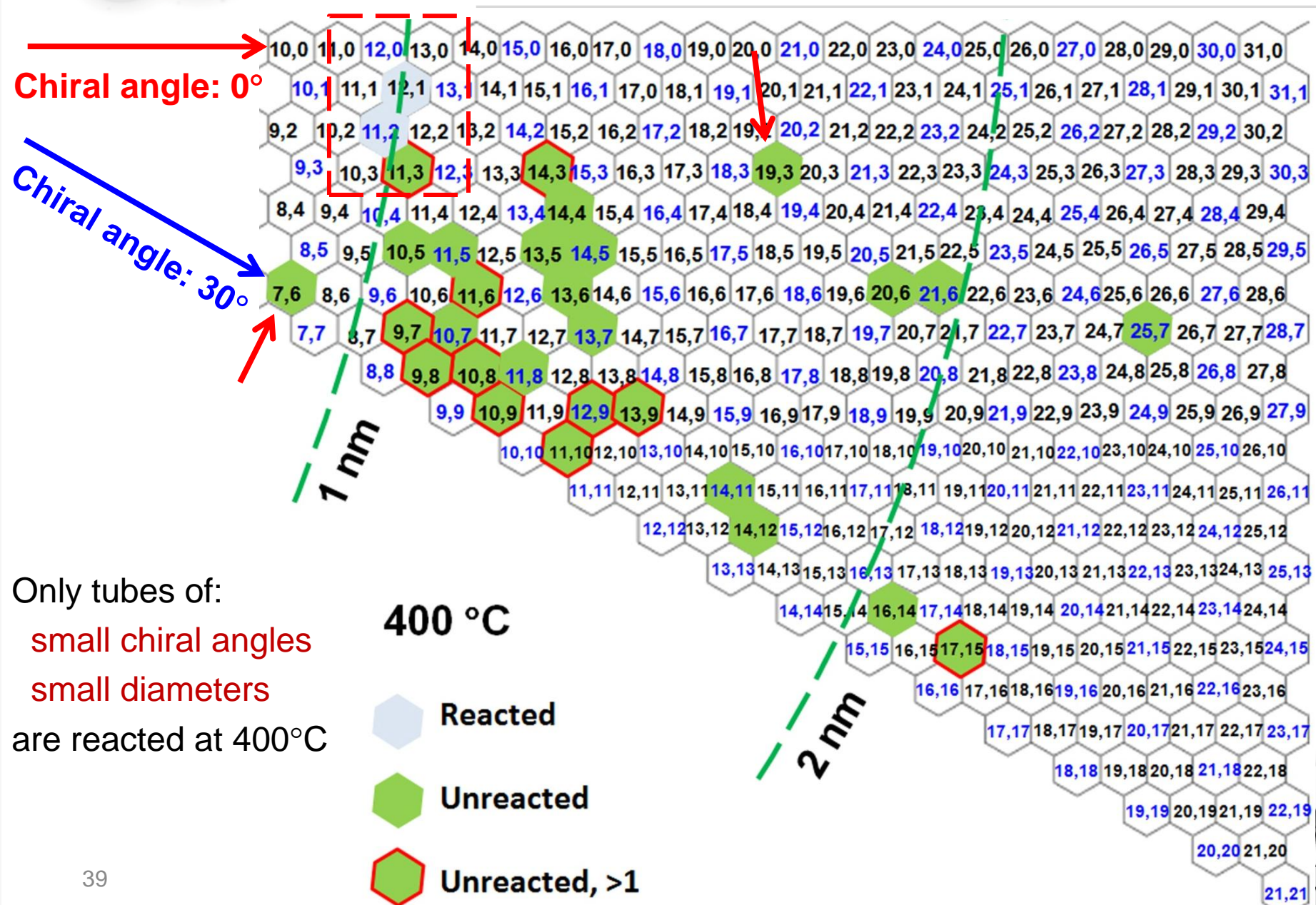
Evolution of a SWCNT under heat treatment in air

An example: a (11, 10) SWCNT was found reacted at 490 °C



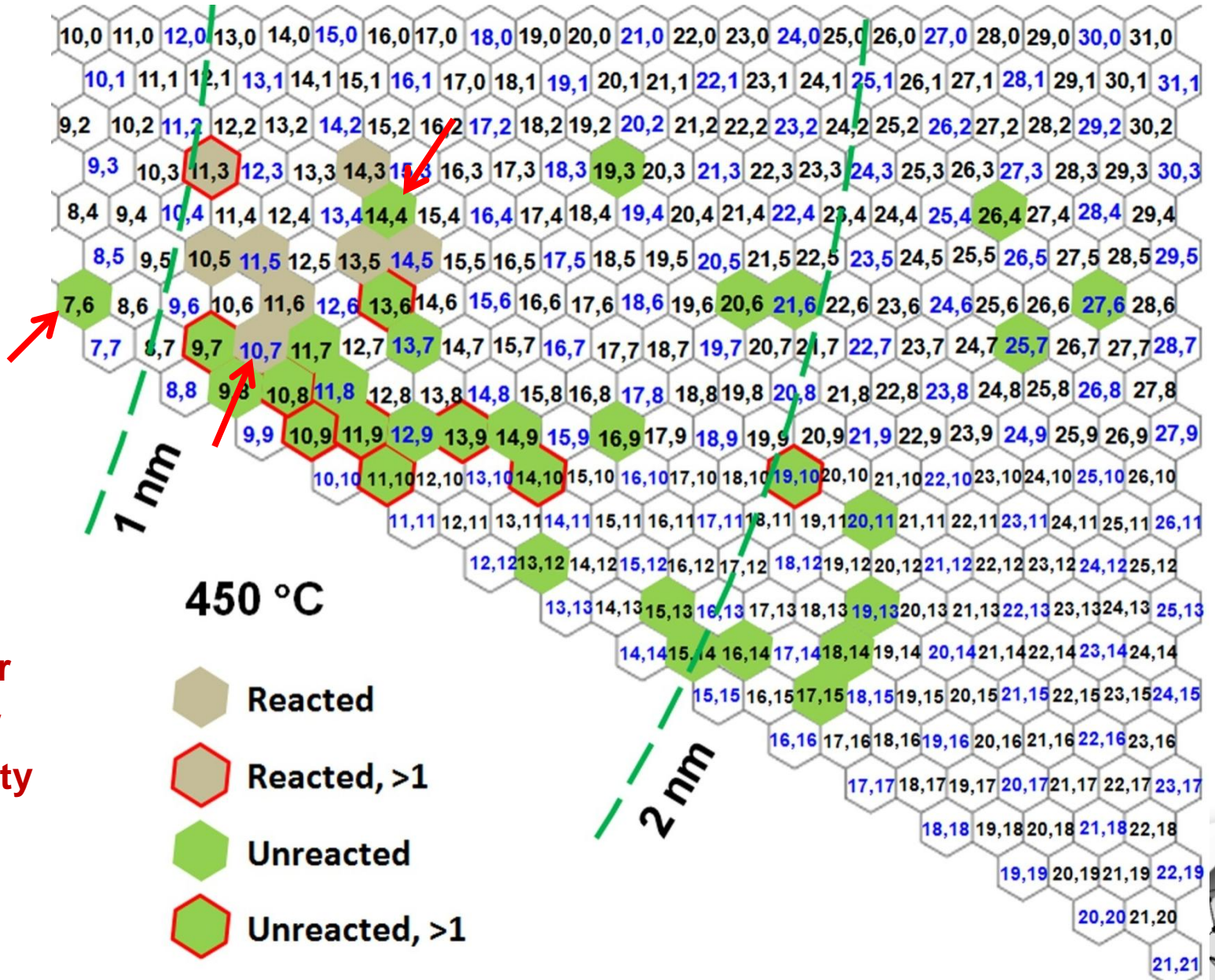
400 °C

Reaction status of CNTs at 400 °C



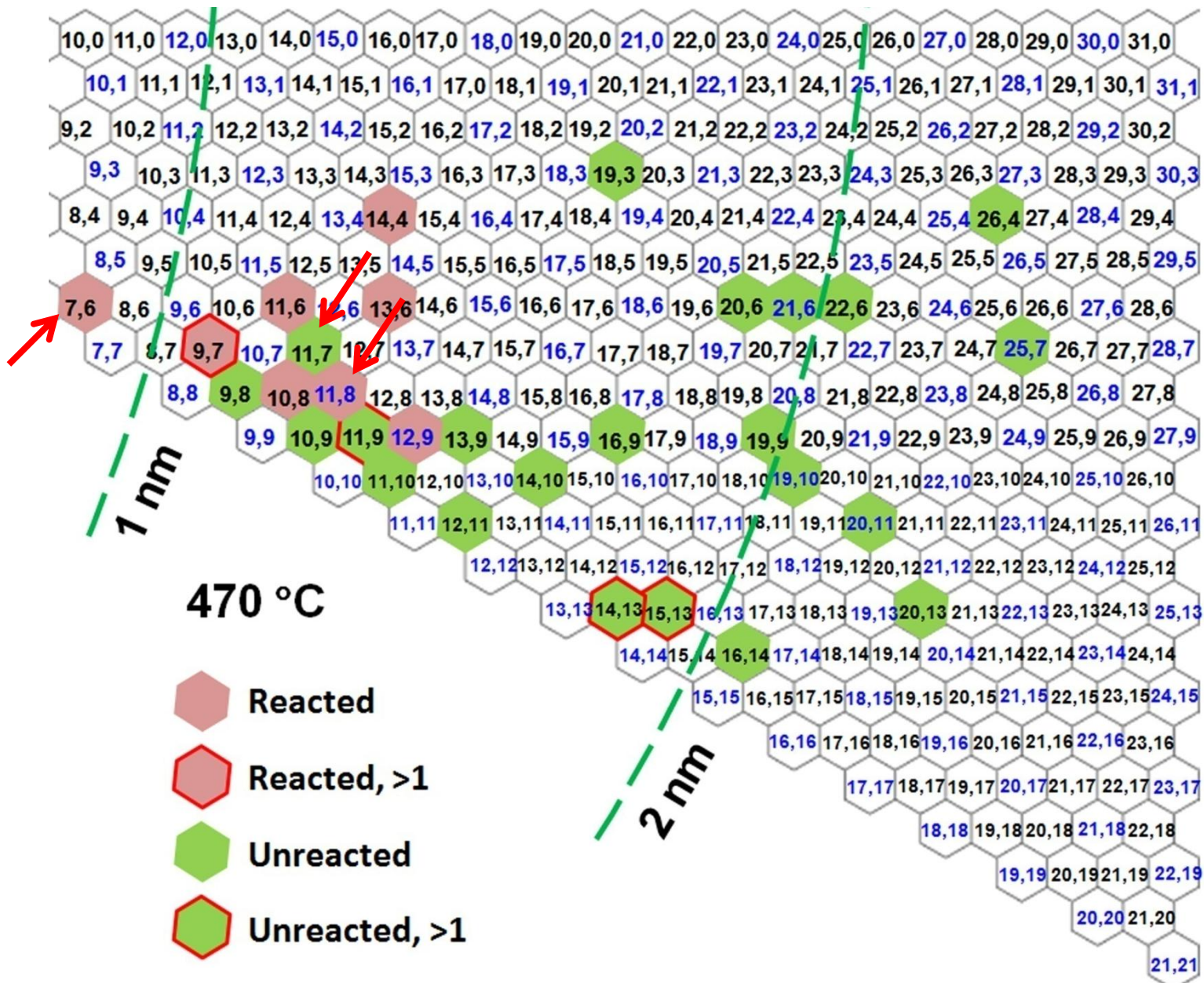
450 °C

Reaction status of CNTs at 450 °C



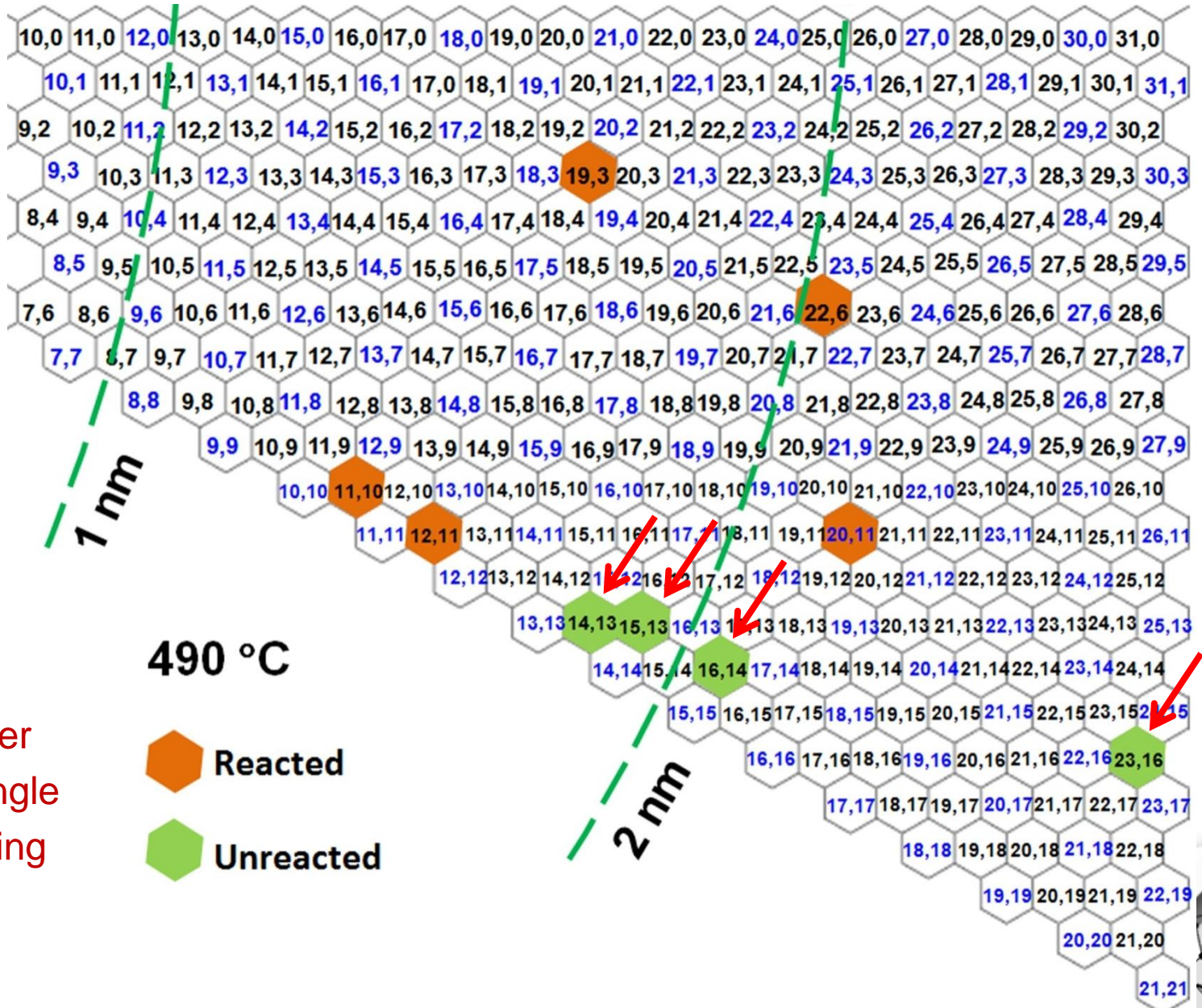
470 °C

Reaction status of CNTs at 470 °C



490 °C

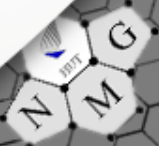
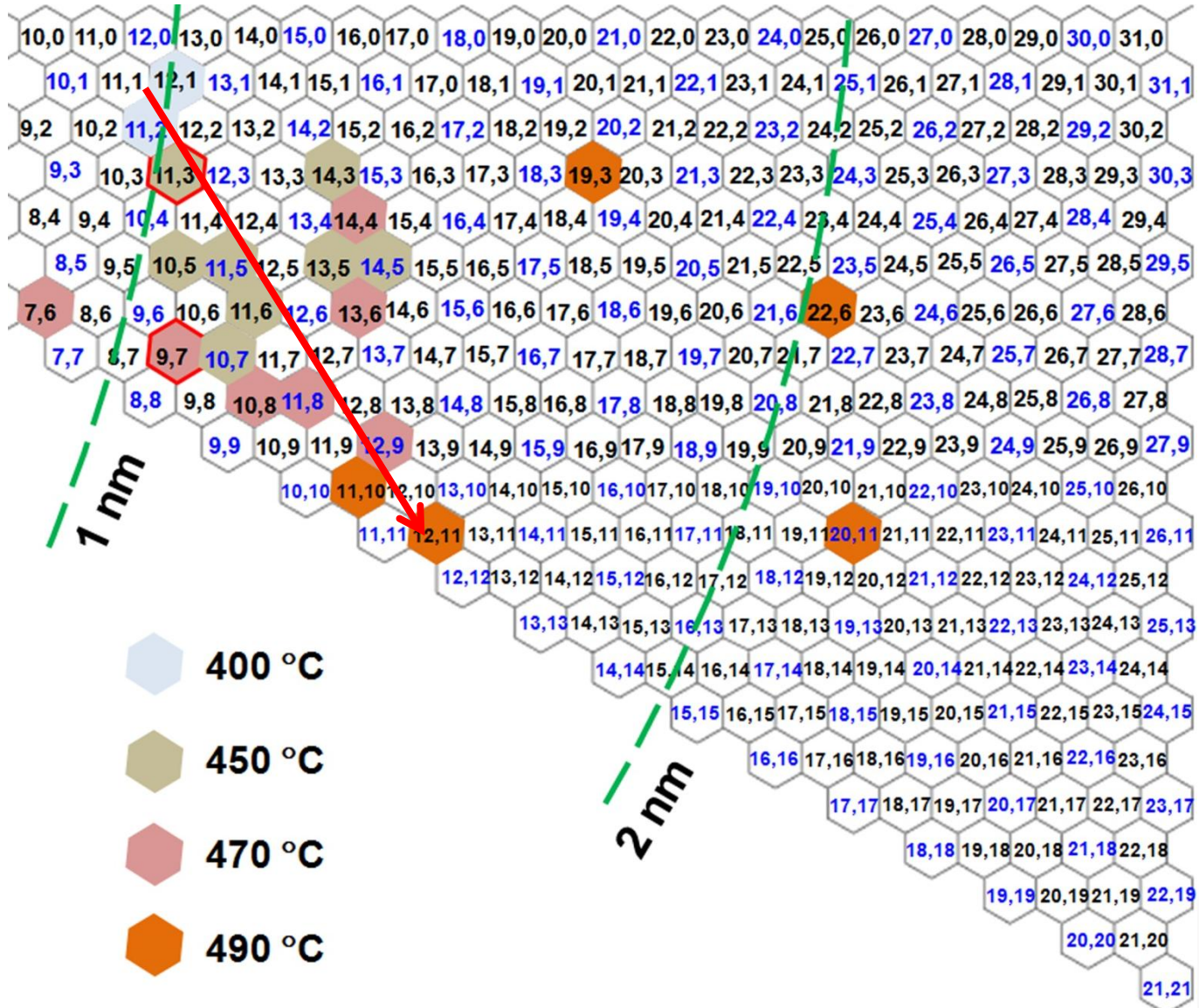
Reaction status of CNTs at 490 °C



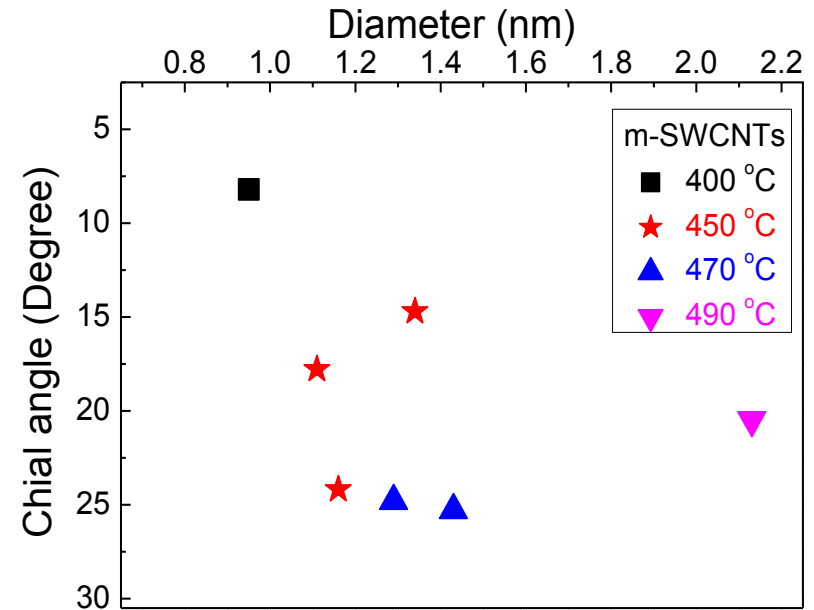
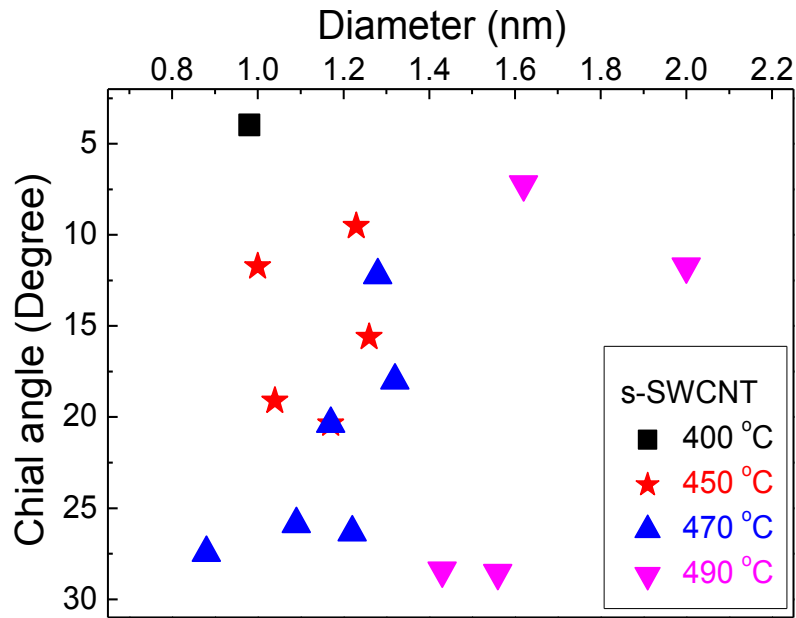
All remaining SWCNTs:

- Large diameter
- High chiral angle
- Semiconducting

Chirality-dependent reaction sequence of SWCNTs



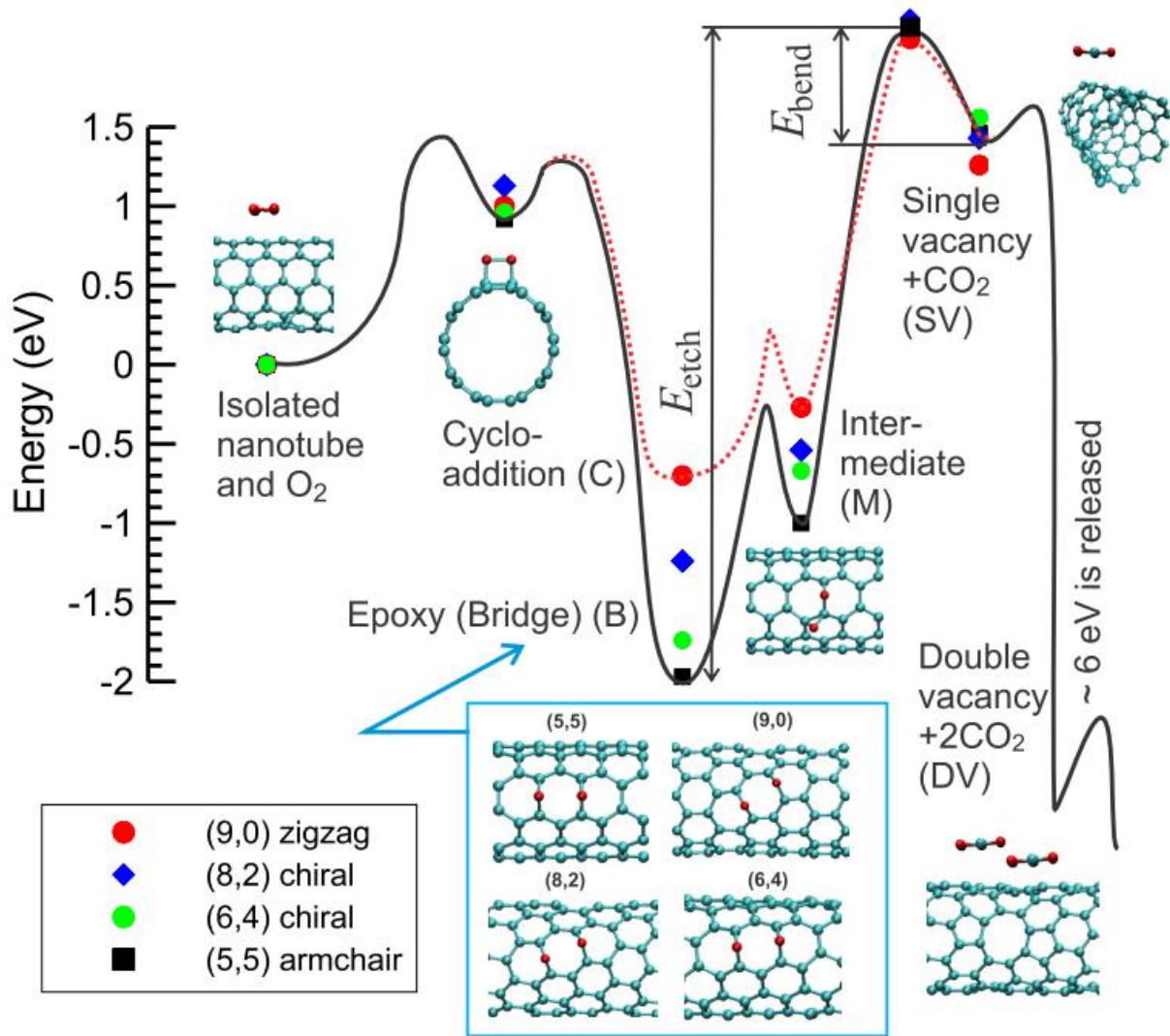
Chirality-dependent reaction sequence of SWCNTs



- ✓ Small diameter and small chiral angle SWCNTs more reactive
- ✓ m-SWCNTs more reactive
- ✓ Simple air treatment enrich larger diameter, high chiral angle s-SWCNT



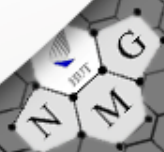
DFT calculations: Reactions with chirality-dependent potential barriers



The required vacancy formation energy is chirality-dependent:

- (9,0): 1.96eV
- (8,2): 2.67eV
- (6,4): 3.30eV
- (5,5): 3.43eV

The Energetics of forming the first vacancy



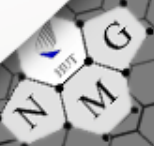
Conclusions

- We present a selective chemical reactivity of SWCNTs in an O₂ atmosphere which was found to be chirality dependent.
- It was demonstrated that the reactivity of SWCNTs to O₂ depends largely on their chiral structure and their conductivities as well. In general, SWCNTs with large diameters, high chiral angles, and of semiconducting properties are less reactive.
- DFT calculations indicated that the potential barriers for SWCNT oxidation is highly chirality dependent, thus quantitatively explains our experimental observations.
- Our results gain a new insight into the interplay between chemical reactivity of SWCNTs and their electronic structure, thus imply an application in modification of electronic structure and chirality separation of SWCNTs – **support the role of CO₂ during our FFCVD of SWCNTs**

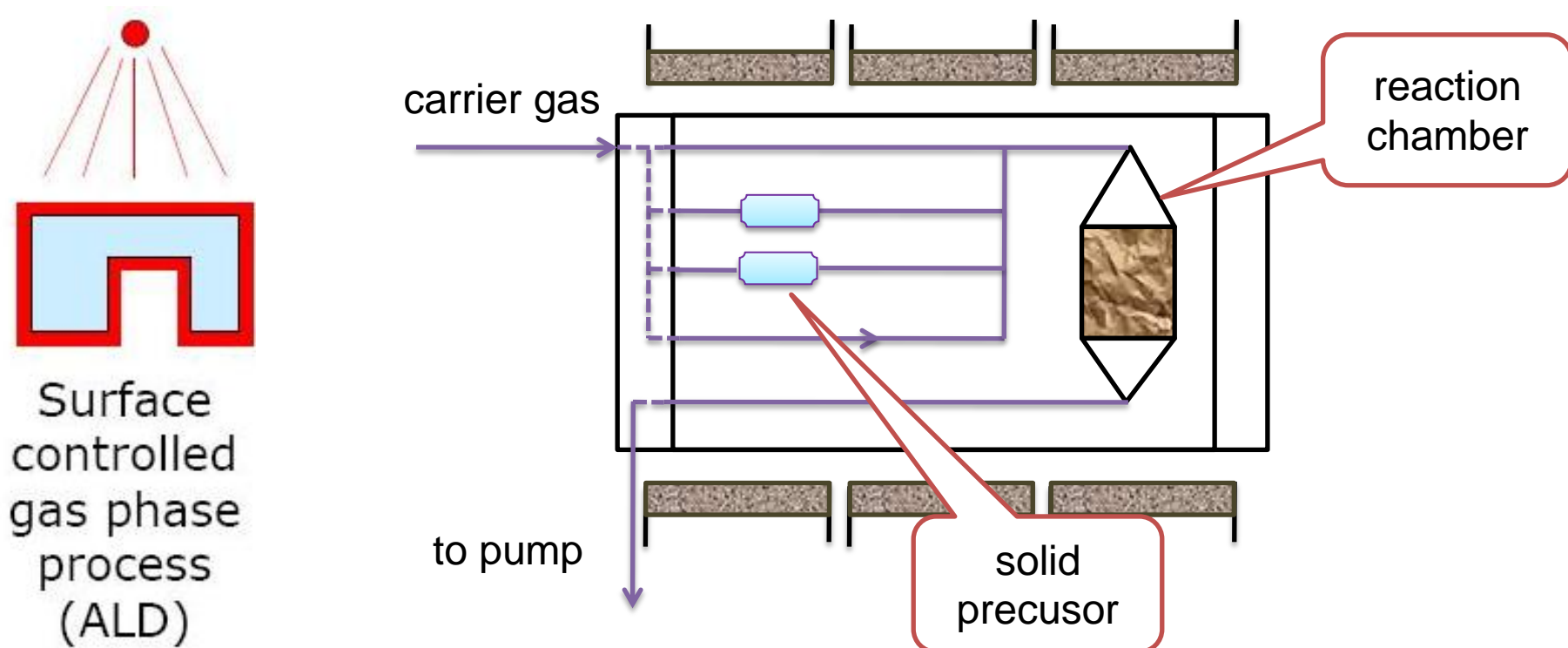


In-situ TEM growth - experimental Setups

- Growing SWNTs in an ETEM
- Catalyst preparation
 - FeCu-MgO: ALD prepared
 - Co-MgO I: ALD prepared
 - Co-MgO II: impregnation prepared



Preparation of catalysts by atomic layer deposition



Surface
controlled
gas phase
process
(ALD)

Precursors: $M(\text{acetylacetonate})_x$; $M = \text{Fe, Co, Ni, Cu}$. $X = 2$ or 3 .
Supports: or MgO .



I. Preparation of FeCu-MgO by ALD

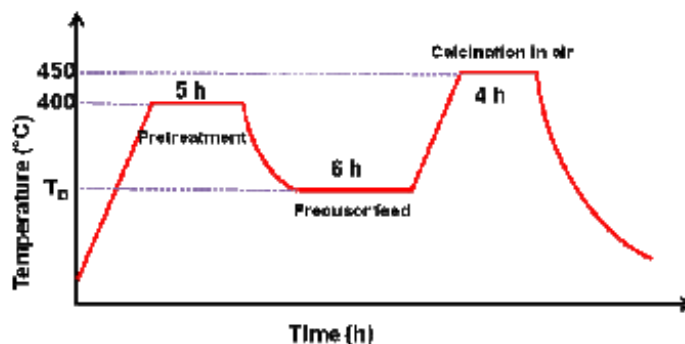
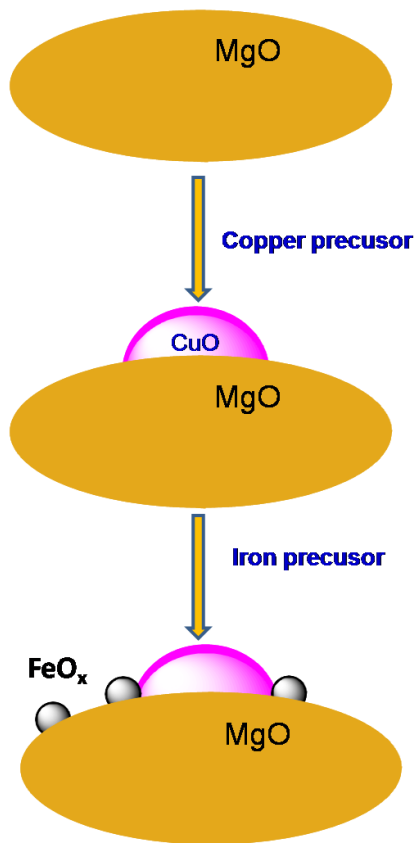
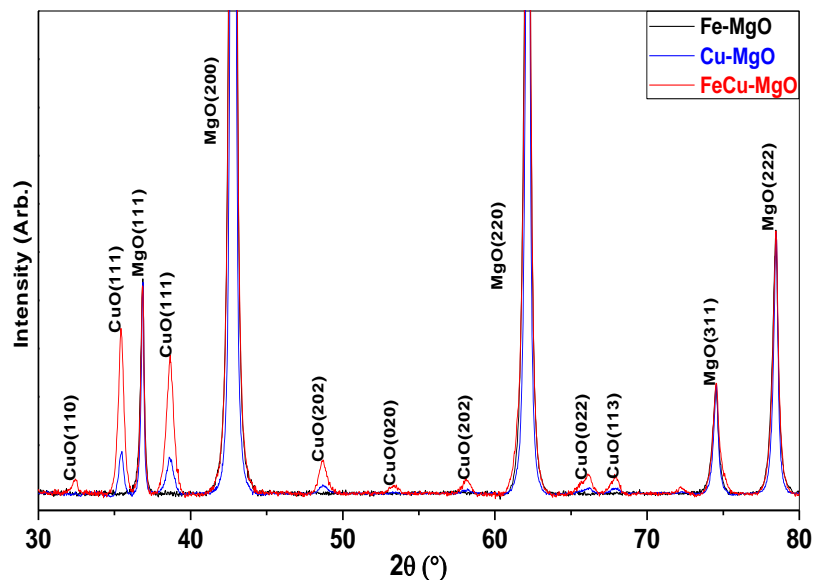


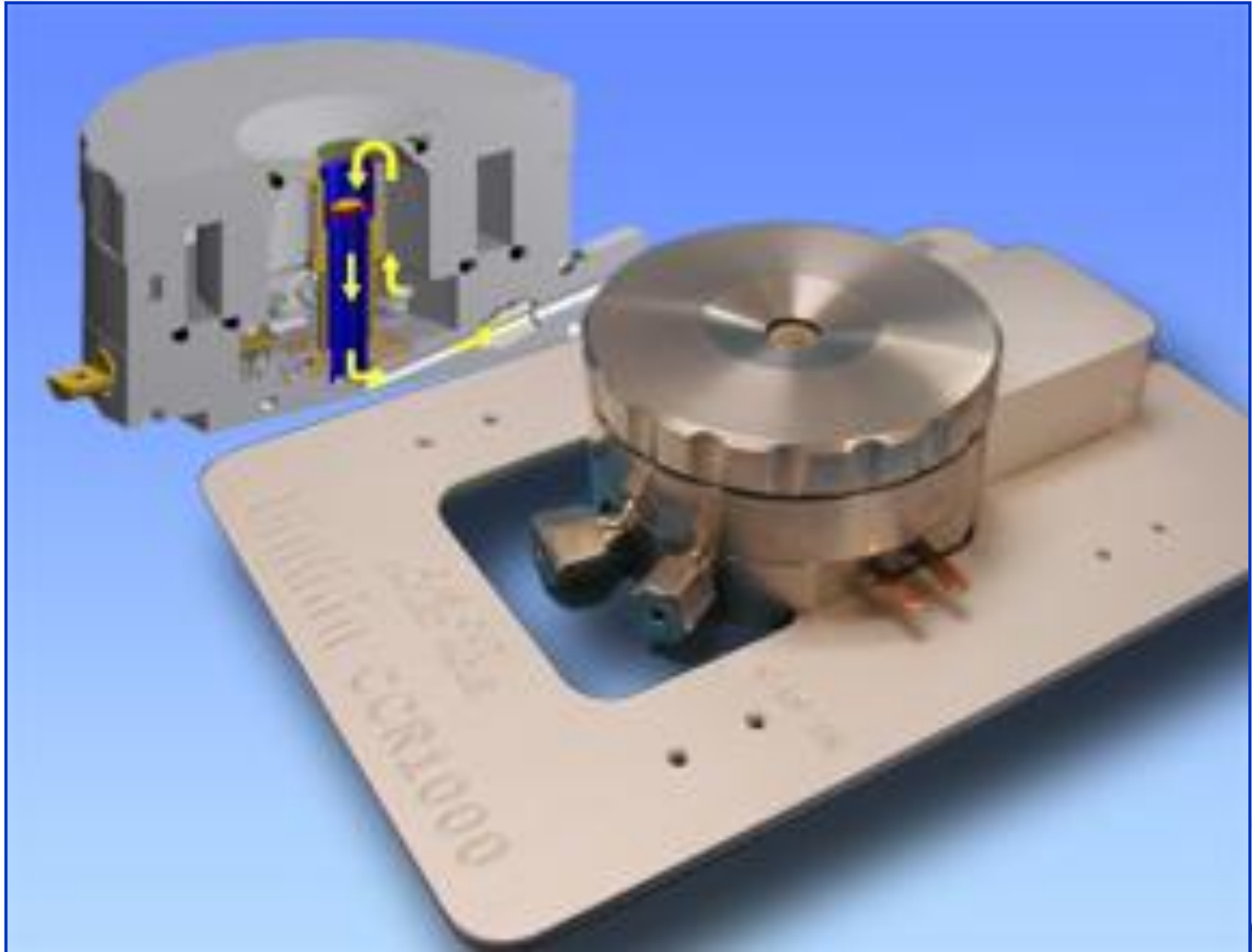
Figure S1. Schematic illustration of the ALD process.



The FeCu/MgO catalyst was prepared by consecutive deposition of Cu and Fe onto the MgO support. XRD patterns do not show the formation of FeCu alloy.

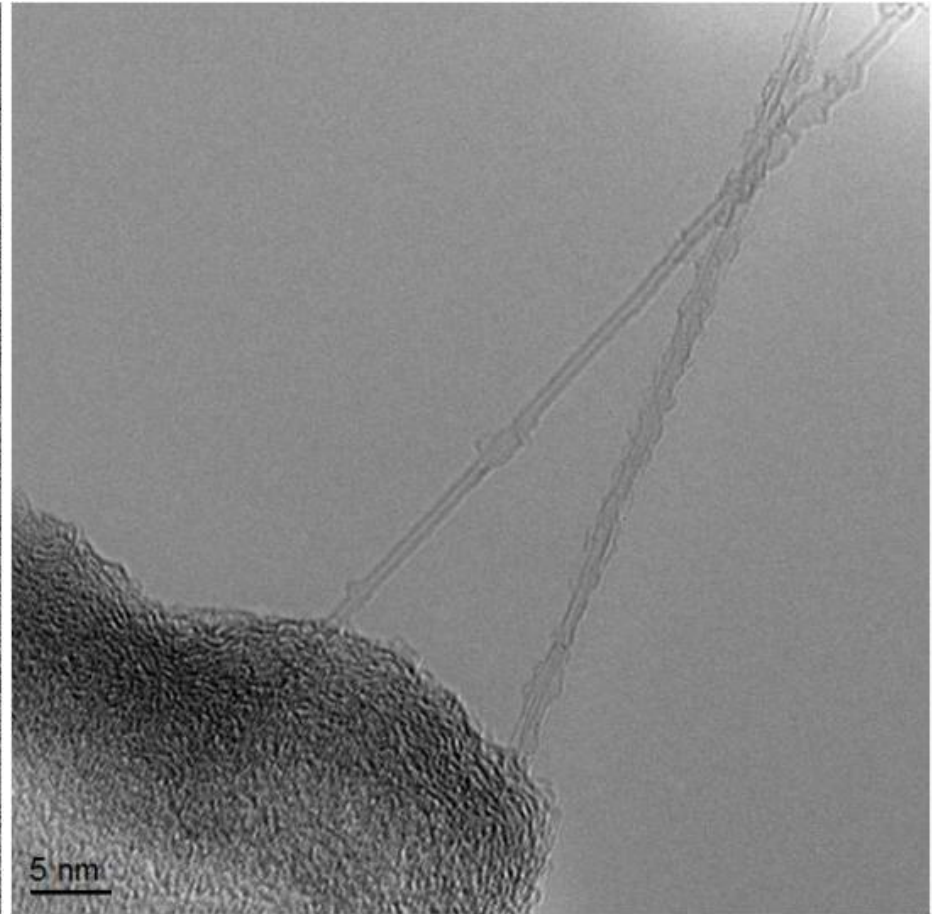
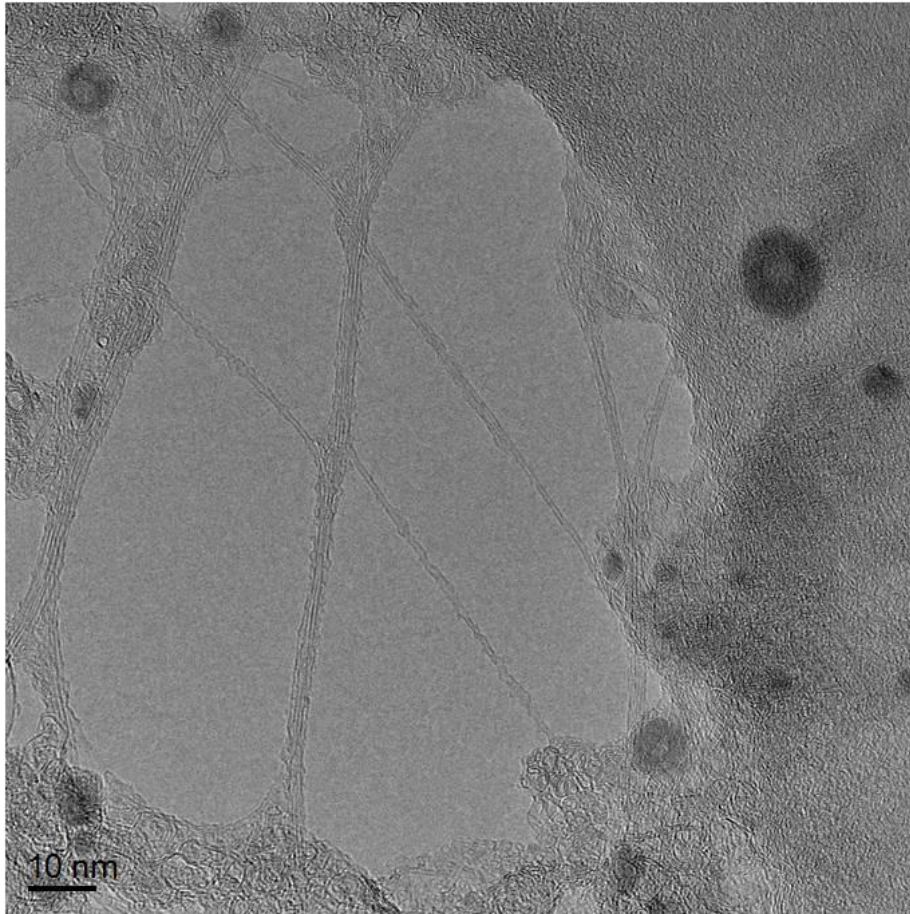


Ambient pressure growth experiments using Linkam in situ reaction chamber of Jobin Yvon Microscope Raman/FTIR spectrometer

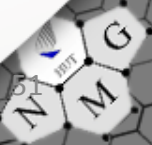


TEM characterization results

FeCu-MgO by ALD

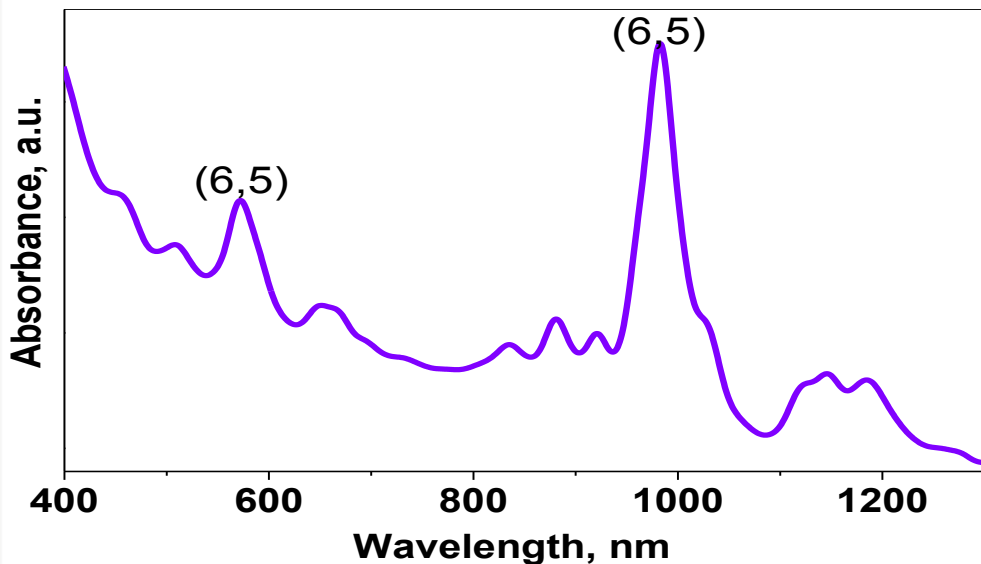


Carbon source: CO; Growth temperature: 600 °C

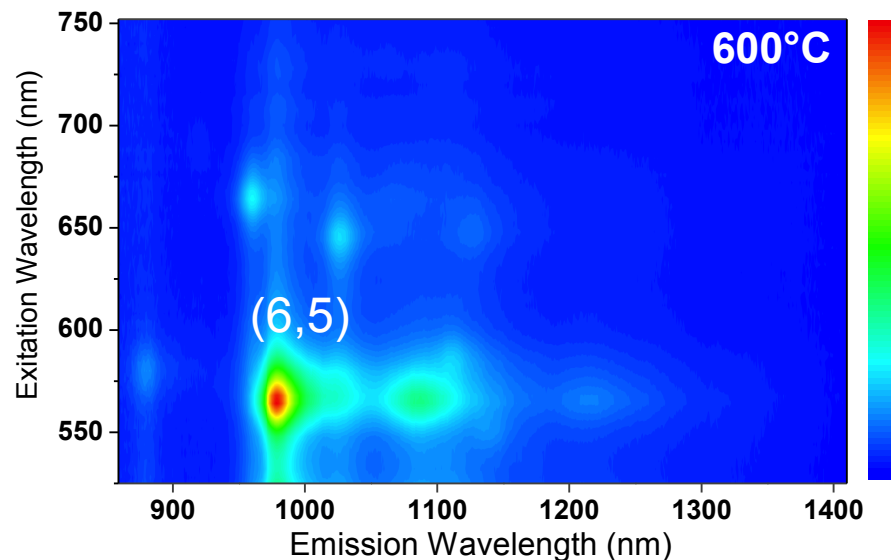


Spectroscopic characterization of SWNTs grown at 600 °C

FeCu-MgO by ALD



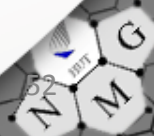
UV-Vis-NIR absorption



Photoluminescence

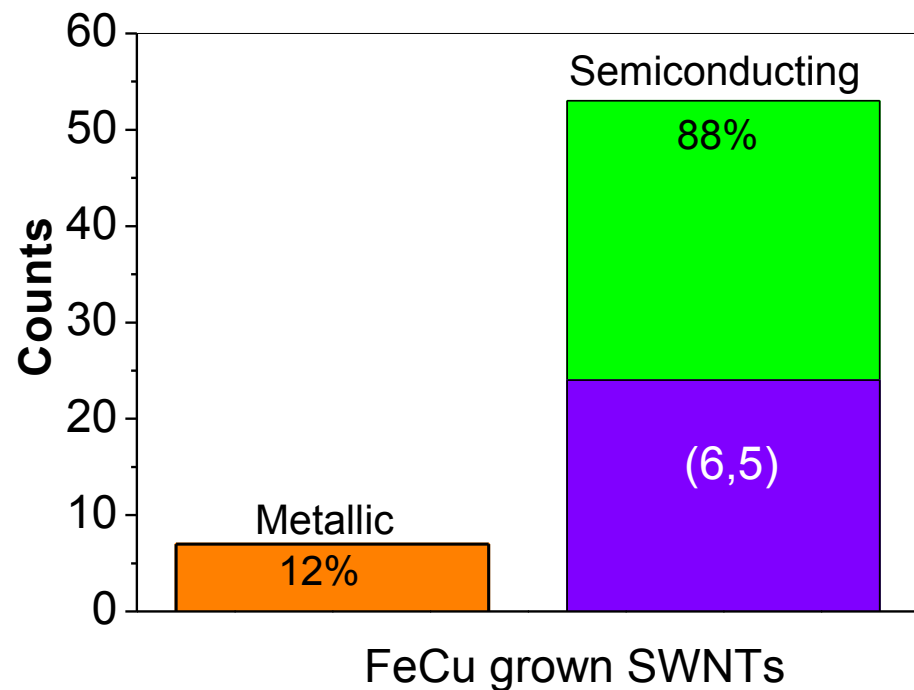
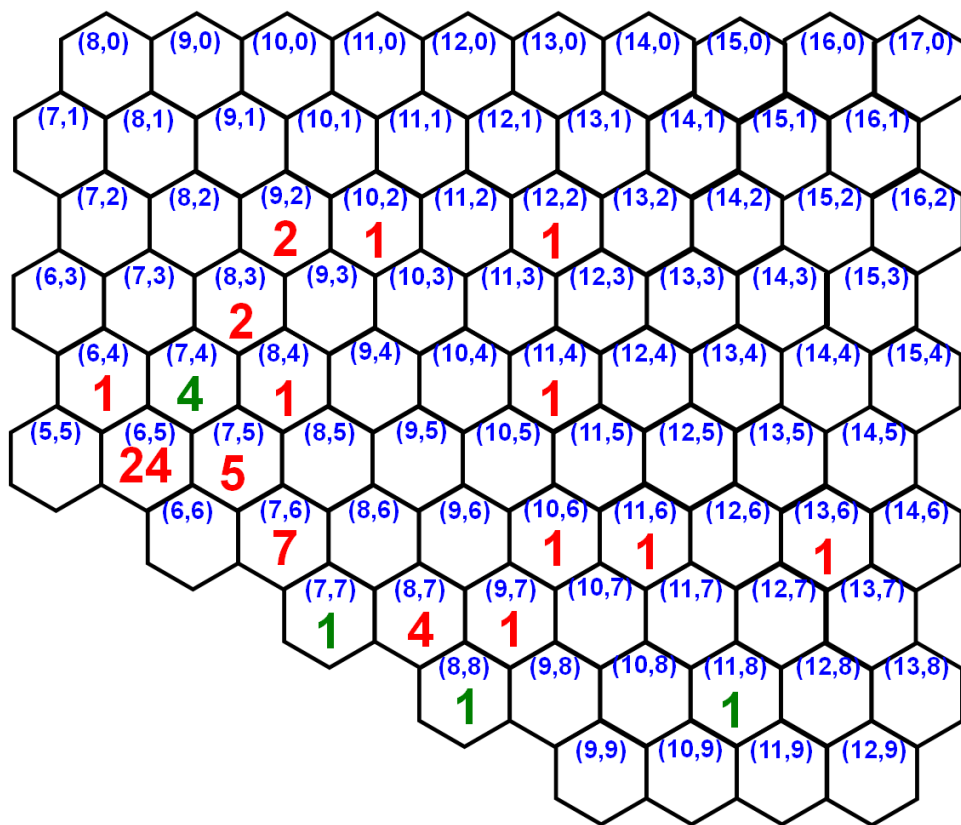
Predominant (6,5) SWNT growth was achieved

He et al. J. Am. Chem. Soc. **2010**, *132*, 13994-13996



Preferential growth of semiconducting SWNTs

FeCu-MgO by ALD



Preference of growing semiconducting SWNTs (S:M = 7)

He et al. Chem. Mater. **2012**, 24, 1796-1801



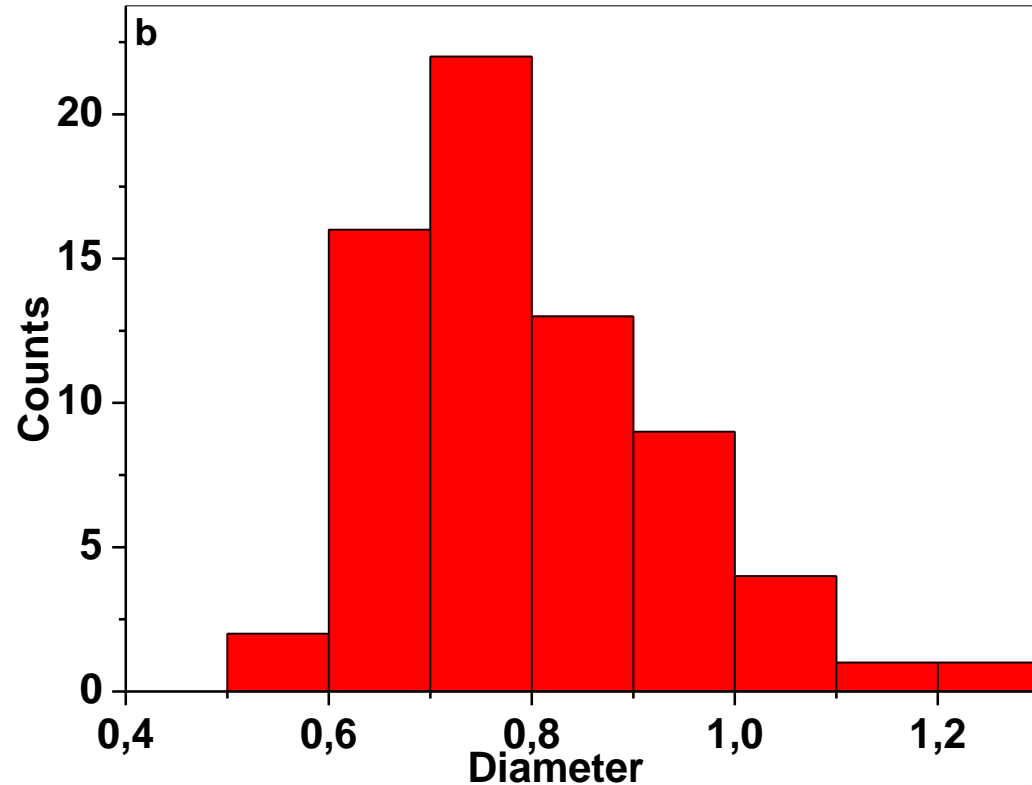
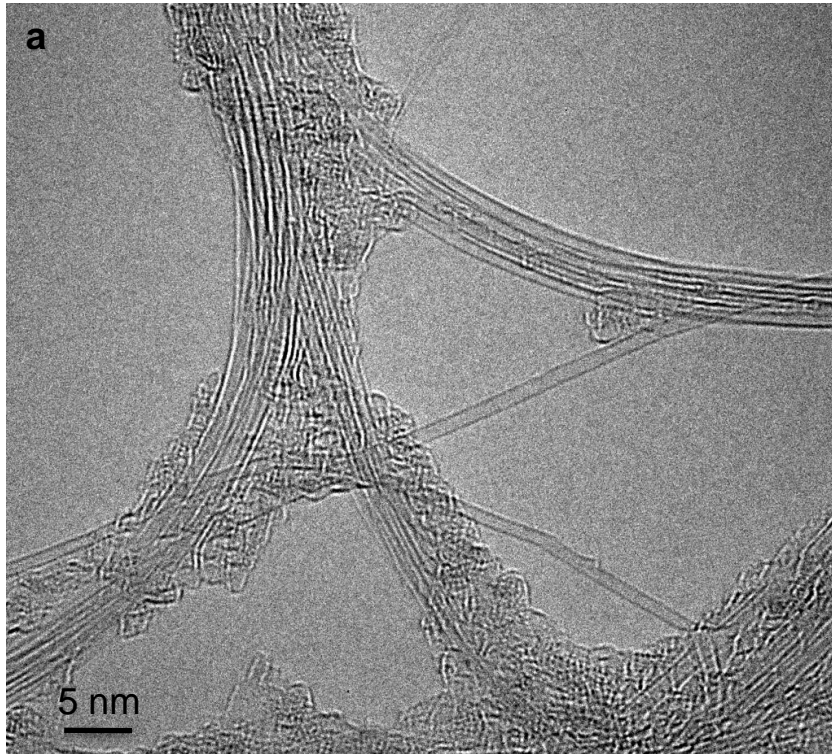
Preparation of Co-MgO I by ALD

Porous MgO obtained from the thermal decomposition of magnesium carbonate hydroxide hydrate was loaded into the ALD reactor (F120). The MgO carrier was first annealed in N₂ at 400 °C for 5 h. The deposition temperature was set at 190 °C for the cobalt (III) acetylacetonate (98%, Aldrich). After finishing the 6 h reaction, the catalyst was further annealed in air at 450 °C for 4 h.



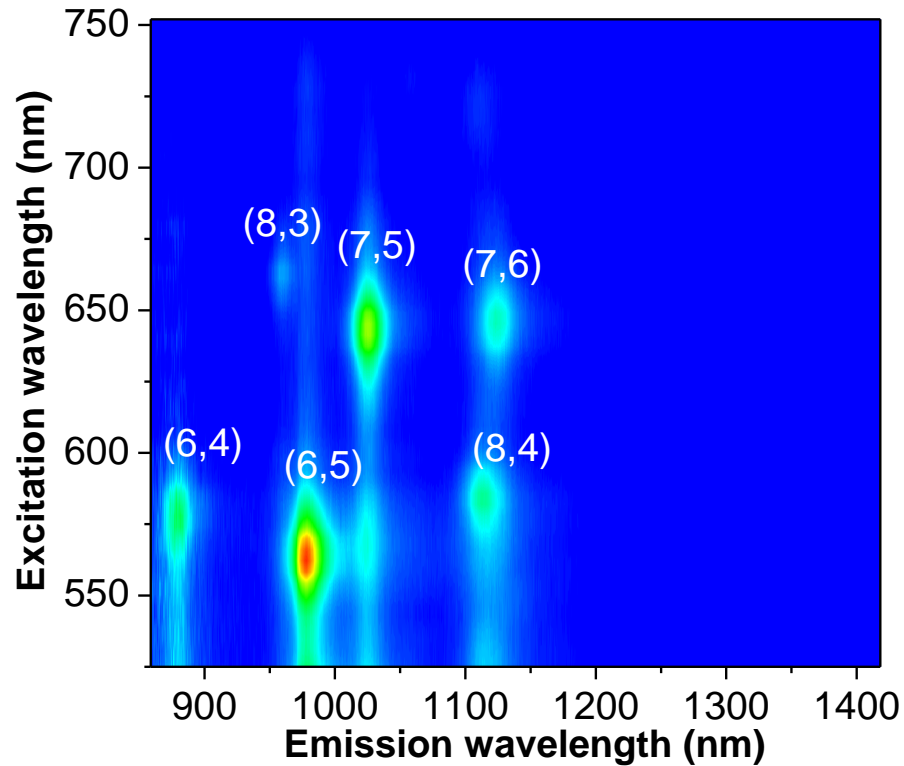
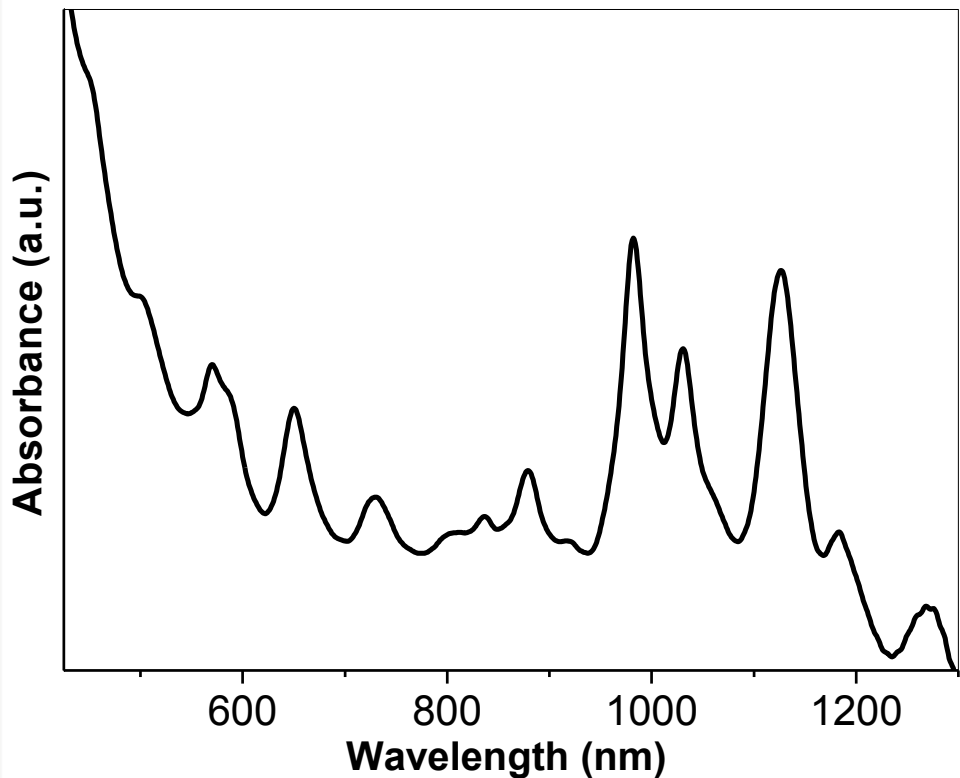
TEM characterization and diameter distribution

Co-MgO I by ALD



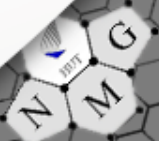
Spectroscopic characterization of SWNTs grown at 600 °C

Co-MgO I by ALD



Preparation of Co-MgO II by impregnation

The $\text{Co}_x\text{Mg}_{1-x}\text{O}$ catalyst was prepared by an impregnation technique followed by high temperature calcination. Porous MgO support was obtained by thermal decomposition of magnesium carbonate hydroxide hydrate (Aldrich, 99%) at 400°C for 1 h. $\text{Co}(\text{NO}_3)_2 \cdot 6\text{H}_2\text{O}$ (1.40 g, 98%, Aldrich), which was first dissolved in 100 mL distilled water and then mixed with 4.0 g MgO under stirring. After drying in air at around 90°C overnight, the catalyst was annealed at 1000°C in a muffle furnace.



Characterization of catalyst - Co-MgO II by impregnation

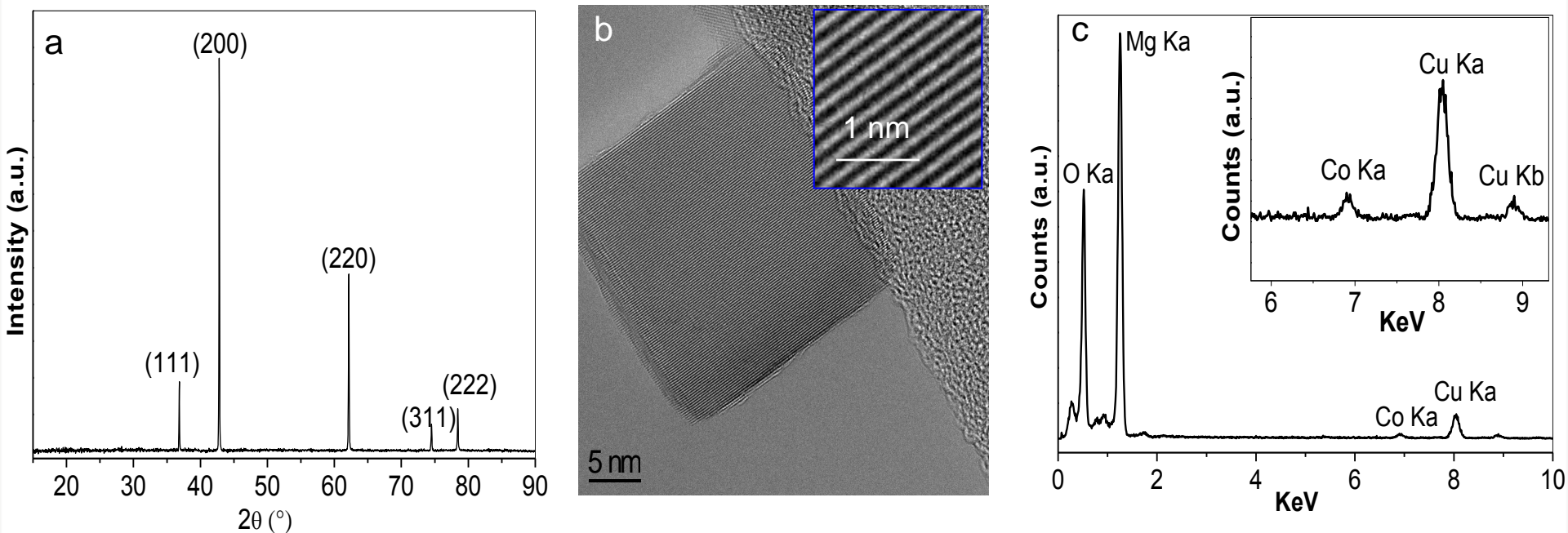
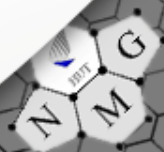
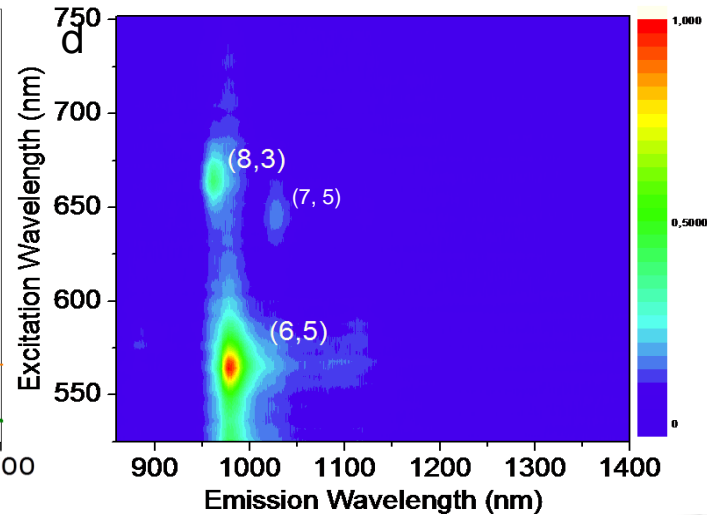
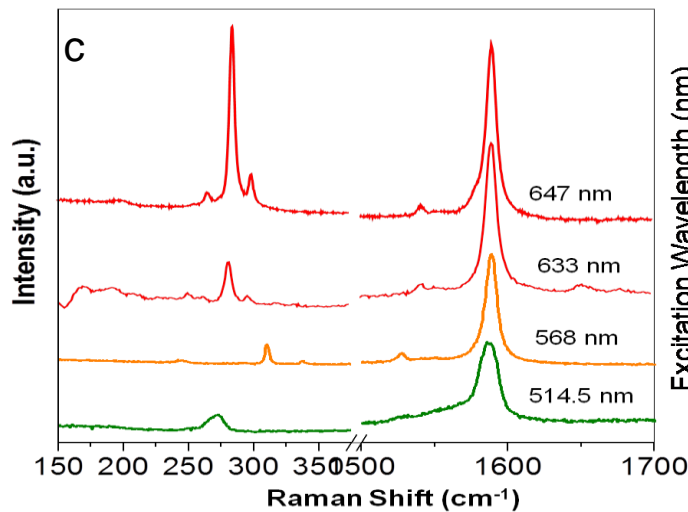
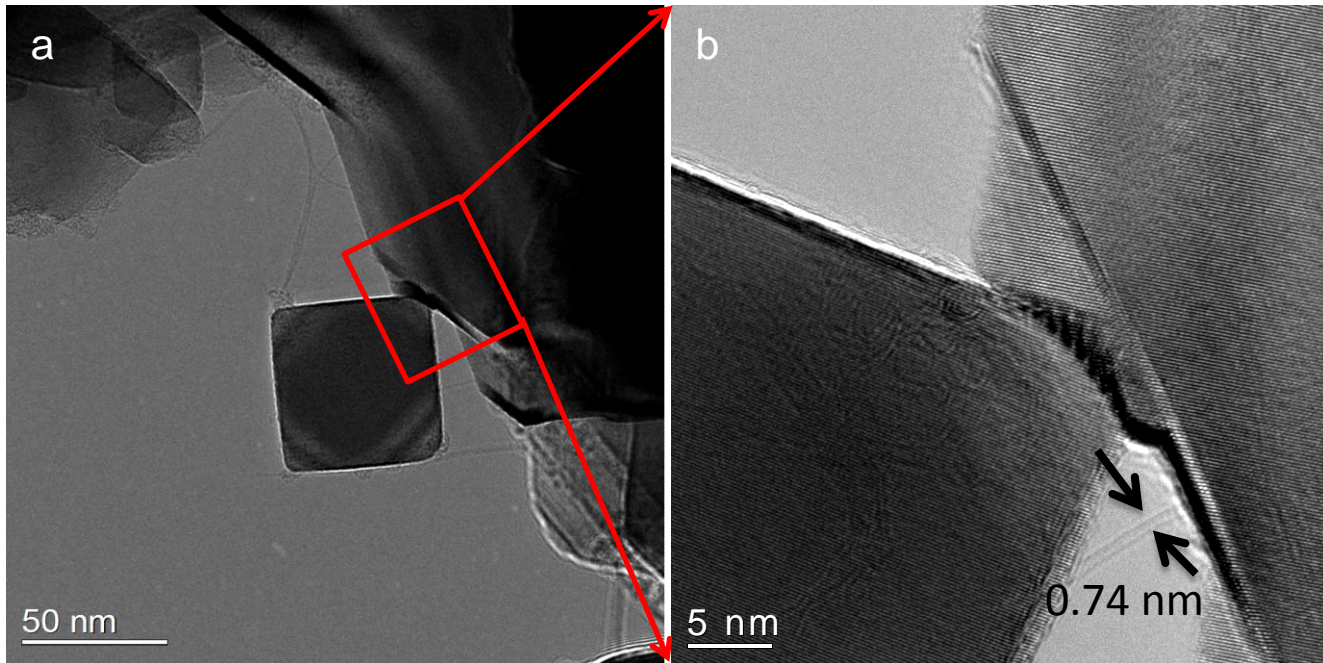


Figure. (a) XRD pattern of the $\text{Co}_x\text{Mg}_{1-x}\text{O}$ solid solution. (b) A TEM image of a cube particle of $\text{Co}_x\text{Mg}_{1-x}\text{O}$ solid solution. Inset is a close view of the particle with clear crystalline fringes. (c) An EDX spectrum of the $\text{Co}_x\text{Mg}_{1-x}\text{O}$ solid solution.



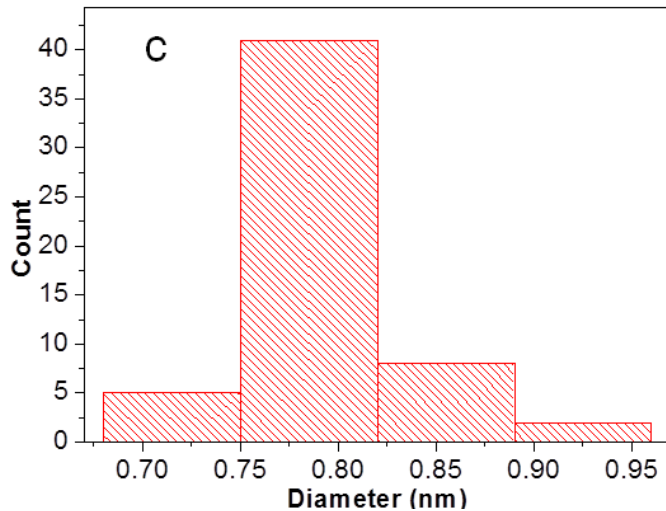
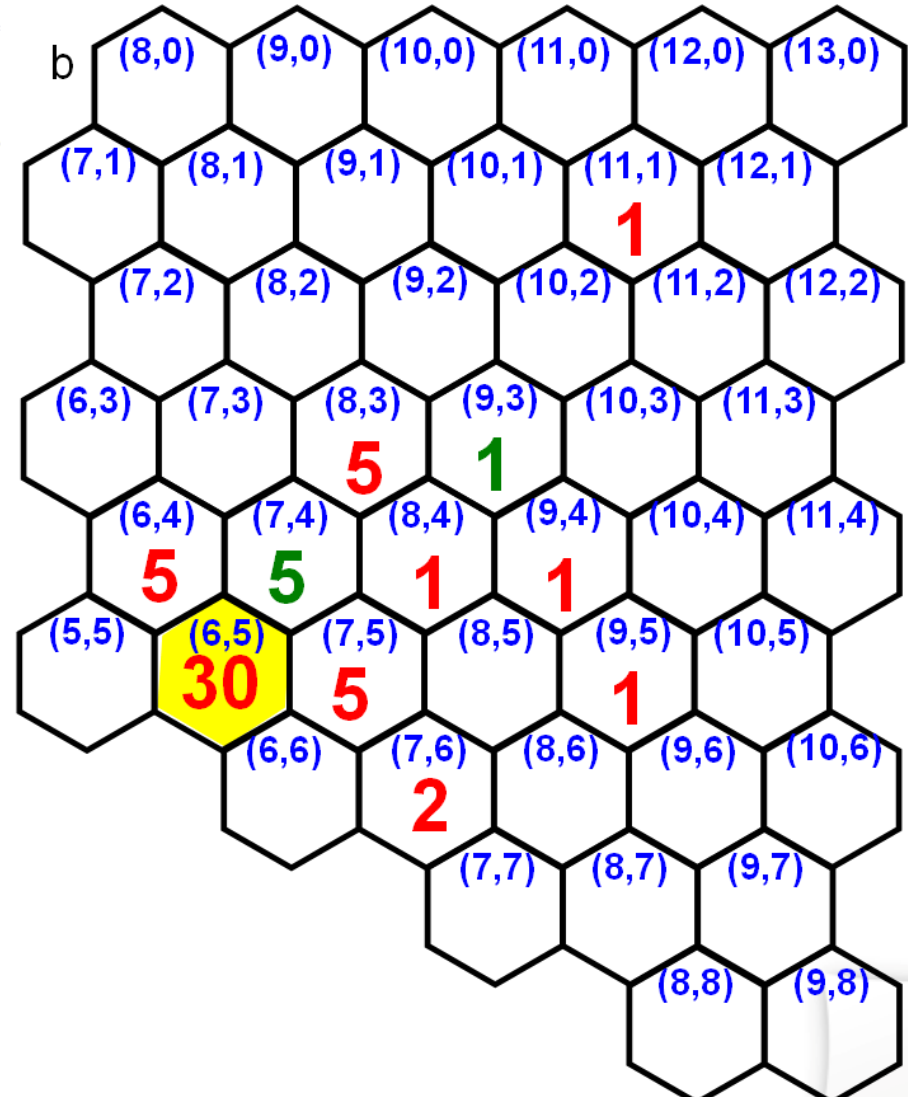
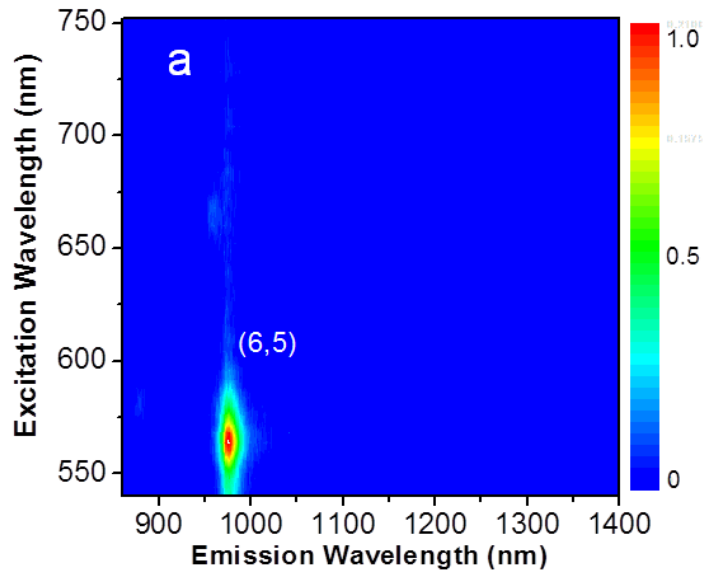
Characterization results on SWNTs grown at 600 C

Co-MgO II by impregnation



Characterization results on SWNTs grown at 500 C

Co-MgO II by impregnation



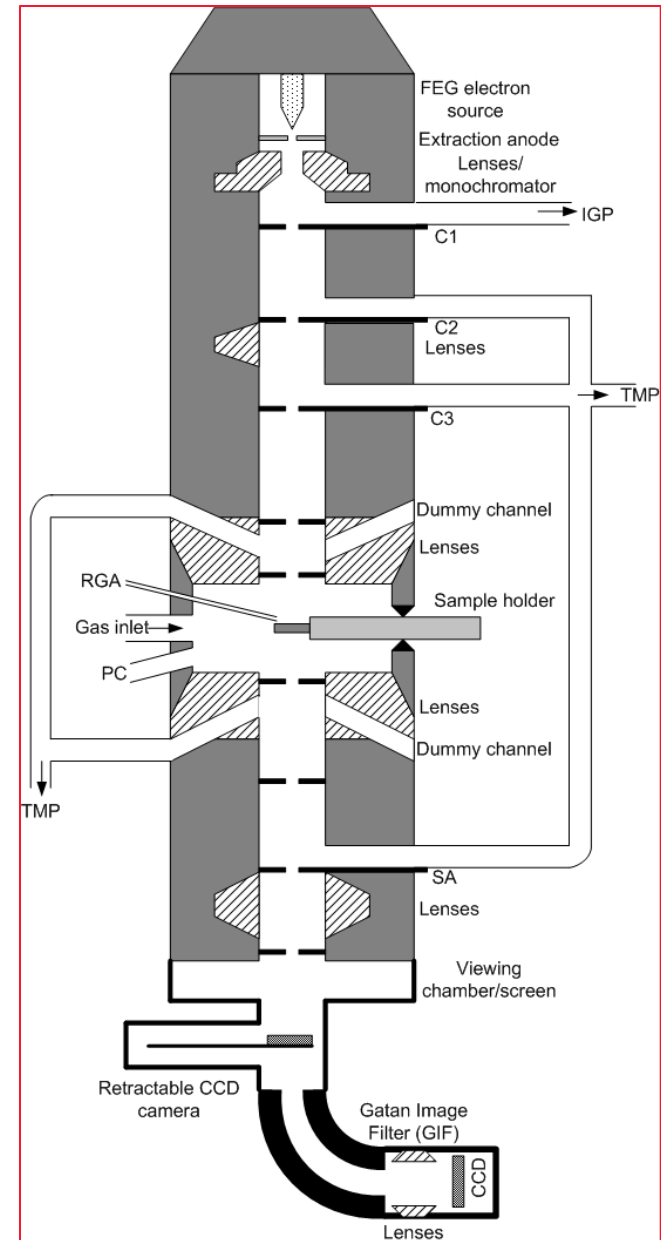
Preferential growth of semiconducting SWNTs (~90%)



Environmental TEM - Titan E-Cell 80-300ST with image Cs-corrector at DTU, Ljungby, Denmark (<http://www.cen.dtu.dk>)



Work conditions:
Accelerating voltage: 300 kV,
CO pressure: < 10 mbar.
Temperature: 600 °C ~ 700 °C



Catalyst: FeCu-MgO: *in-situ* growth

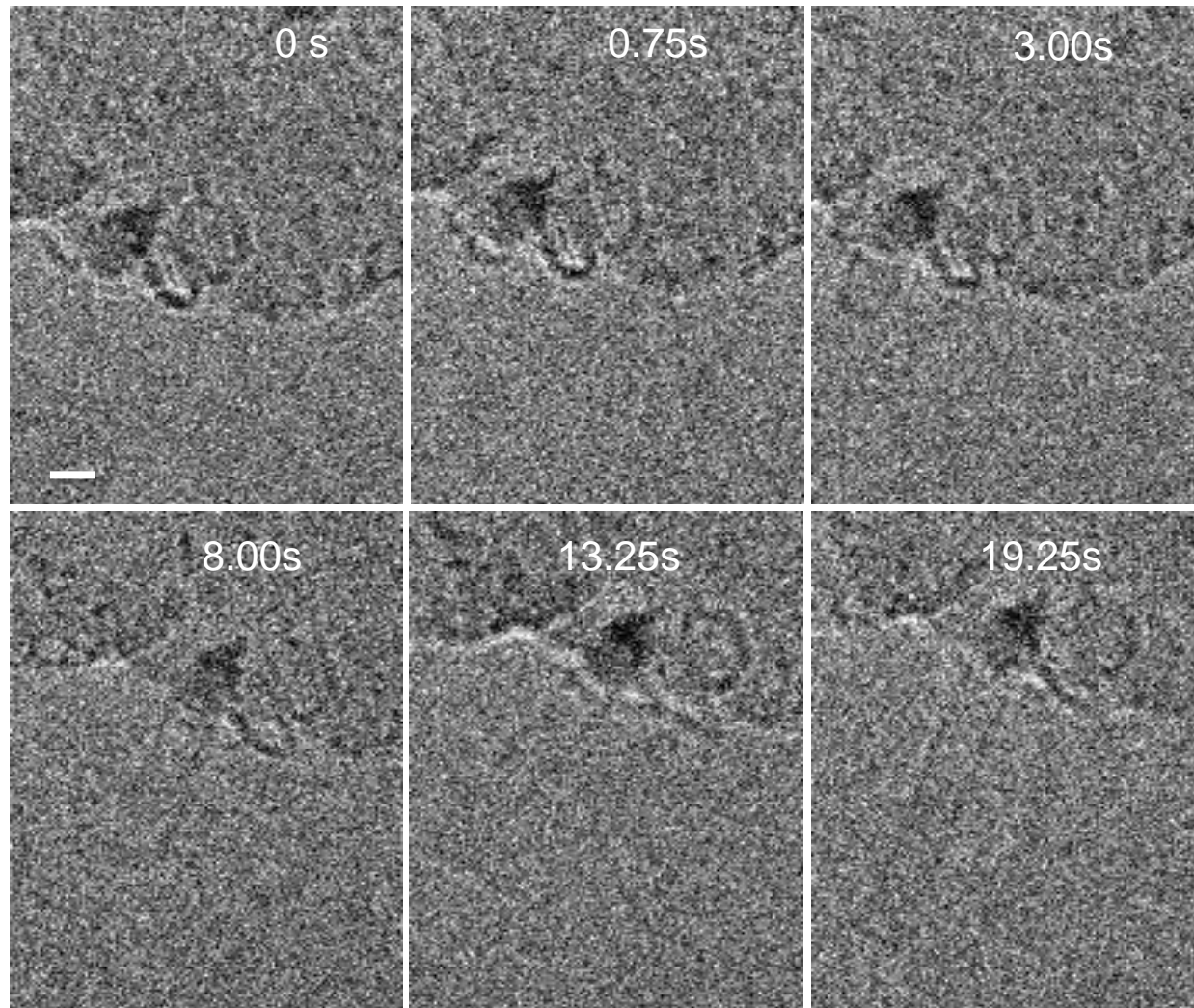


FeCu-MgO catalyst, CO= 6.9 mbar, T= 690 °C, 4 frames/s

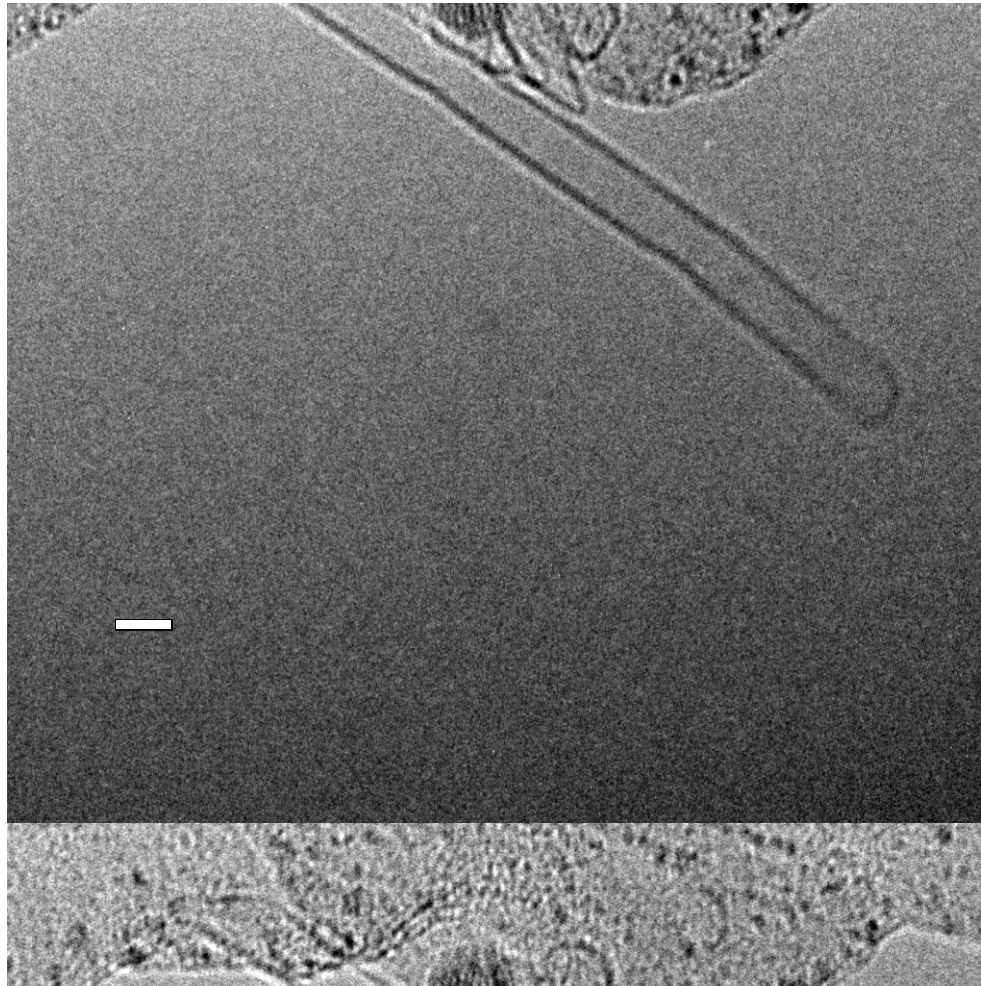


Growth of the SWNT in different stages

FeCu-MgO: ALD prepared



Termination of growth – initiation to grow new tubes
FeCu-MgO: ALD prepared

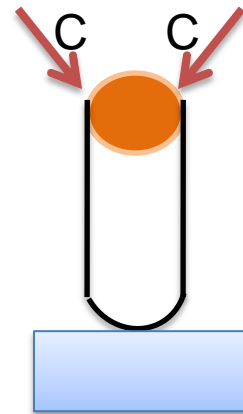


Nanoparticle escaped the
SWNT

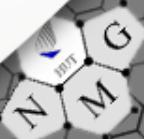
Catalyst: Co-MgO I: ALD prepared

Movie

Tip Growth



Movie– 1 frame/s, CO=9.5 mbar, T=700 °C



SWNT growth rate

Catalyst: Co-MgO I: ALD prepared

SWNT ID	particle size	SWNT size	Growth rate
1	3.7	3.2	0.23 nm/s
2	3.2	2.8	0.38 nm/s
3	2.1	1.8	0.82 nm/s
4	3.6	2.6	1.9 nm/s
5	2.8	2.3	0.12 nm/s

Growth conditions: 9.5 mbar CO at 700 °C

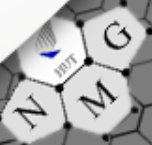


Catalyst: Co-MgO II: impregnation prepared - *in-situ* growth

Base-growth
mode

Movie 1

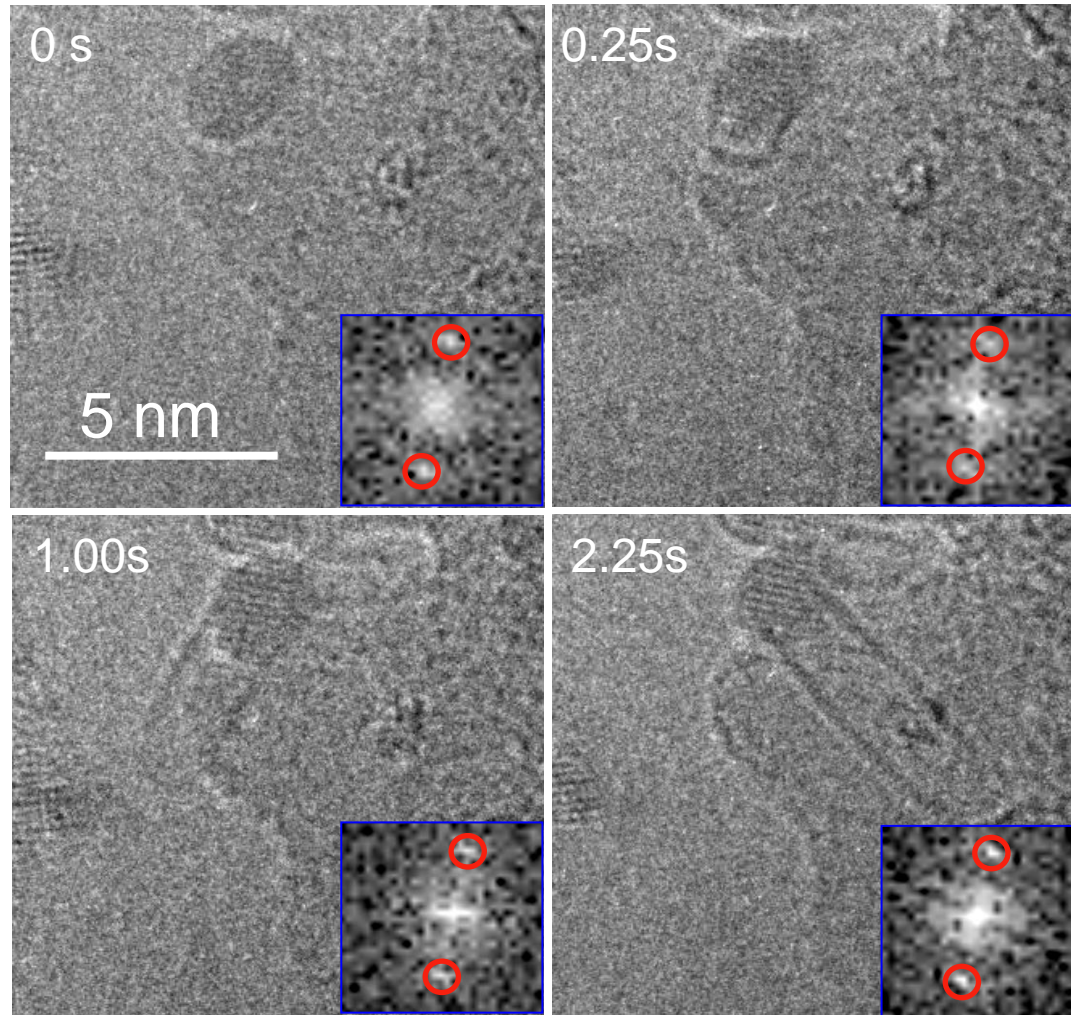
Co-MgO catalyst, CO= 6.9 mbar, T= 690 °C
4 frames/s



Evolution of the Co particle

Co-MgO II: impregnation prepared

CO= 6.9 mbar,
T= 600 °C



The particle preserves its crystalline orientation during SWNT growth process



Catalyst: Co-MgO II: impregnation prepared - *in-situ* growth

Base-growth
mode

Movie 2

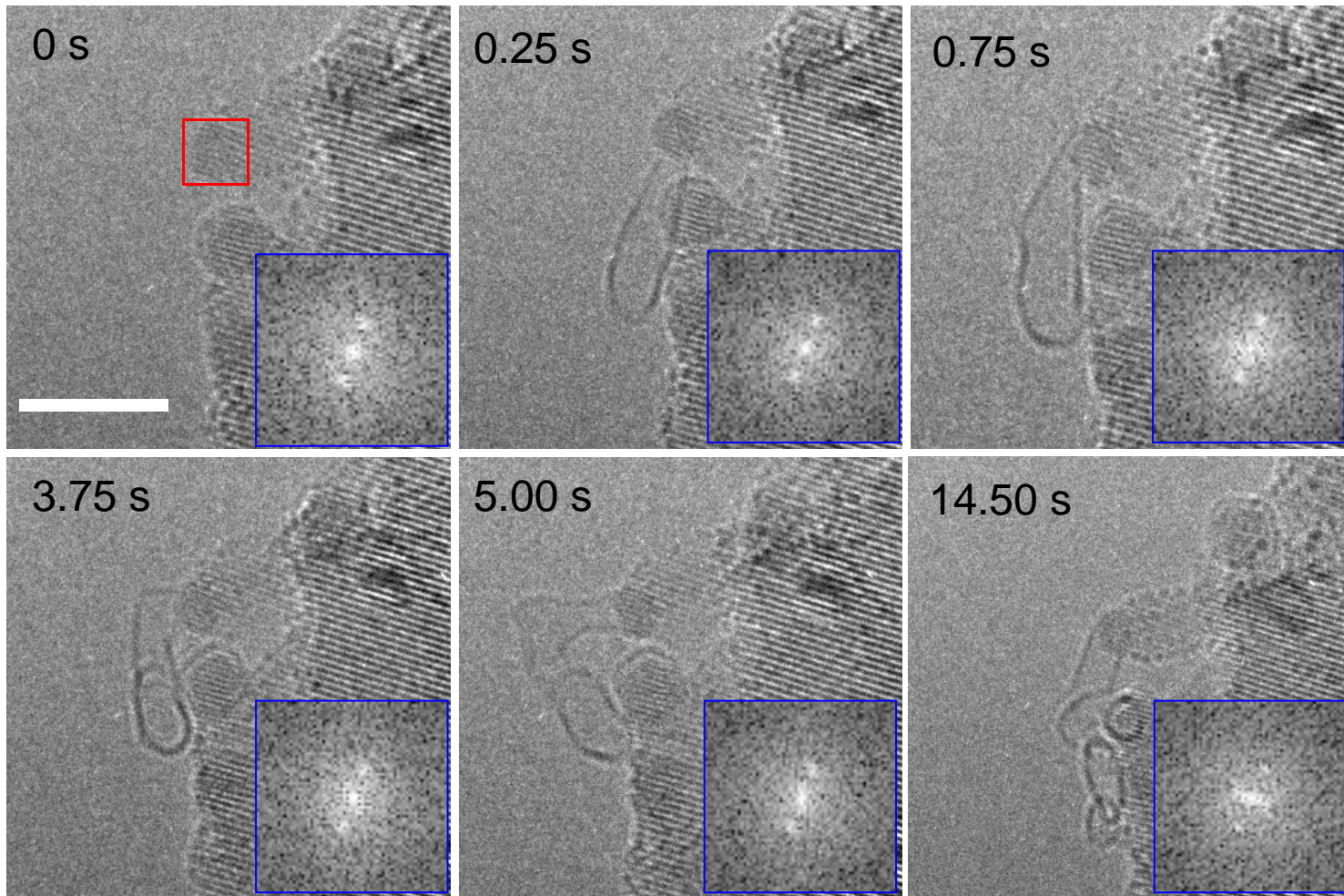
Co-MgO catalyst, CO= 6.9 mbar, T= 690 °C
4 frames/s



Evolution of the Co particle

Co-MgO II: impregnation prepared

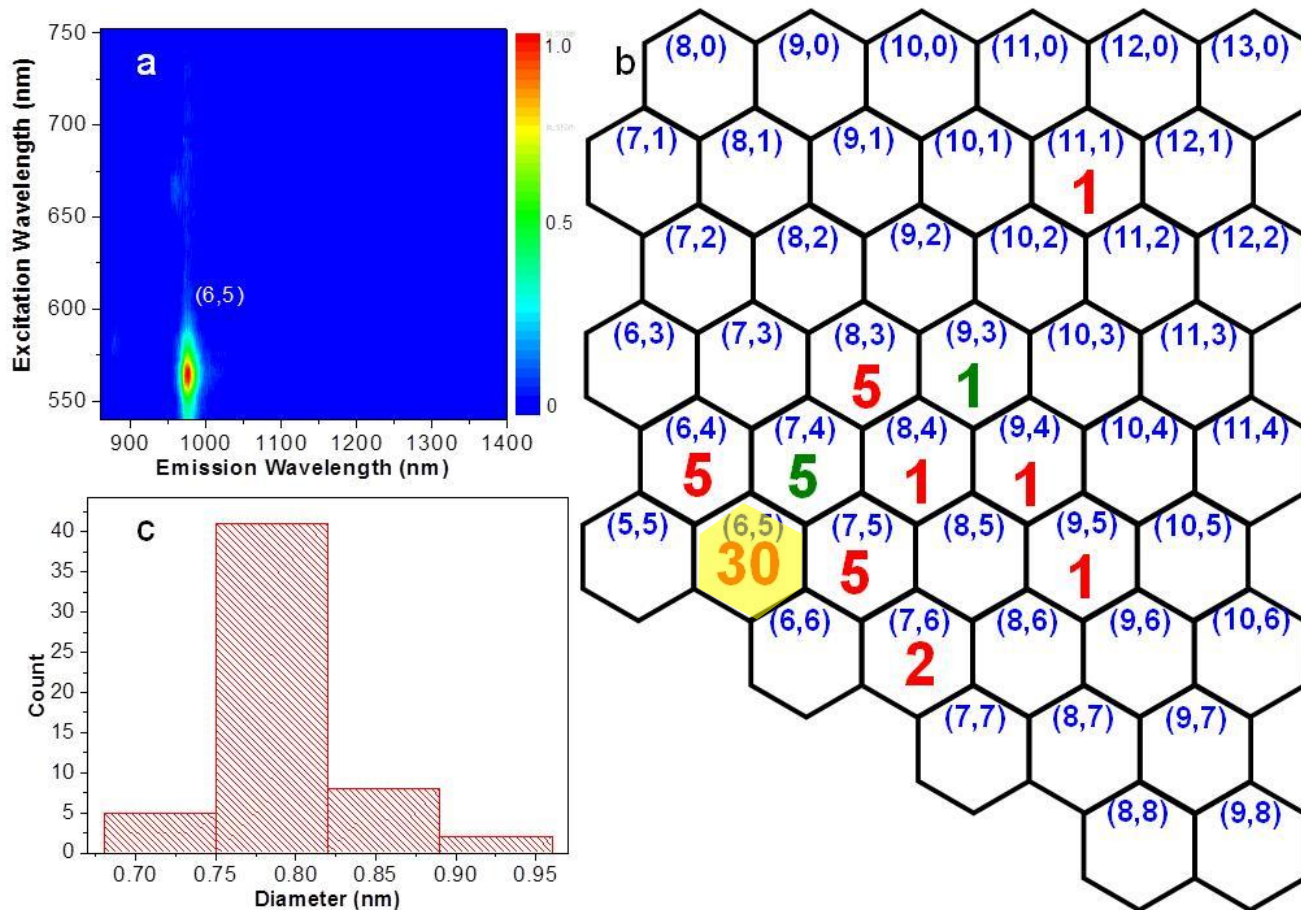
CO= 6.9 mbar,
T= 600 °C



- ❑ Strong interactions between Co and MgO support;
- ❑ Possible growth modes: Pendendicular VS Tangential;

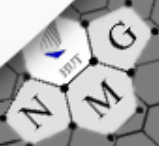
Catalyst: Co-MgO II: *Ex-situ* Growth

Narrow Chirality distribution of SWNTs grown at ambient CO pressure



Growth temperature: 500 °C

Preferential growth of semiconducting SWNTs: 89%.



In-situ studies - Summary

1. Several catalyst systems have been developed for studying SWNT growth by ETEM.
2. The SWNT growth rate, the evolution of metal nanoparticles and the growth modes of SWNTs being determined and compared to model predictions
3. Preferential growth of semiconducting SWNTs can be achieved on catalysts with strong metal-support interactions.



NanoMaterials Group, Aalto University School of Science

Department of Applied Physics

Antti Kaskela

Dr. Albert G. Nasibulin

Dr. Hua Jiang

Zhen Zhu

Dr. Ilya Anoshkin

Dr. Anton Anisimov

Dr. Maoshuai He

Ying Tian

Marina Y. Timmermans

Dr. Toma Susi

<http://www.fyslab.hut.fi/nanomat/>



Acknowledgement for Funding

- * Academy of Finland
- * EU FP6 & FP7
- TEKES FinNano Program
- NEDO, NICT

Prof. Y. Ohno, Dr. DM. Sun
Nagoya University, Japan



Acknowledgements

Alexander I. Chernov, Pavel V. Fedotov,
Elena D. Obraztsova



Filippo Cavalca , Thomas W. Hansen , Jakob B. Wagner



Inkeri Kauppi, Emma Sairanen, Sonja Kouva, Juha Linnekoski, Marita Niemelä,
Juha Lehtonen



Annick Loiseau, Christophe Bichara

